DOKUZ EYLÜL UNIVERSITY
GRADUATE SCHOOL OF NATURAL AND APPLIED SCIENCES

PRODUCTION OF NANO-SIZED BORON PRODUCTS FROM BORON DERIVATIVES

by

Mehmet Baran TUFAN

July, 2014
İZMİR

PRODUCTION OF NANO-SIZED BORON PRODUCTS FROM BORON DERIVATIVES

A Thesis Submitted to the
Graduate School of Natural and Applied Sciences of Dokuz Eylül University
In Partial Fulfillment of the Requirements for the Degree of Doctor of Philosophy in Mining Engineering, Mineral Processing Program

by

Mehmet Baran TUFAN

July, 2014

İZMİR

Ph.D. THESIS EXAMINATION RESULT FORM

We have read the thesis entitled "**PRODUCTION OF NANO-SIZED BORON PRODUCTS FROM BORON DERIVATIVES**" completed by **MEHMET BARAN TUFAN** under supervision of **PROF. DR. TURAN BATAR** and we certify that in our opinion it is fully adequate, in scope and in quality, as a thesis for the degree of Doctor of Philosophy.

Prof. Dr. Turan BATAR

Supervisor

Prof. Dr. Üner İPEKOĞLU

Thesis Committee Member

Prof. Dr. Erdal ÇELİK

Thesis Committee Member

Prof. Dr. Mehmet POLAT

Examining Committee Member

Doç. Dr. Sezai ŞEN

Examining Committee Member

Prof. Dr. Ayşe OKUR

Director

Graduate School of Natural and Applied Sciences

ACKNOWLEDGMENTS

Foremost, I would like to express my sincere gratitude to my advisor Prof. Dr. Turan Batar for the continuous support throughout my Ph.D. studies and research and for his faith, patience, motivation, enthusiasm and immense knowledge.

I would also like to thank the rest of my thesis committee; Prof. Dr. Üner İpekoğlu and Prof. Dr. Erdal Çelik, for their encouragement, insightful comments and guiding questions.

My sincere thanks also goes to my professor Dr. Bayram Kahraman and my fellow colleagues Dr. Erkan Güler, Dr. Mete Kun, Dr. Tahir Mallı, Fatih Turan, all EMUM personnel and especially Ertuğrul Torun for the enlightening discussions, endless guidance and helping hands offered for these whole four years of my research.

Last but not the least, I would like to thank my family; my wife and colleague Ebru Tufan and my parents, for supporting me spiritually throughout my life.

Mehmet Baran TUFAN

PRODUCTION OF NANO-SIZED BORON PRODUCTS FROM BORON DERIVATIVES

ABSTRACT

Turkey has the most abundant boron reserves in the world; however, the boron end products to be used in advanced technology are not available since the existing production plants in Turkey do not possess the technology to produce advanced boron end products. Though, several boron derivatives such as borax pentahydrate, borax decahydrate and boric acid used in this study are produced in Turkey, there is no production of boron end products from these derivatives.

The production of boron end products such as boron carbide, boron nitride, boron carbonitride and elemental boron are possible on industrial scale. However, these processes which consume large amounts of energy and cause unacceptable levels of environmental problems (carbon dioxide emission) stop short of being economical.

The main objective of this thesis is to assess the production of nano-sized boron end products from boron derivatives by electro-deposition as powders or coating. The possibility of nano-sized boron end product manufacturing by a relatively cheap and energy conscious chemical method is investigated. It was found that, production of boron end products could be achieved by electro-deposition at low temperatures without any carbon dioxide emission regardless of the path of sintering and thermal treatment. The optimum experimental parameters for the process are provided through an in depth analysis of test results.

Keywords: Electro-deposition, boron carbide, boron nitride, nano-particles, boron derivatives, boron end product

BOR TÜREVLERİNDEN NANO BOYUTLARDA BOR UÇ ÜRÜNLERİ ÜRETİMİ

ÖZ

Türkiye, dünyadaki en büyük bor rezervlerine sahip olmasına rağmen ileri teknoloji ürünlerde kullanılan bor uç ürünlerinin fabrikasyonu için gerekli tesislere sahip değildir. Var olan tesisler ise bor uç ürün üretimi için yeterli teknolojiye sahip değillerdir. Kısacası, ülkemizde boraks pentahidrat, boraks dekahidrat ve borik asit gibi bor türevleri üretilirken, bu ürünlerden asıl katma değeri oluşturan bor uç ürünlerinin eldesini sağlayacak tesisimiz bulunmamaktadır.

Endüstriyel çapta bor karbür, bor nitrür, bor karbonitrür ve elementel bor gibi uç ürünler çok yüksek enerji gideri ve çevresel sorunlar (karbondioksit emisyonu) ile üretilmektedir.

Bu çalışmanın amacı ise, elektro depozitleme yöntemi kullanarak nano boyutlarda toz yada kaplama olarak bor uç ürün eldesini sağlamaktır. Düşük maliyetli, düşük enerji giderli ve çevre dostu bu kimyasal yöntem ile bor uç ürün eldesinin mümkün olup olmadığı araştırılmıştır. Sonuç olarak, elektro depozitleme yöntemi ile karbondioksit emisyonu, sinterleme ve ısıl işlemler olmadan, düşük sıcaklıklarda bor uç ürünlerinin eldesi sağlanmıştır. Kullanılan her bor türevi ve üretilen bor uç ürününe göre gerekli analizler ışığında en uygun deneysel koşullar belirlenmiştir.

Anahtar Kelimeler: Elektro-depozitleme, bor karbür, bor nitrür, nano parçacıklar, bor türevleri, bor uç ürünleri

CONTENTS

Page

LIST OF FIGURES

Page

LIST OF TABLES

Page

CHAPTER ONE
INTRODUCTION

Boron and boron compounds have increasing strategical significance in the world for several decades. Though, Turkey has the most abundant boron reserves in the world; production of boron end products to be used in advanced technology are still possible since the existing production plants in Turkey do not have the required technology to manufacture advanced boron end products.

The main objective of this research is the production of nano-sized boron end products from boron derivatives by electro-deposition as powder or coating products. Several boron derivatives among borax pentahydrate ($Na_2B_4O_7.5H_2O$), borax decahydrate ($Na_2B_4O_7.10H_2O$), boric acid (H_3BO_3), anhydrous borax ($Na_2B_4O_7$), tincal concentrate ($Na_2B_4O_7.10H_2O$) and calcined tincal (compacted $Na_2B_4O_7$) used in this study are produced in Turkey by Eti Mine, nevertheless there is no production plant for boron end products emerged from these derivatives.

The boron ores can be easily and economically extracted in Turkey, although the production capacity and exportation values are under expectations. The refined boron derivatives, as well as raw boron compounds and their concentrates (colemanite, ulexite and tincal), are being sold without any further process for decades which brings out a great financial loss regarding the economics of Turkey. In the long run, extensive usage of boron is going to be accomplished by application of this modified electro-deposition method for boron end product fabrication in local scale which will close the deficit of Turkey in end product export.

The production of boron end products such as boron carbide (B_4C, BC_5 and $B_{13}C_2$), boron nitride (BN), boron carbonitride (BCN) and elemental boron (B_{28}) are possible in industrial scale. However, the procedures require large amounts of energy, cause excessive environmental problems (CO_2 emission) and are not economical. This thesis is going to explore the possibility of production of nano-sized boron end products by a very cheap and energy-saving chemical method,

namely electro-deposition. The production of boron end products are achieved at low temperatures without CO_2 emission, regardless of sintering and thermal treatment. This new, modified method of production is going to provide an opportunity for improvement in mining industry with respect to boron production.

Unlike the traditional production methods which require high energy consumption due to high temperatures involved, the modified electro-deposition method brings in the opportunity of environment friendly boron end product fabrication with lower energy consumptions. The production of advanced materials with such environmentally friendly and low energy consuming method will address the gap in the literature regarding the boron end products.

Nanotechnology is a promising route to manufacture advanced materials, in other words; materials with high purity, technological performance and economic value and carries a great significance in industrial development. By the same token, utilization of boron resources as feed materials in nanotechnology based manufacturing processes presents a high added value solution for Turkish economy.

The importance of the results gathered here is not limited to boron end product production. The possibility of utilization of produced boron end products is also quite significant in fabrication of nano-composites and advanced materials. In this manner, a further study with a multidisciplinary research team is attempted to utilize these boron end products in a daily use or military purposes under financing and support of public enterprises. The suitability of products is going to be determined and evaluated with respect to fabrication of nano-composites and advanced materials afterwards.

CHAPTER TWO
LITERATURE REVIEW AND CURRENT SITUATION

The progress of boron carbide, boron nitride, boron carbonitride and elemental boron productions have been developed in years. The use of electro-deposition method in several operations regardless of boron end product fabrication was also developed by determining the optimum parameters for each product. The combination of electro-deposition method with boron end product production has not been applied yet in literature and this research is going to be the first under these circumstances. The literature review is classified under several topics with respect to boron strategies, boron end products, production methods and boron end product market.

2.1 Boron, Boron Products, Boron Industry and Previous Studies

Turkey and the United States are by far the largest producers of boron minerals, accounting for 73% of the global production in 2010. After a sharp decline in consumption during the economic downturn, the market recovered to the pre-crisis level in 2010. Only a few of the many minerals that contain boron are commercially valuable. Substances containing boron oxide are commonly known as borates. The major borate minerals produced are borax, colemanite, datolite, kernite, probertite, szaibelyite, tincal and ulexite. Major deposits occur in South America, Turkey and the United States in the form of ores and brines (IHS Incorporation, 2011).

The most important boron deposits are in Turkey, Russia and USA; whereas the world's commercial boron reserves are grouped under 4 regions. These are; "Mojave Desert" in California, USA, "Andean Zone" in North America, "South-Middle East Orogeny Zone" covering Turkey and Eastern Russia (Boren National Boron Research Institute, 2013).

In 2010, Turkish production provided 41% of the world supply, based on B_2O_3 content, and the United States provided another 31% of supply. Other countries that

are significant exporters include Argentina, Chile and Malaysia. Europe and Japan rely on imports for their boron mineral and chemical supplies. China is the world's third-largest producer of primary boron chemicals after Turkey and the United States and is the third-largest consumer of boron chemicals after the United States and Europe (IHS, 2011).

Boron is a commonly existing element in the earth, soil, rocks and water. Although boron content of the soil is approximately 10-20 ppm, it is found at high concentrations in the western regions of USA and in the region stretching from Mediterranean to Kazakhstan. Boron content ranges from 0.5-9.6 ppm for sea water and 0.01-1.5 ppm for fresh water. Boron deposits with high concentrations and economical values are found mainly in Turkey and in arid, volcanic and high hydrothermal activity regions of U.S. as boron compounds bound with oxygen (Boren, 2013).

Boron, shown by the symbol B in the periodic table, having an atomic number of 5 and atomic mass of 10.81, is an element in between metal and non-metal with semi conducting property. It is the first and the lightest element of 3A group in the periodic table. Boron element is composed of ^{8}B, ^{10}B, ^{11}B, ^{12}B and ^{13}B isotopes. The most stable isotopes are ^{10}B and ^{11}B. The occurrence rates of these isotopes in nature are 19.1-20.3% and 79.7-80.9%, respectively. ^{10}B isotope shows a very high thermal neutron capture property. Hence, it can be used in nuclear materials and nuclear energy stations. There are boron deposits with high ^{10}B isotope ratios in Turkey. The chemical properties of the boron element depend on its morphology and particle size. Micron sized amorphous boron reacts easily and sometimes intensely, whereas crystalline boron does not react easily. Boron reacting with water at high temperatures forms boric acid and some other products. The reaction of boron with mineral acids can be slow or explosive depending on the concentration and temperature and boric acid is formed as the main product (Garrett, 1998; Helvacı & Palmer, 1997). The relevant chemical and physical properties of boron are listed in Table 2.1.

Table 2.1 Chemical and physical properties of boron (Garrett, 1998; Helvacı & Palmer, 1997)

Material Properties	Specifications
Crystal Structure	Rhombohedral
Electron Configuration	$1s^2\ 2s^2\ p^1$
Electron Number (neutral)	5
Number of Neutrons	6
Number of Protons	5
Atomic Weight	10.811
Boiling Point	4275K-4002°C-7236°F
Density	2.34 g/cc @ 300K
Appearance	Yellow-Brown Nonmetallic Crystal
Heat of Vaporization	489.7 kJ/mol
Melting Point	2573K-2300°C-4172°F

About 230 naturally occurring borate minerals were identified as of 1996 and the increasing sophistication of analytical instruments, computer assistance, and crystallographic identification ensures that many new ones will be found in the future. Most of the newly reported minerals contain multiple cations or anions, are very large molecules, or have changed cation or anion proportions in large families of borates such as borosilicates, rare earths, boracites, and others. The number of nonmineral borates produced in the laboratory is also very large. The reason for this abundance is boron's ability to form boron-oxygen compounds (the borates) in many molecular and polymer forms. Its tri and tetra (negatively charged) bonded groups with oxygen can combine in a very large number of geometric combinations and polymer types. Also, the borates can combine with any cation, as well as form double or multiple salts with many other compounds. Boron readily crystallizes with silicates, and can replace aluminum or silicon in varying proportions in some minerals. However, despite these long lists, only a comparative few of the borates are important in commercial deposits (Table 2.2). This includes the hydrogen borate sassolite (H_3BO_3); the two sodium borates, borax ($Na_2B_40_7.10H_20$) and kernite ($Na_2B_4O_7.4H_2$); the calcium borates, colemanite ($Ca_2B_6O_{ll}.5H_20$), inyoite ($Ca_2B_6O_{ll}.13H_20$), and priceite ($Ca_4B_{10}O_{l9}.7H_20$); the sodium-calcium borates,

ulexite ($NaCaB_5O_9.8H_20$) and probertite ($NaCaB_5O_9.5H_20$); the magnesium borates, szaibelyite, inderite or kurnakovite and pinnoite; the magnesium-calcium borate, hydroboracite; the borosilicates datolite and ludwigite; and the magnesium chloride double salt, boracite. Each of these minerals is being, or has been, mined and processed on a commercial scale (Garrett, 1998).

Table 2.2 Some commercially available boron minerals (Garrett, 1998)

Mineral	**Formula**	**%**		**Location**
		B_2O_3	**H_2O**	
Colemanite	$Ca_2B_6O_{11}.5H_2O$	50.8	21.9	Turkey, USA, Mexico
Ulexite	$NaCaB_5O_9.8H_2O$	43.0	35.6	Turkey, USA, Argentina, Chile, Peru, Tibet
Tincal, Borax	$Na_2B_4O_7.10H_2O$	36.5	47.2	Turkey, USA, Argentina
Tincalconite	$Na_2B_4O_7.5H_2O$	47.8	30.9	Turkey, USA, Argentina
Kernite	$Na_2B_4O_7.4H_2O$	50.9	26.4	USA, Argentina
Pandermite, priceite	$Ca_4B_{10}O_{19}.7H_2O$	49.8	18.1	Turkey
Hydroboracite	$CaMgB_6O_{11}.6H_2O$	50.5	26.2	Russia, Argentina
Inyoite	$Ca_2B_6O_{11}.13H_2O$	37.6	42.2	Kazakhstan, Russia, Argentina
Probertite	$NaCaB_5O_9.5H_2O$	49.6	25.6	USA
Sassolite	H_3BO_3	56.3	43.7	Italy
Boracite	$Mg_3B_7O_{13}Cl$	62.2	-	Turkey
Meyerhofferite	$Ca_2B_6O_{11}.7H_2O$	46.7	28.2	Turkey

All borates contain combinations of the three (triangular) or four-bond (tetragonal; negatively charged) B-O structures. Boron always maintains its valence state of +3, so the tetrahedral bonding has a negative charge and seeks attachment to a cation. Cations may occasionally replace hydrogen on some of boron's OH groups at very high temperatures. Hydrogen bonding is also especially strong with the borates, forming many hydrates, double salts and polymers. In all cases except for the comparatively few mono and diborates, the B-O grouping tends to form one or more

ring structures, allowing electrons to resonate around the ring, thus strengthening its bonds (Figure 2.1).

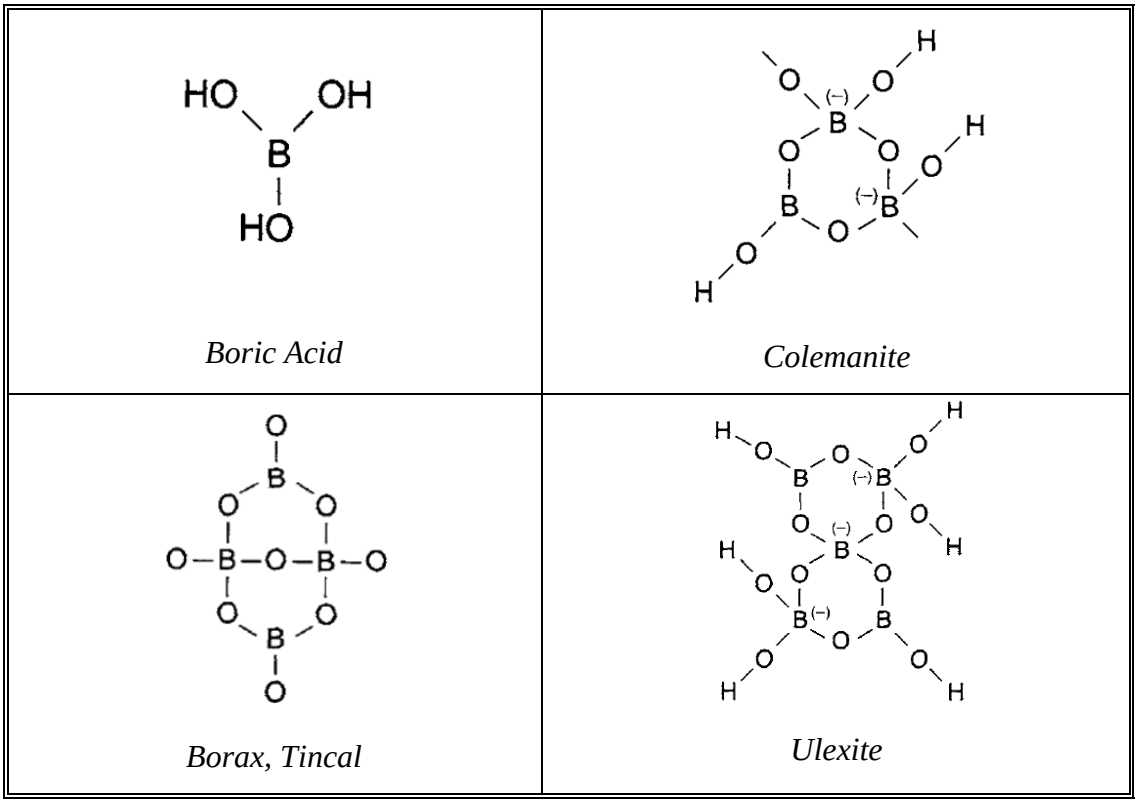

Figure 2.1 Crystal structure examples of borates (Garrett, 1998)

Boron compounds are used in over 100 industries for the production of borosilicate glass, enamels, leather, detergents, cosmetics, insulation and textile grade fibers, fire retardants, artificial fertilizers, insecticides, disinfectants and drugs. Boron compounds are also used as an alternative energy source, and new application fields of boron continue to be discovered. The world boron consumption is greater than 1.5 million tons/year in terms of boron oxide and it increases gradually. (Domenech-Carbo et al., 2004; Özdemir & Kıpçak, 2010). For nearly twenty years, Turkey has been the major source of boron mineral for direct use in the United States and Europe (IHS, 2011).

Consumption of borates in borosilicate glasses was the second-largest end use in 2010. Boron added to glass in amounts between 4% and 15% reduces the viscosity of the melt, assists with fiber formation during processing, allows for improved specific

optical properties, increases resistance to aqueous or chemical attack, enhances certain mechanical properties, and reduces the thermal-expansion coefficient and thermal-shock resistance of the product (IHS, 2011).

In order to summarize, Turkey is on the top of the list of total boron reserve with a share of nearly 73%. When total boron reserve of the world and current consumption values are considered, it is seen that there will not be any deficit in boron ore needs in the world for long years. The known boron deposits are mainly located at Kırka/Eskişehir, Bigadiç/Balıkesir, Kestelek/Bursa and Emet/Kütahya. The most common boron ores in terms of reserve in Turkey are tincal ($Na_2O.2B_2O_3.10H_2O$) and colemanite ($2CaO.3B_2O_3.5H_2O$). The important tincal deposits of Turkey are located in Kırka and important colemanite deposits are located around Emet and Bigadiç. In addition to this, a small reserve of ulexite is found in Bigadiç and ulexite is obtained as a side-product in Kestelek from time to time (Boren, 2013). The production plants in Turkey under management of Eti Mine are Bandırma Boron Works, Emet Boron Works, Bigadic Boron Works and Kırka Boron Works (Figure 2.2).

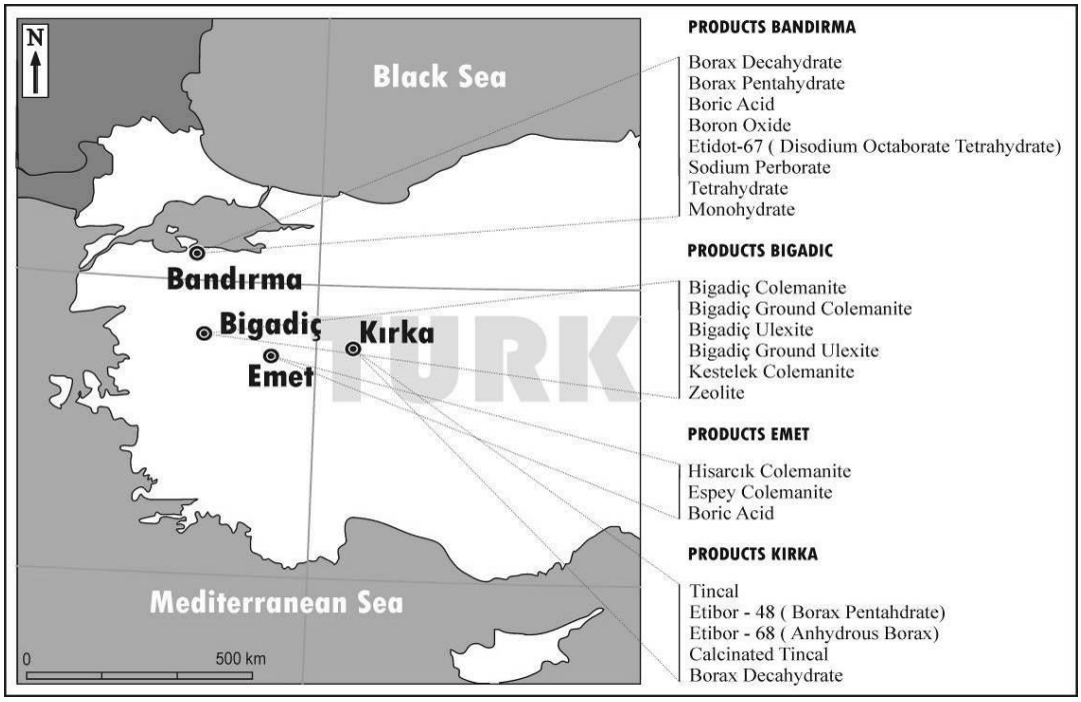

Figure 2.2 Boron production plants of Eti Mine and list of products in Turkey

There are many other researches in literature including the thermal treatment, beneficiation, tailing utilization, characterization and market evaluation of boron products and derivatives. Some of these researches are mentioned below as examples of serious and continuous work on extending the area of usage for boron compounds and derivatives.

Batar et al. (1998) stated that the majority of boron minerals exist in the hydrated form and lose their water of crystallization upon heating to a certain temperature. Boron minerals such as colemanite ($Ca_2B_6O_{11}.5H_2O$), ulexite ($NaCaB_5O_9.8H_2O$) and borax ($Na_2B_4O_7.10H_2O$) undergo different alterations when subjected to temperatures up to 500ºC. Thermal treatment of boron minerals usually results in some structural modifications due to formation of micropores and the resultant expansion of the crystal matrix upon development of uneven distribution of stresses. Such internal stresses subsequently induce fractures and in some cases fragmentation of the crystals. For instance, when heated to the decomposition temperature, colemanite decrepitates into a fine powder of 80% less than 0.2 mm (Batar et al., 1998; Çelik et al., 1994).

In a research by Yılmaz (2006), froth flotation technique was applied to wastes of Eti-Bor A.S. boron processing plant at Bigadic in Turkey and a recovery of tailings was partially achieved. At first step, traditional flotation tests were carried out on grounded and sieved tailing samples in associated with various depressant and collector agents. In this step, no recovery has achieved, but it was established that oleic acid collector is suitable for oxide minerals (Yılmaz, 2006).

Two boron minerals; colemanite and pandermite were studied as well as the solubility of calcined products derived from these minerals in pure water, acetic acid, hydrochloric acid and sulphuric acid solutions by Gedikbey et al. (2004). The concentrations of acid solution were 0.025M, 0.05M and 0.075M for each acid. The solubilities of colemanite and pandermite in aqueous environment were detected as 22.09% and 10.02% respectively. The solubilities of colemanite and pandermite in

water that these minerals were calcined at 500°C are detected, as 52.34% and 48.41% respectively (Gedikbey et al., 2004a).

Buluttekin (2008) stated that, Turkish boron trade depends on pure boron product export which is sold at a very low price. While Turkey exports pure boron to the developed countries; she leaves the advantageous and high valued boron products market of borax, sodium perborate to the USA. The average price of World "boron products" is 317 USD$ while pure boron is 198 USD$. Turkey has produced 33% of the World production while USA has produced 27% since 2004. Despite this, while Turkey earned 250 million USD$ export income of the 1.5 billion USD$ market, USA earned 650 million USD$. By aiding and confronting local potential sectors in boron market and with the corporation of universities, research institutes and industry conducting research and development activities, Turkey should have a national boron policy, focused on increasing market share and base on increasing the production capacity of the accretion valued ground boron products, aiming to increase the product variety by developing boron technologies and new production methods (Buluttekin, 2008). Another detailed investigation on boron economics of Turkey was conducted by Kahraman (Kahraman, 2010).

In a study by Yersel et al. (2010), the influence of boron derivatives such as calcined tincal concentrate, boric acid and borax pentahydrate on the physical properties and microstructure of the standard floor tile body composition was investigated. Fired strength, water absorption, and shrinkage tests on the incorporated ceramic bodies and reference body were carried out. Microstructures of sintered floor tiles were examined by a scanning electron microscope. The results revealed that boron additives to the ceramic body enhanced the physical properties of the tiles (Yersel et al., 2010).

Ediz & Özdag (2002) stated that, boron minerals have a wide and intensive usage in modern technology in the fertilizer, pharmacy, detergent and nuclear industries. This important and indisputable position of boron minerals will continue in the future. In their research, a new technique for processing boron ores and wastes was

developed. For this purpose, a helical transporter, which is used for solid-liquid separation and material conveyance in industrial applications, was re-designed and manufactured. With the single stage helical transporter, direct processing of tincal ores (-25 mm), fed to the concentrator in the Etibor Kırka Mine, and the wastes from the concentrator was carried out. The optimum operational parameters of the transporter were determined by testing under various processing conditions. After the tests with tincal ores were carried out under optimum conditions, B_2O_3 solubility of 88.66% was obtained. The maximum B_2O_3 solubility in clay waste was 87.83% (Ediz & Özdag, 2002).

In another work, two boron minerals; tunellite ($Sr0.3B_20_3.4H_20$) and ulexite ($Na_20.2Ca0.5B_20_3.16H_20$) were studied as well as the solubility of calcined products derived from these minerals in pure water, acetic acid, hydrochloric acid and sulphuric acid solutions. The concentrations of acid solution were 0.025M, 0.05M and 0.075M for each acid. The solubilities of tunellite and ulexite in aqueous environment were detected as 46.52% and 61.15% respectively. The solubilities of tunellite and ulexite in water that these minerals were calcined at 500°C and detected as 81.50% and 55.19% respectively (Gedikbey et al., 2004b).

Another study was directed towards determining the usability of clay and fine wastes (CW and FW) of boron from the concentrator plant in Kırka (Turkey) as a fluxing agent in production of red mud (RM) brick by Kavas (2006). Both laboratory studies on the characterization of materials and industrial-scale tests for production of bricks were carried out. CW and FW, which have similar chemical composition but include different types and amounts of oxides, were added in amounts of 5, 10 and 15 wt% to RM, which consists of high amounts of Fe_2O_3, Al_2O_3, SiO_2 and alkalis. Six different sets of the samples have been produced and fired at 700, 800 and 900^oC. Dry shrinkage of green body, bending and compressive strength, firing shrinkage, water absorption, frost resistance and harmful magnesia and lime tests on heat-treated bodies have been performed. The mineralogical and mechanical tests showed that usability of boron wastes as a fluxing agent in the production of RM

bricks was possible. In addition, the samples obtained by adding 15wt% CW and FW to RM showed the best mechanical characteristic (Kavas, 2006).

2.1.1 Fabrication Process of Tincal Concentrate and Boron Products

A brief explanation should be necessary in tincal, tincal concentrate production and the further stages of boron product fabrication which are benefited in this research. In tincal ores, two different flowsheets are applied. The flow sheet in Figure 2.3, attrition scrubbing to the ore is followed by classification by the use of screens and cyclone. Then concentrate is produced in -6 mm +0.1 mm fraction. As Na borate is soluble in water so that all the water is kept at near saturation with boron. At Kırka Concentration Plant, 1.2 million tons of tincal ore, having 26% B_2O_3 is treated to produce a concentrate of 34.5% B_2O_3 content with a total of 800,000 tons per year (Acarkan et al., 2005; Onal & Burat, 2008).

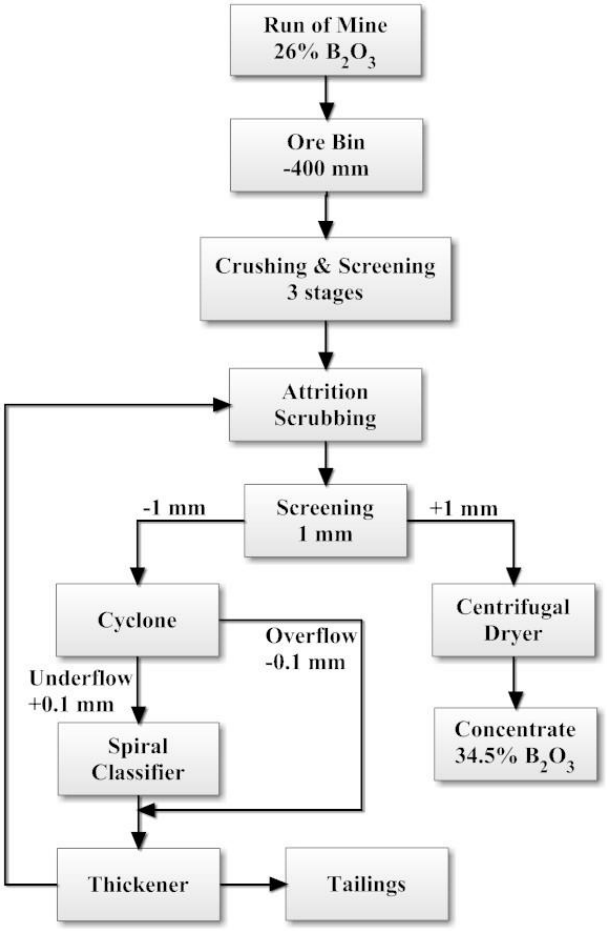

Figure 2.3 Flowsheet of Kırka tincal concentration plant (Onal & Burat, 2008, revised)

In another process, where the effect of environmental impact is minimized, tincal ore is solubilized and solution is sent directly to produce boron salts. Solid waste is stored in a suitable area as indicated in Figure 2.4. In solubilization plant, the tincal ore having 26% B_2O_3 is treated at 200,000 tons per year (Acarkan et al., 2005; Onal & Burat, 2008).

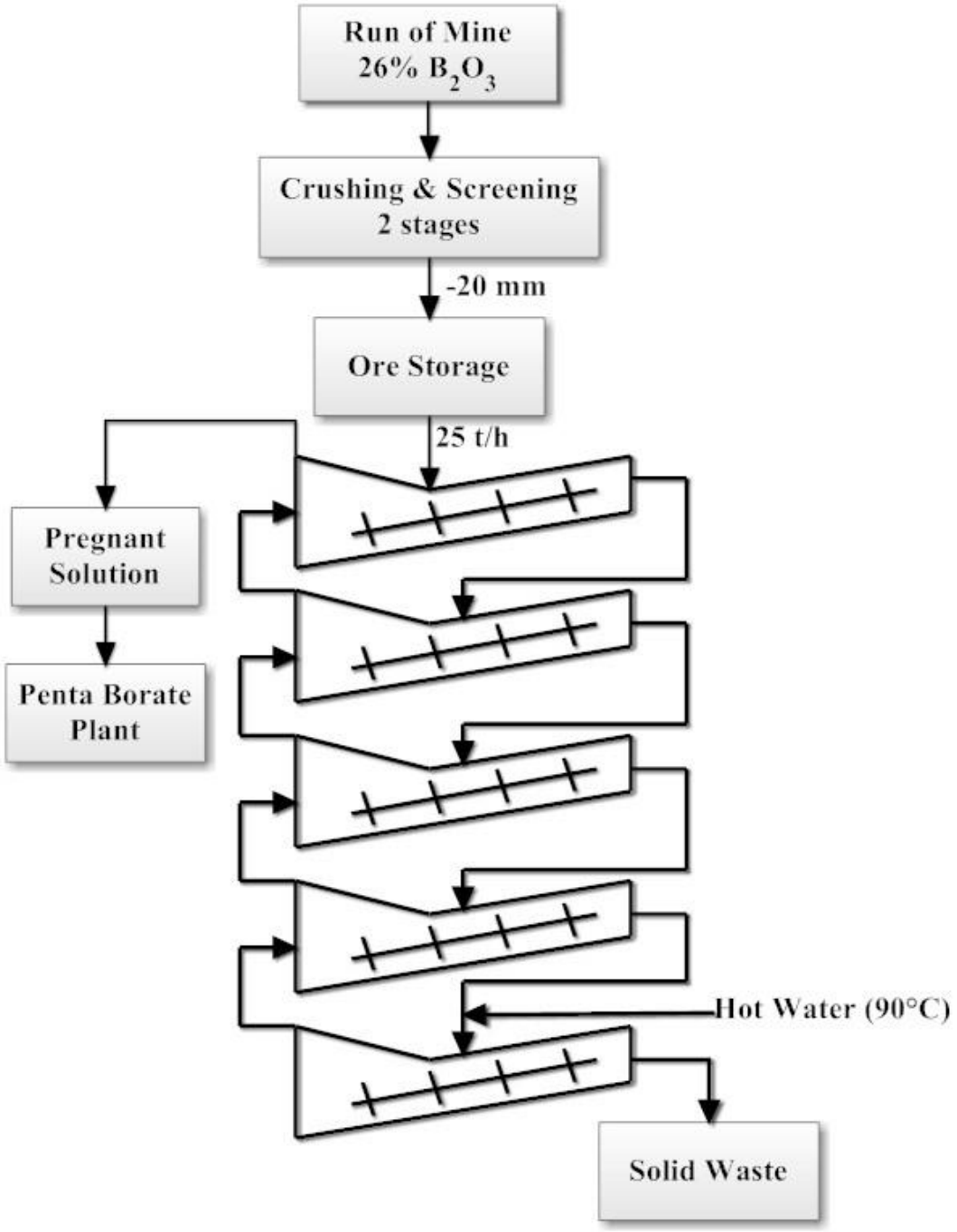

Figure 2.4 Flowsheet of Kırka solubilazation plant (Onal & Burat, 2008, revised)

The fabrication process of borax pentahydrate, decahydrate and anhydrous borax from tincal concentrate is illustrated in Figure 2.5.

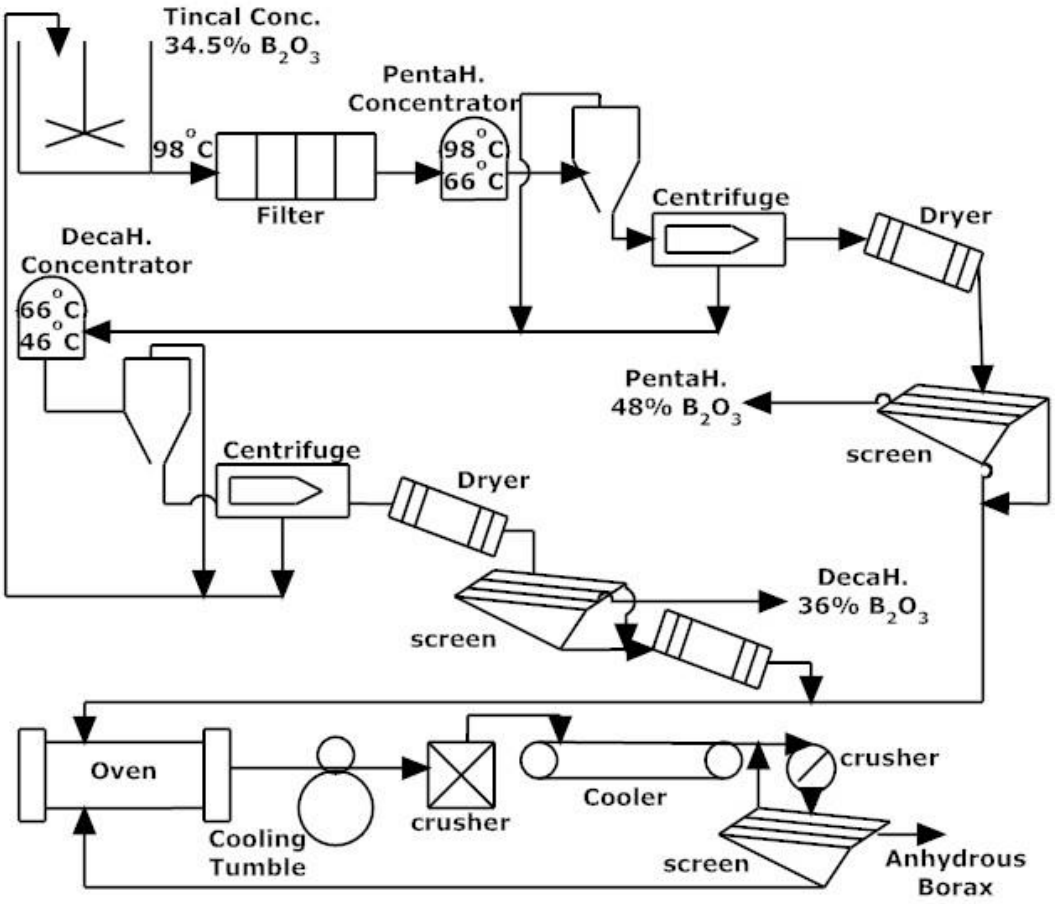

Figure 2.5 Production flowsheet of borax pentahydrate, decahydrate and anhydrous borax (Batar & Aytekin, 2012; revised)

2.2 Production Methods of Boron Carbide and Previous Studies

Boron carbide is an advanced ceramic material. It occupies a significant place in the group of most important nonmetallic hard materials. It is the third hardest material known and hardest material produced in tonnage quantities. Its high melting point (2450^{o}C), high modulus, large neutron capture section, low density, chemical inertness, outstanding thermal and electrical properties make boron carbide a strong candidate for high technology applications. In comparison with other refractory materials, such as diamond, silicon carbide, boron nitride, alumina, relatively little effort has been put into studying and developing boron carbide deposition methods. This has started to change in recent years due to the need of high quality boron

carbide based materials especially in microelectronics, nuclear, military, space and medical industries (Roy et al., 2006; Sezer & Brand, 2001).

In 1883, Joly reported the preparation of boron carbide and identified it as B_3C and then Moissan reported the production of B_6C. The stoichiometric formula of B_4C was identified in 1934. The boron carbide has a rhombohedral structure with 12-atom icosahedral clusters which are linked by direct covalent bonds and through three-atom intericosahedral chains (Figure 2.6). Boron carbide has single phase throughout the entire range. Its high wear and impact resistance and low specific weight makes it suitable for application in ball mills, nozzle, wheel dressing tools, wire drawing dies, rocket propellant, light weight armor plates, etc. (Alizadeha et al., 2004; Jung et al., 2004; Khanra, 2007; Sezer & Brand, 2001; Tokmak, 2004). The interest in boron carbide microelectronic devices and high-temperature thermo-electronic conversion devices started in the 1950's (Sezer & Brand, 2001). It can also be used as a reinforcing material for ceramic matrix composites. It is an excellent neutron absorption material in nuclear industry due to its high neutron absorption coefficient (Reynaud, 2010; Sinha et al. 2002). The relevant physical properties of boron carbide are listed in Table 2.3.

Table 2.3 Physical properties of boron carbide (Reynaud, 2010)

Material Properties	**Values**
Melting Point	2450-2750 K
Boiling Point	3770 K
Bulk Density	2520 kg/m^3
Hardness (Knoop, 100g)	2900-3580 kg/mm^2
Young's Modulus	450-470 GPa
Shear Modulus	180 GPa
Electrical conductivity	140 Ωm^{-1}
Thermal conductivity	29-67 W/(m-K)

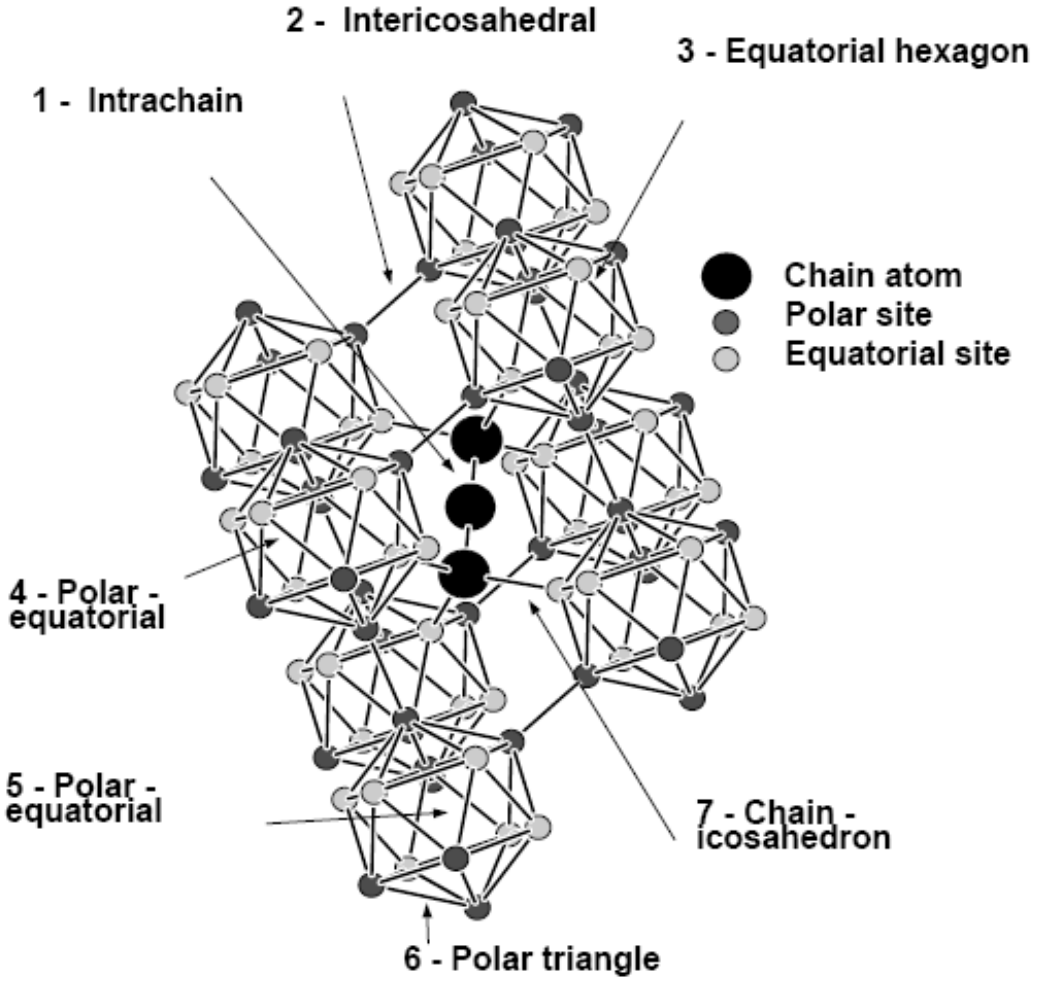

Figure 2.6 Atomic structure of boron carbide (Reynaud, 2010)

There are several different production methods of boron carbide in literature, some of which are already applicable in industry. A brief summary of these researches are compiled below.

Boron carbide can be fabricated by several high temperature methods. These methods can be grouped in the following major categories (Kumar, 2006; Thevenot, 1990):

- ✓ Boron carbide synthesis using virgin elements
- ✓ Boron carbide synthesis by magnesiothermic route
- ✓ Boron carbide synthesis by gaseous route
- ✓ Boron carbide synthesis by carbothermal reduction

Elemental route of B_4C production gives the best quality product. Boron, in its elemental form, can be synthesized by reduction of boron halides with H_2, reduction of boron halides with Zn or reduction of boron oxide with Mg (White et al., 1993). The reaction between amorphous boron and carbon is kinetically fast compared to crystalline form. Initially the raw material is thoroughly mixed in ball mill to get homogeneous product. The reaction between boron and carbon is completely diffusion controlled. High temperature, of the order of 1800K, is required for the preparation of boron carbide. Due to the susceptibility of boron for oxidation, the reaction is carried out under vacuum of the order of 10^{-3} mbar.

Soh et al. discovered a method of producing fine particle size boron carbide by heating a mixture of boron oxide, carbon and magnesium. Overall reaction can be written as:

$$2B_2O_3 + C + 6Mg \rightarrow B_4C + 6MgO \qquad (2.1)$$

Oxidation of Mg is strongly exothermic and the heat liberated during the oxidation is used for the reaction to form boron carbide from boric acid. The boron carbide, produced by the this method, is unsatisfactory for high purity applications because the boron carbide is contaminated with the magnesium, the starting material, and even after repeated digestions with hot mineral acids the magnesium is difficult to remove (Soh et al., 1999).

Very fine powders of boron carbide have been produced by vapor phase reactions of boron compounds with carbon or hydrocarbons, using laser or plasma energy sources. These reactions tend to form highly reactive amorphous powders. Due to their extreme reactivity, handling in inert atmospheres may be required to avoid the contamination by oxygen and nitrogen. These very fine powders have extremely low bulk densities (Kumar, 2006).

Pulse laser technique is used for the synthesis of boron carbide crystallite encapsulated in graphite particles via chemical vapor deposition of $C_6H_6 + BCl_3$ gas

mixture. Gas mixture consisting of C_6H_6 + BCl_3 or C_6H_6 + CCl_4 is introduced into the pyrex glass reactor chamber which is further connected to a vacuum system. Before the introduction of gas mixture into the reactor chamber, it is first baked out. Raw material is then irradiated with laser which is focused with a lens. The reaction gets completed because of intense laser pulse (Reynaud, 2010).

Carbothermal reduction of boric acid has scientific and economic advantages over the other methods of boron carbide production. Powders prepared by carbothermic reduction have excellent morphology and surface characteristics (Reynaud, 2010). In carbothermal reduction process, boric acid or boron oxide as a source of boron and carbon active or petroleum coke as reducing agent is used as the main raw material. Depending upon the method or process adopted, there are many ways of producing boron carbide such as using boron oxide and carbon black, using arc furnace process and resistance-heating furnace process.

In a previous research, for carrying out the carbothermic reduction reaction, a reactive mixture of a boric oxide source such as boric acid and a carbon source such as carbon black was prepared by mechanically mixing them together. This reactive mixture was then heated at a reaction temperature for a sufficient length of time to form B_4C. The temperature of firing the reactive mixture was in the range of 1700-2100^oC. The particle size of boron carbide ranged anywhere between 0.5 and 150 μm with no control of particle size distribution (Treacy et al., 1996).

In an arc furnace trial, the reactant used for the process was a mixture of old mix and fresh charge. Old mixture was from the previous run and differs from the fresh charge in that some part of it is partially converted B_4C material (Treacy et al., 1996). In other words, the old mix has some boron compounds having less oxygen than B_2O_3 and some boron carbide having more carbon than B_4C. The arc furnace in comparison to resistance furnace requires only 59% of the power. Production rate in this method is much greater than that of the resistance furnace. The major drawback of this process is that the control of the temperature above 2300K is not possible. This leads to the vaporization of boron from the system affecting the B/C ratio.

Therefore, more than 65% of excess B_2O_3 was used to compensate for the loss of boron during the process (Kumar, 2006; Thevenot, 1990).

Industrially, boron carbide on large scale is produced by carbothermal reduction process using boric acid and petroleum coke in graphite resistance-heating furnace (Reynaud, 2010). Operation and design wise this furnace is similar to the Acheson furnace which is used for SiC synthesis. Resistance heating furnace is cylindrical in shape, with a graphite electrode as the heating element. Since, graphite has a very high melting point so it is an ideal choice for heating electrode in the resistance heating furnaces. Boron carbide reaction is highly endothermic reaction; therefore, the heat generated due to resistance heating is responsible for heating the charge which surrounds the electrode. Once the reaction temperature is reached, the raw material reacts to form B_4C (Kumar, 2006). The overall carbothermal reduction reaction is described by;

$$2B_2O_3\ (l, g) + 7C\ (s) \rightarrow B_4C\ (s) + 6CO\ (g)\ \Delta H^o = 1812\ kj/mol \quad (2.2)$$

In a study of Khanra (2007), boron carbide (B_4C) powder has been produced by carbothermal reduction of boric acid–citric acid gel. Initially a gel of boric acid–citric acid was prepared in an oven at 100°C. This gel was pyrolyzed in a high temperature furnace over a temperature range of 1000-1800°C. The reaction initiation temperature range for B_4C formation was determined by thermal analysis. The optimal pyrolysis temperature of B_4C synthesis was investigated. During pyrolysis, the evaporation of boron-rich phases resulted in presence of free carbon in B_4C powder. A mixture (10 g) of boric acid and citric acid (molar ratio 12:7) was dissolved in distilled water and then the solution was heated in an oven at 100°C for 3h. The solution became golden yellow gel, which was crushed into powder for pyrolysis. The dissociation reactions are given below;

$$2H_3BO_3 \rightarrow B_2O_3 + 3H_2O \quad (2.3)$$

$$C_6H_8O_7.H_2O \rightarrow 3C + 5H_2O + 3CO \quad (2.4)$$

The overall pyrolysis reaction of gel was written as;

$$2B_2O_3 + 7C \rightarrow B_4C + 6CO \quad (2.5)$$

The B_4C powder can be produced by carbothermal reduction of gel material prepared from boric acid–citric acid mixture. During pyrolysis, the B_4C formation started over the temperature range of 1050-1100°C. The optimum pyrolysis temperature of B_4C was found to be at 1600°C. The generation of fine B_4C powder was confirmed from the SEM, particle size analysis and TEM studies (Khanra, 2007).

Similarly, Alizadeh et al. (2004) have studied carbothermic reduction process and stated that carbothermic reduction process is an economic method to produce boron carbide powder. Boric acid as a source of boron, and carbon active and petroleum coke as reducing agents were used. Mixtures of boric acid and carbon bearing material with a particle size of less than 44 mm were placed in a graphite crucible and heated under a flow of argon atmosphere in a tube furnace to 1400-1550^{o}C for 1 to 5h. It was found that the optimum weight ratio of boric acid to carbon bearing material was 3.5 and 3.3 for petroleum coke and carbon active, respectively. Boron carbide powder was synthesized from elemental boron and carbon directly. The high cost of these elements made this method economically unattractive (Alizadeha et al., 2004).

Jung et al. (2004) also studied the carbothermic reduction process and offered a modified carbothermal reaction to minimize free carbon residue in the boron carbide (B_4C) powder. Because of boron loss in the form of B_2O_2 gas during the carbothermal reaction of the stoichiometric starting composition, the final B_4C powders contained carbon residues. Thus, an excess B_2O_3 was used in the reaction to compensate the loss and to obtain stoichiometric powders. Parameters of the process for obtaining the carbon free B4C powder by the carbothermal reduction have been determined using X-ray diffraction analysis and scanning electron microscopy (Jung et al., 2004).

B_4C ultrafine powders were successfully synthesized at 450^oC through a new co-reduction route by Shi et al. (2003). The synthesis was carried out in an autoclave by using BBr_3 and CCl_4 as the reactants and metallic Na as the co-reductant. The X-ray powder diffraction pattern and Raman spectra indicated the formation of B_4C (Figure 2.7). A low temperature route to crystalline B_4C was reported and described as (Shi et al., 2003);

$$CCl_4 + 4BBr_3 + 16Na \rightarrow B_4C + 4NaCl + 12NaBr \quad (2.6)$$

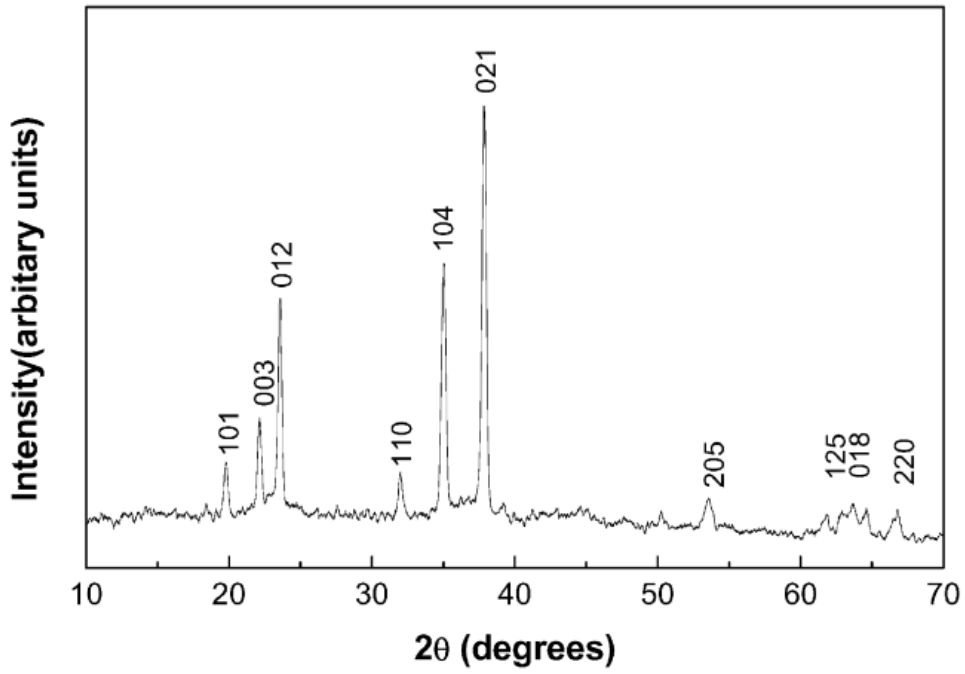

Figure 2.7 XRD patterns of the B_4C sample (Shi et al., 2003)

In another study, boron-doped amorphous carbon powders were produced at 1000^oC and under one atmosphere of pressure using a simple tube furnace by Burgess et al. (2008). Doping was monitored using XRD and Raman spectroscopy, and boron content was confirmed by XPS. The XPS data showed a peak at 188 eV which coincides with the B1s energy when bound to carbon (Burgess et al., 2008).

The plasma-enhanced chemical vapor deposition (PECVD) of boron carbide was investigated on quartz glass and alumina substrates from a gas mixture of BCl_3, H_2, and CH_4 in inductively coupled plasma (ICP) medium produced by a radio frequency (RF) discharged onto the gases passing through a tubular reactor under atmospheric

pressure by Eroglu et al. (2003). A thin solid boron carbide coating with a gray color was deposited on both substrates. The results of XRD revealed that the major solid phase formed in the coating material was b-rhombohedral B_4C. The SEM analysis (Figure 2.8) showed that the surface homogeneity increased with an increase in the exposure time, and different boron carbide structures were formed at different RF powers and exposure times (Eroglu et al., 2003).

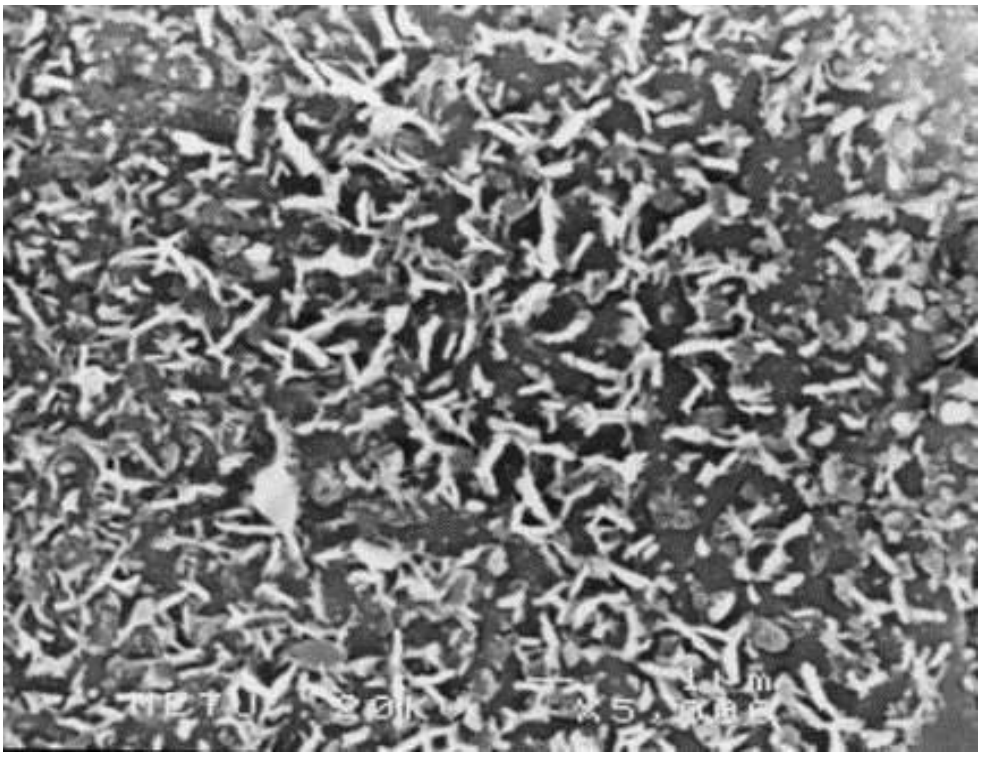

Figure 2.8 SEM micrographs of boron carbide coating on quartz glass, 1000x (Eroglu et al., 2003)

Ion beam sputtering deposition technique was employed to prepare boron carbide films at different substrate temperatures by Chen et al. (2000). The structure and mechanical properties of the B_4C films have been studied over the substrate temperature range of 50 to 350^{o}C in order to study the temperature effect. Infrared spectroscopy, Auger electron spectroscopy, X-ray diffraction and X-ray photoelectron spectroscopy were used to evaluate the structural properties. The formation of B_4C was found to strongly depend on the deposition temperature. It was shown that a higher deposition temperature was beneficial for the boron carbide synthesis. Hardness of these films was also thoroughly studied by micro-indentation

facility. The hardness increased and reached a very high value of 43 GPa at a substrate temperature of 350^{o}C (Chen et al., 2000).

Sinha et al. (2002) stated that they prepared boron carbide (B_4C) powder by carbothermal process using boric acid and citric acid as raw materials. Aqueous solution of boric acid in presence of citric acid formed a stable gel under controlled pH condition. The gel on subsequent pyrolysis under vacuum yielded a precursor powder consisting of boron oxide and carbon. The precursor was heated under vacuum at 50^{o}C up to 1450^{o}C and the product obtained has been characterized by X-ray diffraction (XRD), chemical analysis, and particle size analysis and scanning electron microscopy. XRD pattern showed that the product consisted of B_4C and carbon (graphite). Presence of free carbon (11.1 wt. %) indicated the boron loss in the carbothermal reaction. Boron loss has been calculated to be 11.3 wt. % (Sinha et al., 2002).

Synthesis of boron carbides by the reduction of boron oxides with carbon and magnesium in mechanical alloying process using a planetary ball mill has been studied by Deng et al. (2006). XRD and TEM have been used to characterize the product and the results showed submicron B_4C particles were obtained at the mass ratio of ball to load about 5:1 and the mass ratio of B_2O_3:C:Mg about 10:1:11 (Deng et al., 2006).

Boron carbide was produced in a heat resistance furnace using boric oxide and petroleum coke as the raw materials by Rao et al. (2009). The product yield was very low. Heat transfer played an important role in the formation of boron carbide. Temperature at the core reached up to 2600K. Therefore, a laboratory scale hot model of the process has been setup to measure the temperatures in harsh conditions at different locations in the furnace using various temperature measurement devices such as pyrometer and various types of thermocouple. The recorded data were analyzed to understand the heat transfer process inside the reactor and the effect of it on the formation of boron carbide (Rao et al., 2009).

The oxidation kinetics of various types of boron carbides (pellets, powder) was investigated by Steinbrück (2005) in the temperature range between 1073 and 1873K. Oxidation rates were measured in transient and isothermal tests by means of mass spectrometric gas analysis. Oxidation of boron carbide was controlled by the formation of superficial liquid boron oxide and its loss due to the reaction with surplus steam to volatile boric acids and/or direct evaporation at temperatures above 1770K. The overall reaction kinetics was paralinear. Oxidation was strongly influenced by the thermohydraulic boundary conditions and in particular by the steam partial pressure and flow rate. On the other hand, the microstructure of the B_4C samples had a limited influence on oxidation. Very low amounts of methane were produced in these tests (Steinbrück, 2005).

Boron carbide nanoparticles were made by Chen et al. (2004) via a reaction of boron, obtained from thermal decomposition of magnesium diboride, with multiwall carbon nanotubes at 1150^{o}C for 3h in vacuum. The size of the nanoparticles was smaller than 100 nm. The bamboo structure of the multiwall carbon nanotubes was the key to the successful synthesis of such nanoparticles. Good crystallinity was demonstrated by scanning electron microscope images and X-ray diffraction patterns. The single-crystal nature of each nanoparticle was evidenced by a high-resolution lattice image obtained using a transmission electron microscope. The single-crystal nature of each B_4C nanoparticle was well demonstrated by SEM, XRD, and TEM characterizations (Chen et al., 2004).

Sezer & Brand (2001) stated that boron carbide is an important non-metallic material with outstanding hardness, excellent mechanical, thermal and electrical properties. Its low density, high chemical inertness and neutron capture section make boron carbide an attractive material for micro-electronics, nuclear, military, space and medical applications. Boron carbide based materials has been widely deposited by chemical vapor deposition methods (CVD). Structure, properties and potential application areas of this material were also reviewed. The status of the theoretical modeling of boron carbide deposition and the developments on the experimental processes were reported (Sezer & Brand, 2001). A similar study by Liu et al. (2001)

stated besides chemical vapor deposition (CVD), laser vaporization was also established to form well-constructed carbon and boron nanoparticles (Liu et al., 2001).

The chemical vapor deposition (CVD) of boron carbide was investigated on a tungsten substrate from a gas mixture of BCl_3, H_2, and CH_4 in a dual impinging-jet reactor that was connected to an FT-IR spectrometer for on-line analysis of the reactor effluent stream by Dilek et al. (2001). During CVD of boron carbide, the formation of $BHCl_2$ was experimentally verified, and rhombohedral B_4C was formed. Conversion to boron carbide was found to increase with an increase in the BCl_3/CH_4 ratio. However, conversion to dichloroborane decreased with an increase in the BCl_3 concentration in the inlet gas stream (Dilek et al., 2001).

Boron carbide powder was fabricated by combustion synthesis (CS) method directly from mixed powders of borax, magnesium and carbon by Guojian et al. (2009). The adiabatic temperature of the combustion reaction of $Na_2B_4O_7$+6Mg+C was calculated. The control of the reactions was achieved by selecting reactant composition, relative density of powder compact and gas pressure in CS reactor. The effects of these different influential factors on the composition and morphologies of combustion products were investigated (Guojian et al., 2009).

Wang et al. (2004) achieved nano-structured B_4C by mechanical milling under hydrogen atmosphere, in which hydrogen was absorbed simultaneously. The IR measurements provided clear evidence of hydrogen trapping by boron. At elevated temperatures, molecular hydrogen and CH_4 were detected in the desorption process. With increasing milling time, the desorption behavior of molecular hydrogen and CH_4 changed substantially, which was suggested to be related to the structural change of BC_4 during the milling process (Wang et al., 2004). A similar study was also accomplished by Woodman et al. (Woodman et al., 2005).

The processing of boron carbide by pressureless sintering with and without additives to obtain dense pellets for use as neutron absorber in fast breeder reactors

was reported by Roy et al. (2006). The effect of particle size and sintering temperature on density and microstructure was studied. Pressureless sintering of boron carbide powder (0.5 mm) at 2375^{o}C yielded a pellet with a micro hardness value of 32 GPa. In the samples sintered with the addition of zirconium oxide the formation of zirconium boride (ZrB_2) was noticed (Roy et al., 2006).

Gosset & Provot (2001) studied boron carbide as a potential inert matrix. They prepared and characterized ceramic composites with B_4C to evaluate the utilization (Gosset & Provot, 2001).

B_4C matrix ceramics with different content of Al and TiO_2 were fabricated by hot-press sintering, and sinterability of B_4C matrix ceramics was investigated by addition of TiO_2 and Al in the study of Sun et al. (2009). X-ray diffraction analysis showed that in situ reaction between B_4C and TiO_2 happened, and TiB_2 was formed during sintering. Results showed that the densification rate and mechanical properties of B_4C matrix ceramics were significantly improved due to the introduction of TiO_2 and Al (Sun et al., 2009).

Polyvinyl borate (PVBO) was prepared by the condensation of poly vinyl alcohol (PVA) and boric acid, and used as a precursor for boron carbide by Yanase et al. (2009). Boron carbide powder was synthesized by the pyrolysis of the PVBO precursor in air at 600°C for 2h, followed by heat treatment in air flow at 1300°C for 5h. Pyrolysis of the PVBO precursor resulted in submicron-size particles of B_2O_3 dispersed in a carbon matrix (Yanase et al., 2009).

Laser physical vapor deposition was used to deposit thin films of boron carbide on Si (100) and WC–Co substrates at 550°C under different pressures of methane atmosphere by Jagannadham et al. (2009). Grazing incidence X-ray diffraction was used to identify a boron carbide phase, which exhibited weak peaks. The presence of particulates in the size range of 50nm–3μm embedded in an amorphous matrix was observed by scanning electron microscopy (Jagannadham et al., 2009).

In the study of Tavşanoglu et al. (2010), boron carbide powders were obtained from the carbothermal reduction of boric acid in a graphite resistance furnace at 2000ºC (Figure 2.9). The powder thus obtained was hot pressed in pure nitrogen atmosphere with 100 MPa applied force at 2100°C for 15 minutes to obtain boron carbide (Tavşanoglu et al., 2010).

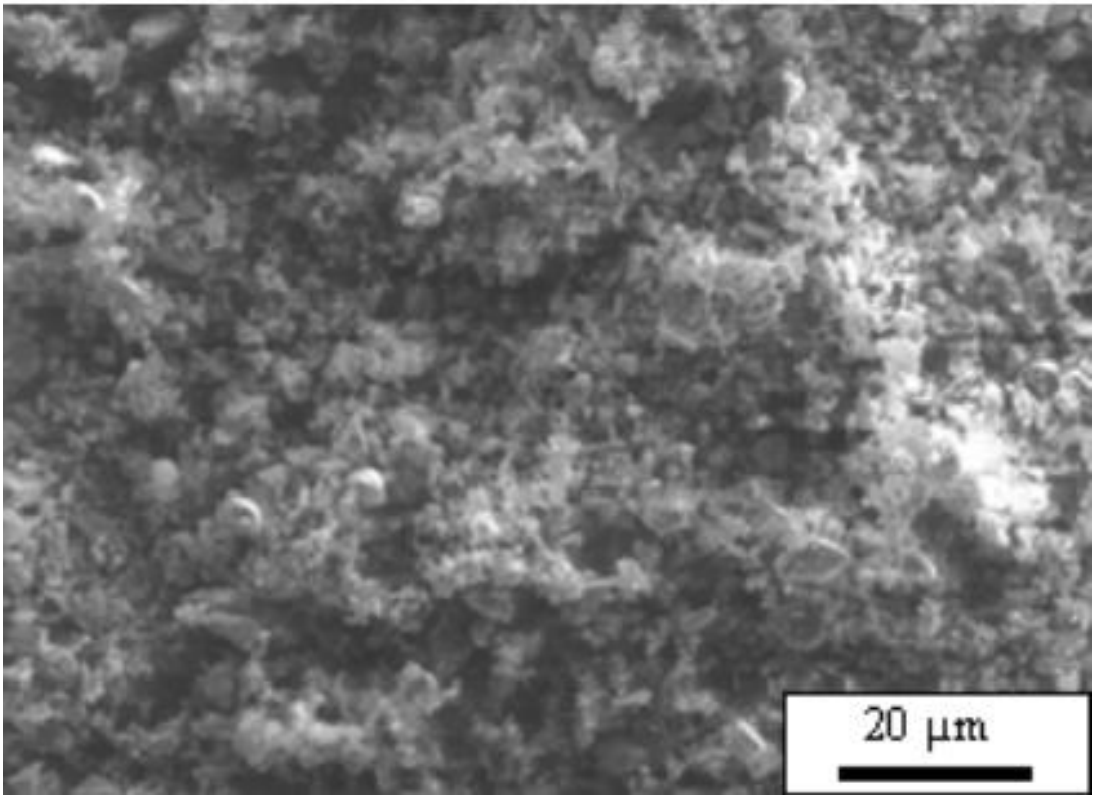

Figure 2.9 SEM of boron carbide powders (Tavşanoglu et al., 2010)

The production of boron carbide nanoparticles was investigated in a conventional high temperature furnace reactor by Chang et al. (2007). The reaction was carried out by heating a mixture of amorphous carbon and amorphous boron at 1550^{o}C to efficiently obtain a quantity of B_4C. Scanning electron microscopy studies showed the average size of B_4C particles was 200 nm, ranging from 50 nm to 350 nm. X-ray diffraction transmission electron microscopy and electron diffraction studies indicated that the prepared nanoparticles were crystalline B_4C with a high density twin structure (Chang et al., 2007).

B_4C-TiB_2 composite powders have been synthesized with the temperature of 1650-1800^oC by carbothermal reduction process using boron acid, carbon black and TiO_2 powder as the starting materials in a study by Pei & Xiao (2009). XRD and EDS results show that the composite powders are composed of B_4C and TiB_2. The boron carbide powder contained 78.03% of B and 21.75% of C by weight (Pei & Xiao, 2009).

The mechanical properties of particulate-reinforced metal-matrix composites based on aluminum alloys at high temperatures were studied by Onoroa et al. (2009). Boron carbide particles were used as reinforcement. All composites were produced by hot extrusion. The tensile properties and fracture analysis of these materials were investigated at room temperature and at high temperature to determine their ultimate strength and strain to failure. The fracture surface was analyzed by scanning electron microscopy. B_4C particles provided high stability in the aluminum 6061 and 7015 matrixes in the fabrication process, heat treatments and the temperature testing that were considered (Onoroa et al., 2009).

Boron carbide whiskers and platelets have been synthesized via a carbothermal vapor–liquid–solid (VLS) growth mechanism starting with B_2O_3 and carbon black as sources of boron and carbon, respectively by Carlsson et al. (2002). The reactions were studied in the temperature range 1200-1800^oC, testing Co, Ni and Fe as catalyst metals. The best result was obtained at a synthesis temperature of 1700^oC with a reaction mixture containing B_2O_3:C:NaCl:Co in the molar ratios of 1:6:0.25:0.1 (Carlsson et al., 2002).

Hayun et al. (2009) have applied spark plasma sintering on consolidated boron carbide powder without any sintering additives. Fully dense boron carbide bodies were obtained by a short high temperature SPS treatment. The mechanical properties of the SPS-processed material, namely hardness (32 GPa), Young's modulus (470 GPa), fracture toughness, flexural strength and elastic limit were stated (Hayun et al., 2009).

In addition, a classification of ternary metal boron carbides was presented (Figures 2.10) with respect to types of phase equilibria and types of crystal structures (Rogl & Bittermann, 1999).

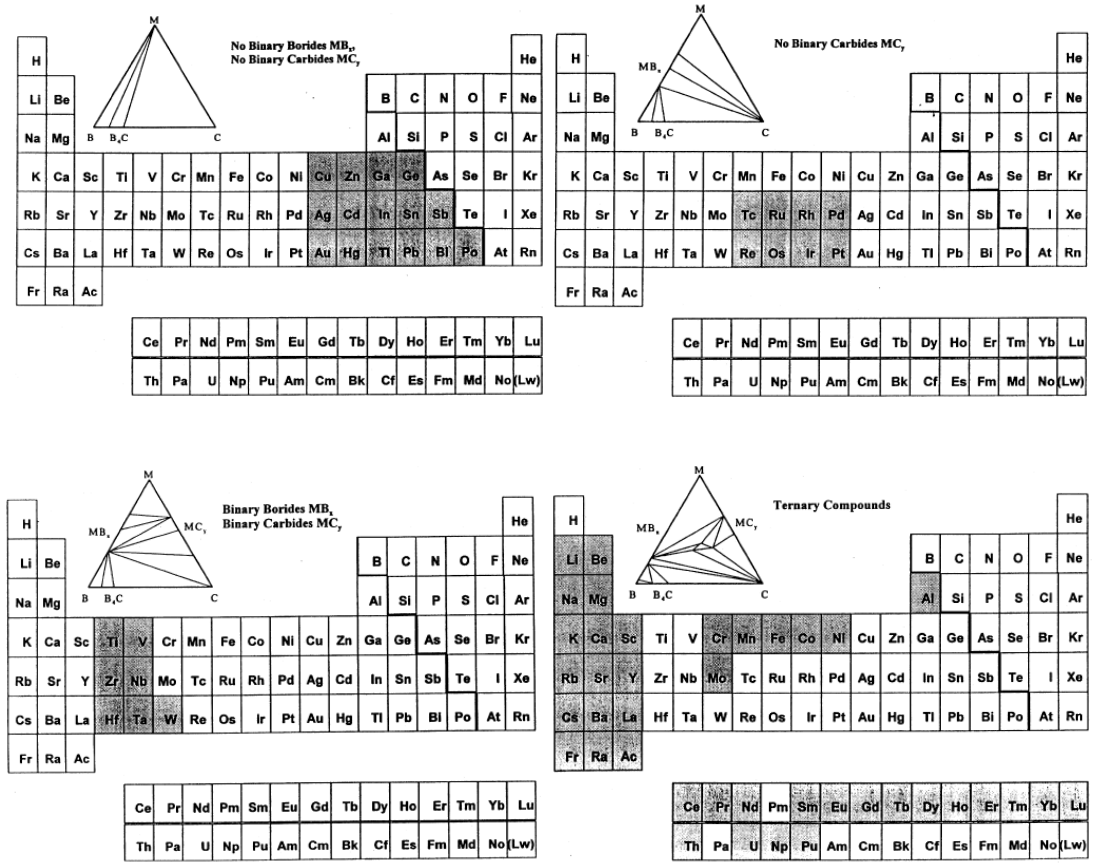

Figure 2.10 Classification of types of phase equilibria in ternary metal-boron-carbon systems; types of phase equilibria are indicated schematically by the phase triangle for each group of elements (Rogl & Bittermann, 1999).

High purity boron carbide nanowires with mean diameter of around 50 nm and with typical lengths of several tens to hundreds of micrometers were produced in thermal evaporation of $B=B_2O_3=C$ powder precursor under argon atmosphere without the presence of catalyst by Ma and Bando (2002). XRD, EELS and high-resolution transmission electron microscopy revealed the single crystallinity of these nano-wires (Figure 2.11) (Ma & Bando, 2002).

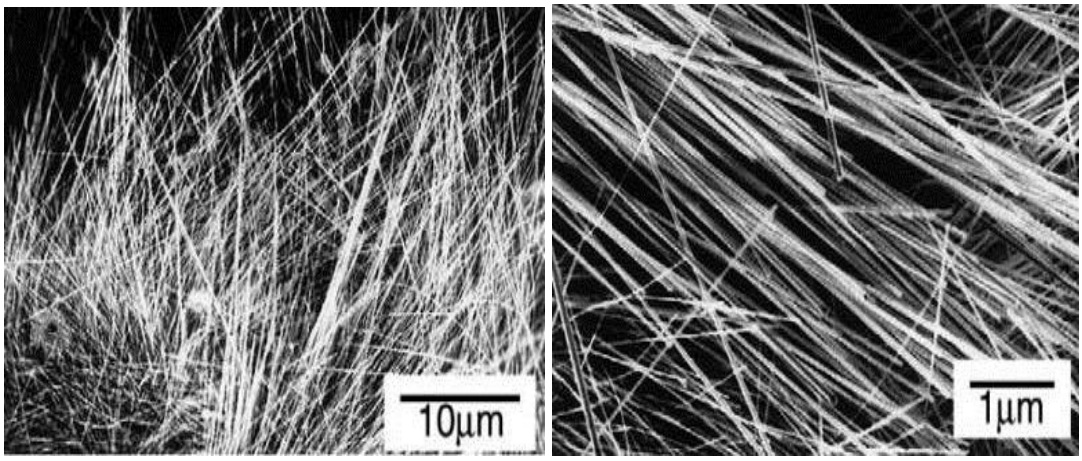

Figure 2.11 SEM images of the deposit of dense nano-wires (Ma & Bando, 2002)

2.3 Production Methods of Boron Nitride and Previous Studies

Boron nitride (BN) is a synthetically refractory material, which is widely applied due to its fascinating physical and chemical properties. BN exists in the form of hexagonal BN (h-BN), cubic BN (c-BN), turbostratic BN (t-BN), wurtzitic BN (w-BN), rhombohedral BN (r-BN), and explosive BN (e-BN) (Shi et al., 2008; Yang et al., 2005).

Hexagonal boron nitride (h-BN) is one of the key advanced ceramics with excellent solid lubricity, high thermal conductivity, good electrical insulation properties and low density 2.27 g/cm^3 (Çamurlu et al., 2009; Paine & Narula, 1990). h-BN does not display a normal melting behavior but a temperature of 2600^{o}C is given as the melting point (Eti Mine, 2003). It is stable in air up to 1000^{o}C, non-wettable and inert to many metallic melts such as Al, Cu, Zn, Fe and nonmetallic melts such as Si, B and glasses. In addition, it has high thermal shock resistance and low thermal expansion which makes it an indispensable material for refractory and crucibles in molten metal handling. h-BN is applied in high temperature lubrication and used as insulators and coolers in electronic circuits, as well as additives in other ceramics and polymers (Çamurlu et al., 2009; Ruh et al., 1992; Shi et al., 2008). It is possible to utilize h-BN in many forms including hot pressed solids, powders, fibers, in aerosols and as dispersed powders in liquid media (Rudolph, 1994). The layered structure of h-BN makes the material mechanically weak, but it has great chemical

and thermal stability. The interesting optical properties of h-BN, such as its huge exciton-binding energy, are due to its anisotropic structure. It is a promising material for its optical characteristics (Shi et al., 2008).

There are different methods to synthesis h-BN. Traditionally, h-BN has been prepared by the classical high-temperature synthesis routes and the direct combination of boron with nitrogen (Sachdev & Strauß, 1999; Shi et al., 2008).

Boron nitride is usually produced by the reaction of boric acid or boron oxide with carbon and nitrogen gas or organic carbon and nitrogen carriers. A study by Emrullahoglu et al. (2002) described the procedures and results of a laboratory scale production of boron nitride powder using carbothermic method, the tube furnace. In the first step the mixtures containing carbon and different proportions of boron oxide was shaped using dry press. Boric acid was calcined for transformation to boron oxide before addition of the mixtures. In the second step, shaped samples were reacted in the nitrogen atmosphere for two hours at the increasing temperatures from 1400^{o}C to 1500°C. In the third step; XRD analysis were applied to the sintered samples. Boron oxide amount of the mixtures and the reaction temperatures was changed to observe the effect on the boron nitride production (Emrullahoglu et al., 2002).

Formation of boron nitride by reaction of boric oxide with carbon and nitrogen was studied by Aydogdu & Sevinç (2003). It was found from the results of experiments conducted by holding B_2O_3-activated C mixtures under a flowing nitrogen atmosphere that formation of boron nitride was complete in 120 minutes at 1500^{o}C. After cleaning the reaction product from the ash of the activated carbon and from the unreacted B_2O_3 pure BN powder was obtained (Aydogdu & Sevinç, 2003).

Hexagonal boron nitride (h-BN) powder was fabricated prepared by the spray drying and calcining-nitriding technology by Shi et al. (2008). The effects of nitrided temperature on the phases, morphology and particle size distribution of h-BN powder, were investigated. The synthesized powders were characterized by X-ray

diffraction (XRD), field emission scanning electron microscope (FESEM), Fourier transformed infrared spectrum and photoluminescence (PL) spectrum. The high-energy ball-milling process following 900^{o}C calcining process was very helpful to obtain fully crystallized h-BN at lower temperatures (Shi et al., 2008).

The nucleation and growth of boron nitride films on a chromium (110) surface by thermal decomposition of borazine $(H_2BN)_3$ was investigated by low energy electron diffraction (LEED), X-ray photoelectron spectroscopy (XPS) and X-ray photoelectron diffraction (XPD) by Müller et al. (Müller et al., 2008).

Rubio et al. (1994) proposed that BN-based nanotubes can be stable and study their electronic structure. All the BN nanotubes were found to be semiconducting materials. The higher ionicity of BN was important in explaining the electronic differences between these tubes and similar carbon nanotubes (Rubio et al., 1994).

Simple methods of preparing boron nitride nanotubes and nanowires have been investigated by Deepak et al. (2002). The methods involved heating boric acid with activated carbon, multi-walled carbon nanotubes, catalytic iron particles or a mixture of activated carbon and iron particles, in the presence of NH_3. The study showed that clean BN nanotubes were obtained in high yields by heating boric acid with multi-walled carbon nanotubes in 1000-1300^{o}C range (Deepak et al., 2002).

Chen et al. (2008) studied the chemical vapor deposition growth of one dimensional nano-material on substrates that were coated with a layer of catalyst film. A green process to synthesize boron nitride (BN) nanowires directly on commercial stainless steel foils was proposed by heating boron and zinc oxide powders under a mixture gas flow of N_2 and 15% H_2 at 1100ºC, and a large quantities of pure h-BN nanowires have been produced directly on commercial stainless steel foil. The stainless steel foils not only acted as the substrate but also the catalyst for the nanowire growth. The synthesized BN nanowires were characterized by X-ray diffraction, scanning and transmission electron microscopes (Chen et al., 2008).

Several other studies including production of h-BN are managed by Çamurlu et al. (2008), Jankowski & Hayes (1998), Rebillat et al. (1997), Streletskii et al. (2009) and Tokmak (2004).

Cubic boron nitride is the hardest substance known after diamond. It is prepared by heating the h-BN to between 1400-1700^{o}C under high pressure. Unlike diamond, however, c-BN has excellent heat resistance, remaining stable up to 1370^{o}C, whereas diamond reverts to carbon at 815^{o}C. Due to its excellent thermal conductivity, like diamond, c-BN is used as a cutting tool. Today, crystalline c-BN powders are synthesized industrially, with high pressure and temperature processes, using various catalysts (Figure 2.12) (Lux et al., 1999).

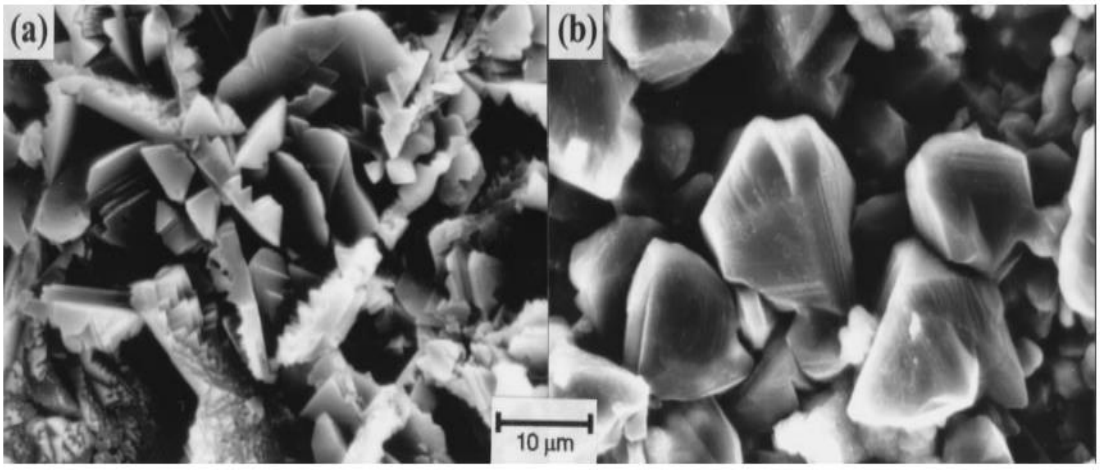

Figure 2.12 c-BN nucleation on Mo-C (a) and polycrystalline BC (b) (Lux et al., 1999)

Cubic boron nitride single crystal was synthesized using the mixture of compound B_2O_3 or element B and Li_3N by chemical reaction under high pressure and high temperature by Ji et al. (2008). The lowest conditions of cubic boron nitride formation in two systems 4.0 GPa, 1400°C or 4.5 GPa, 1450°C were obviously lower than that in Li_3N-hexagonal boron nitride system. Cubic boron nitride was nucleated directly by bond restructuring and the mechanism of crystal growth was the application of crystal seed gravitation and dissolve–precipitate effect together (Figure 2.13). Based on the experimental results, c-BN was synthesized and nucleated directly using compounds or element by chemical reactions under HPHT, and there were no h-BN and catalysts in starting materials (Ji et al., 2008).

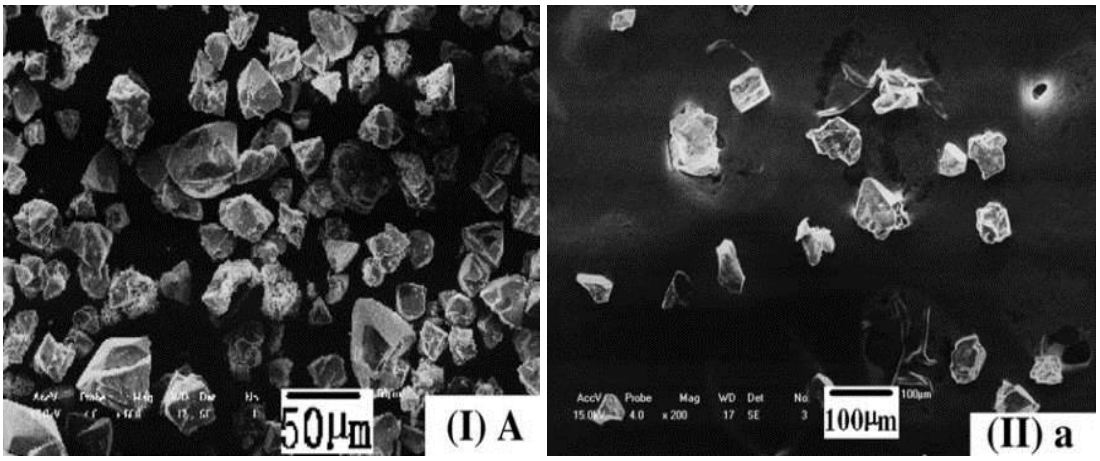

Figure 2.13 SEM images of crystals synthesized in two systems (Ji et al., 2008)

The polycrystalline cubic boron nitride (Pc-BN) was produced using c-BN and ceramic or metal binders under high pressure and high temperature by Zhao & Wang (2009). The cutting tools made from them are widely used for cutting such as hardened steels, cast iron and others (Zhao & Wang, 2009).

The other studies on c-BN production in the literature can be listed as, Deng & Chen (2006) and Singhala et al. (2005).

2.4 Production Methods of Boron Carbonitride and Previous Studies

A technology for obtaining material based on boron nitride and boron carbide powders, called boron carbonitride (BCN), was developed more than 30 years ago. Since then, boron carbonitride has been used in various areas of high temperature technology. However, its structure has not been conclusively studied so far. It has been hypothesized that in addition to the starting components (BN, B_4C), a third phase of the B-N-C compound type is present in the material. (Ulricha et al., 2005) Evidence for this comes from the properties of boron carbonitride, which differ from the properties of a mechanical mixture of the starting components, and specifically: a substantial increase in the crystal lattice parameter c of BN and a decrease in the B_4C content during reactive sintering. The sinterability of the material was also explained by formation of a ternary B-N-C compound, since the components BN and B_4C themselves were not sintered under the synthesis conditions (Grigorev et al., 2005).

The three-component boron-nitrogen-carbon (BNC) system has recently been subject to much attention, owing to BNC nanostructures having predicted higher chemical and thermal stabilities than those of carbon nanostructures. Furthermore, BNC nanotubes have the potential for application as emitters for flat panel displays, photo luminescent materials, high temperature transistors, lightweight electrical conductors and also as high temperature lubricants (Golberg et al., 2003; Han et al., 2002; Moriyoshi et al., 2001; Terrones et al., 2003)

BNC can be synthesized through different routes, including thermolysis of organic, inorganic and polymeric precursors. Arc-methods and laser ablation may additionally be used for direct synthesis of BNC, utilizing solid state sources of B, C and a N compound. The BNC synthesis method utilizing a substitution reaction where the high temperature reaction (2000 K) of carbon nanotubes performed can be managed within a stream of gaseous nitrogen or NH_3 or in the presence of B_2O_3 powder, CuO and Au_2O_3 (Blank et al., 2009; Zhi et al., 2002; Zhuge & Yamanaka, 2008).

There has been much effort to synthesize the new BCN phase by various techniques such as: nitriding of solid phase precursors at relatively high temperature, gas phase reactions using CVD techniques, solid phase's pyrolysis (Watanabe et al., 1996). However, few reports are concerning solvothermal synthesis of boron carbonitride phase. Recently, the solvothermal technique has attracted much attention and has been used to synthesis some important semiconductors (Mannan et al., 2008). In a study by Huang et al. (2004), a solvothermal reaction of $CH_3CN.BCl_3$ and lithium nitride (Li_3N) using benzene as the solvent has been successfully applied to prepare boron carbonitride at 300^oC and less than about 7 MPa by Huang et al. (2004). X-ray photoelectron spectroscopy and Fourier transform infrared spectroscopy were used to confirm their chemical composition and atomic-level hybrid. X-ray diffraction and transmission electron diffraction analysis indicated that the powders have hexagonal network structures (Huang et al., 2004).

BCN films were deposited by plasma-assisted chemical vapor deposition (PACVD) at 390°C by Aoki et al. (2008). A Si wafer, used as a substrate, was placed in a quartz reactor and source gases were introduced into the reactor. Boron trichloride (BCl_3), methane (CH_4), and nitrogen (N_2) were used as source gases. A radio frequency (RF) power of 80W was supplied to produce N_2 remote plasma by induction coupling. BCl_3 was transported with hydrogen (H_2) gas near the substrate. The substrate temperature was maintained at 390°C using an infrared lamp. The deposition time was 30 min. BCN films with thicknesses of 150–250 nm were prepared in this experiment (Aoki et al., 2008).

Transparent and hard BCN films were deposited on polycarbonate and silicon wafer by means of different radio frequency plasma-assisted chemical vapor deposition conditions with two liquid organic compounds as precursors by Ahn et al. (2003). The mechanical and optical properties of BCN films deposited were characterized by nano-indentation. The chemical composition of BCN films was determined by Rutherford backscattering spectroscopy and elastic recoil detection analysis. The influence of the plasma parameters on the mechanical and optical properties of films was described. Hard and transparent BCN films with low refractive index were deposited through low-energy and high-density ion bombardment (Ahn et al., 2003).

Wöhle et al. (1999) have given an overview of the plasma-assisted techniques for coating ceramics on polymer substrates at low temperature. Deposition of boron carbon nitride was carried out on polycarbonate substrates by a radio-frequency plasma-assisted chemical vapor deposition process using different metallo-organics as precursors. The films deposited were found to be stable and adherent under ambient conditions. The chemical composition of the layers varied in a wide range. Nearly stoichiometric BCN layers, as well as films with high carbon content, were obtained. The chemical bonding of boron, carbon and nitrogen was analyzed by X-ray photoelectron spectroscopy (Wöhle et al., 1999).

In a study by Torres et al. (2007), ternary boron-carbon-nitrogen (BCN) compounds have been prepared as nano-metric powders by low-energy ball milling, using as precursors h-BN, graphite and polypropylene micrometric powders. Different proportions of the reactants were used aiming towards the synthesis of BCN, BC_2N, BC_4N and $BCNH_2$ compositions. Ball milling induced chemical reaction between the precursors resulting in ternary BCN materials in the form of nanoparticles with an average diameter of 60 nm, as revealed by Scanning Electron Microscopy. Infrared spectroscopy confirmed the dominant hexagonal bonding structure, although with new spectral features (Torres et al., 2007).

Grigorev et al. (2005) have established that during sintering, in boron carbonitride a secondary disordered rhombohedral boron nitride phase was formed (r-BN), the primary h-BN phase was preserved with small changes in its defect level, and the amount of residual B_4C was inversely dependent on the r-BN formed. The sintered boron carbonitride was a composite consisting of particles of the primary boron nitride h-BN, binding to each other during sintering by particles of secondary r-BN, and grains of residual boron carbide which plays the role of a hardening phase. The ternary compound B-N-C was not observed upon sintering of the composite (Grigorev et al., 2005).

2.5 Elemental Boron Allotropes and Previous Studies

The production of metallic boron is traditionally achieved by reduction of boron oxide with magnesium by magnesiothermic method.

$$B_2O_3 + 3Mg \rightarrow 2B + 3MgO \qquad (2.7)$$

The mid-product (%85-95) is amorphous in structure and gets purified after grinding; treatment with HCl and HF stages (Türkiye Metalurji Mühendisleri Odaları Birliği, 2003).

γ-B_{28} is a recently established high-pressure phase of boron. Its structure consists of icosahedral B_{12} clusters and B_2 dumbbells in a NaCl-type arrangement $(B_2)^{\delta+}(B_{12})^{\delta-}$ and displays a significant charge transfer δ~0.5-0.6. The discovery of this phase proved essential for the understanding and construction of the phase diagram of boron. γ-B_{28} was first experimentally obtained as a pure boron allotrope in early 2004 and its structure was discovered in 2006. The research paper reviews recent results and in particular deals with the contentious issues related to the equation of state, hardness, putative isostructural phase transformation at ~40 GPa and debates on the nature of chemical bonding in this phase. The analysis confirms that (a) calculations based on density functional theory give an accurate description of its equation of state, (b) the reported isostructural phase transformation in γ-B_{28} is an artifact rather than a fact (Figure 2.14), (c) the best estimate of hardness of this phase is 50 GPa, (d) chemical bonding in this phase has a significant degree of iconicity (Oganov et al., 2011).

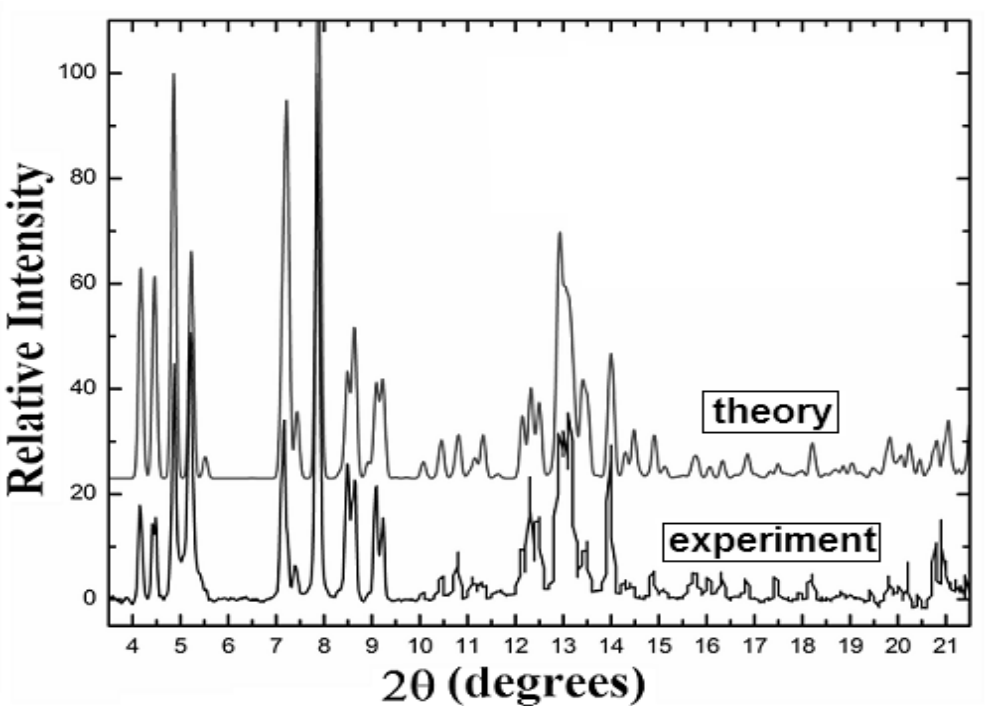

Figure 2.14 Comparison of theoretical and experimental X-ray powder diffraction patterns of γ-B_{28} (Oganov et al., 2011)

Largely due to complicated chemistry, experimental studies of boron proved to be highly non-trivial, often leading to erroneous results even with modern methods. The history of studies of boron has many additional examples of this (Oganov &

Solozhenko, 2009). Major progress has been achieved with the discovery of γ-B_{28}, but one should never forget that boron is still an element of surprise, and many aspects of its behavior remain enigmatic. Out of 16 allotropes that have been reported in the past, 4 (including γ-B_{28}) are now confirmed to be thermodynamically stable pure boron allotropes. It is hard to imagine that these four phases encompass the entire structural variability of this element, and we expect discoveries of new allotropes with new twists of chemistry and interesting physical properties. γ-B_{28}, with its relatively simple and beautiful structure, as well as attractive properties and unique chemical bonding, has attracted tremendous attention in the literature. New chemical thinking that is being produced by such studies and by this tractable material is likely to lead to future breakthroughs in chemistry and materials science (Oganov et al., 2011).

In another study, elemental boron was produced through electrowinning from potassium fluoroborate dissolved in a mixture of molten potassium fluoride and potassium chloride. The characteristics of the electrodeposited boron (raw boron) as well as the water and acid leached product (processed boron) were studied. The chemical purity, specific surface area, size distribution of particles and X-ray crystallite size of the boron powders were investigated. The morphology of the deposits was examined using scanning electron microscopy (SEM). The chemical state of the matrix, as well as the impurity phases present in them, was established using X-ray photoelectron spectroscopy (XPS). In order to interpret and understand the results obtained, a thermodynamic analysis was carried out. The gas phase corrosion in the head space as well as the chemistry behind the leaching process were interpreted using this analysis. The ease of oxidation of these powders in air was investigated using differential thermal analysis (DTA) coupled with thermogravimetry (TG). From the results obtained in this study it was established that elemental boron powder with a purity of 95–99% could be produced using a high temperature molten salt electrowinning process (Jain et al., 2008).

2.6 Electro-deposition Applications

Electro-deposition, although known for some time, has only recently become of commercial importance as a coating application method. Along with the increased use of such methods has been the development of certain compositions which can provide satisfactory coatings when applied in this manner. While many compositions can be electrodeposited, most coating compositions when applied using electro-deposition techniques do not produce commercially usable coatings. Moreover, electro-deposition of many coating materials, even when otherwise successful, is often attended by various disadvantages such as non-uniform coatings. In particular, properties such as corrosion resistance and alkali resistance are difficult to achieve, especially with the resins which are usually employed in electro-deposition processes. Other problems include a tendency for the deposited coating to stain or discolor, attributed to chemical changes and interactions (Bosso & Gaseca, 1971).

In a study by Naik et al. (2002), the electroplating of zinc was carried out in the presence of 3, 4, 5 - Trimethoxy benzaldehyde from a chloride bath. Operating parameters such as pH, temperature, and current density were optimized. The current efficiency and throwing power were measured at different current densities. Polarization study was carried out under galvanostatic conditions. Corrosion resistance test has indicated good protection of steel by the coating. The consumption of brightener was determined in the laboratory scale. SEM photomicrographs revealed fine grained structure of the deposit from the optimum bath. IR spectrum of the scratched deposit showed inclusion of addition agent (Naik et al., 2002).

Nickel foils with nano-size grains were produced by electro-deposition using a sulfamate-based electrolyte by Ebrahimi et al. (1999). The pH of the electrolyte was varied within the 2.8 to 5.1 range. As grain size was reduced, the strength and strain hardening rate increased and the texture became less prominent (Ebrahimi et al., 1999).

In a study by Chen et al. (2011), the electro-treatment of a high strength industrial lead frame nickel-plating wastewater was studied through a newly designed electro-deposition reactor. The electrolyte was circulated rapidly past the anode and cathode at a higher flow rate, allowing for improvements in efficiency and recovery, and nickel electro-deposition on the surface of cathode. The results showed that increasing boric acid concentration could increase the efficiency of nickel removal. The pH decreased during the electro-treatment was due to the production of H^+ on the cathode surface. Therefore, the optimum pH periodically controlled was found to be 2.9±0.2, and the lower current density was accompanied with the higher current efficiency (Chen et al., 2011).

Boron was electro-extracted from boron carbide and deposited on a mild steel cathode by Jain et al. (2013). In order to facilitate its immersion into the molten salt and subsequent withdrawal, it was connected to a long nickel shaft. This shaft was introduced into the retort through a hermetically sealed feed-through provided on the top flange. To start the electrolysis, cathode was lowered and dipped into the molten salt. In order to prevent corrosion at the junction of dissimilar joint between mild steel cathode and nickel shaft, they were connected using a graphite union. The electrolytic cell was placed inside a pit type resistively heated cylindrical furnace. The temperature of this furnace was controlled by a PID temperature controller. Boron was quantitatively estimated by a volumetric method. The trace impurities such as calcium, magnesium and aluminum present in the electrodeposited boron were analyzed by atomic absorption spectroscopy (Jain et al., 2013).

2.7 Literature Based Discussions

The literature review revealed that the minimum temperature of thermal reactions to produce boron carbide or boron nitride is 1500^{o}C and may go up to 2000^{o}C. This research proves the possibility of boron end product fabrication by an environmental friendly, low energy consuming modified electro-deposition method in lower temperature levels (60-80^{o}C) unlike the traditional production methods.

CHAPTER THREE
MATERIALS AND METHOD

There were three different experimental setups established since the start of the trials to produce boron end products by electro-deposition. The electrode substrates, solutes, bath arrangement and redressor were undergone many changes to determine the optimum experimental conditions for each different product throughout this research. The constant and/or variable parameters in conducted electro-deposition experiments can be listed as;

- ✓ Type of solvent
- ✓ Type of solute
- ✓ Solute concentration
- ✓ Type of electrode
- ✓ Electrode surface area
- ✓ Electrode thickness
- ✓ Bath pH level
- ✓ Bath temperature
- ✓ Applied current
- ✓ Applied voltage

The constant parameters for the whole experiment design were the use of purified water as solvent and keeping the bath temperature minimum as to provide enough solubility for the solutes.

3.1 Electrolyte Formation

The electrolyte formation involves the parameters of solvent and solute selection, solute concentration and bath pH and bath temperature. The solvent was fixed as purified water for the experiments.

3.1.1 Solute Selection

Several different solutes were planned to be used to form different electrolyte solutions. These solutes are mainly boron products of Eti Mine Works, such as boric acid, borax pentahydrate, borax decahydrate and anhydrous borax.

3.1.1.1 Boric Acid (H_3BO_3)

Boric acid refers to 3 compounds; orthoboric acid (also called boracic acid, H_3BO_3 or $B_2O_3 \cdot 3H_2O$), metaboric acid (HBO_2 or $B_2O_3 \cdot H_2O$) and tetraboric acid (also called pyroboric, $H_4B_4O_7$ or $B_2O_3 \cdot H_2O$). Orthoboric acid dehydrates to form metaboric acid and tetraboric acid above 170^{o}C and 300^{o}C respectively. Orthoboric acid is derived from boric oxide in the form of white, triclinic crystals. It is poorly soluble in cold water but dissolves readily in hot water, in alcohol and glycerin. Metaboric acid is a white, cubic crystals. It is soluble in water slightly. Tetraboric acid is a white solid soluble in water. When tetraboric and metaboric acid are dissolved, it reverts to orthoboric acid. The main use of boric acid is to make borate salts such as borax and other boron compounds. Boric acid is also used in heat resistant glass, in fireproofing fabrics, in electroplating baths, in leather manufacturing, porcelain enamels and in hardening steels. Boric acid has antiseptic and antiviral activity. Aqueous solutions have been used as mouth-washes, eye-drops, skin lotions and cosmetics. Boric acid and its salts are components of many commercial insecticides and wood preservatives (Görgülü & Arslan, 2003).

The commercially available boric acid bag as a product of Eti Mine Works is represented in Figure 3.1 with structure, XRD analysis (Figures 3.2 and 3.3), chemical specifications, physical and chemical properties, solubility chart and particle size distribution (Tables 3.1, 3.2, 3.3 and 3.4).

Figure 3.1 Commercially available Eti Mine Works boric acid bag (25 kg)

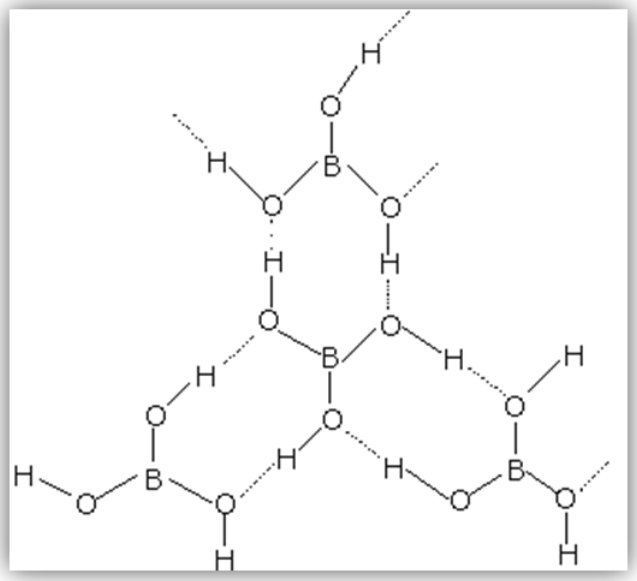

Figure 3.2 Structure of boric acid (dotted lines represent hydrogen bonding)

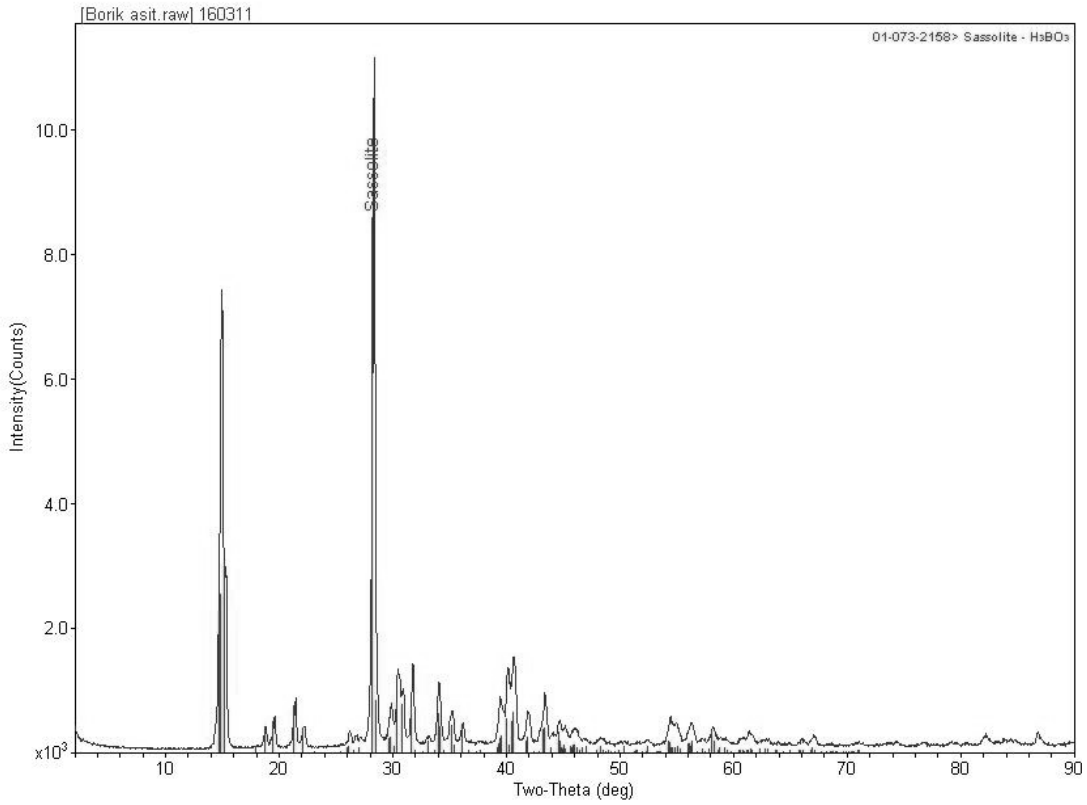

Figure 3.3 XRD analysis of commercial boric acid (Eti Mine,2012)

Table 3.1 Physical and chemical properties of boric acid (Eti Mine, 2012)

Physical & Chemical Properties (H_3BO_3)	
Physical State	White or colorless crystals
Melting Point	450^oC
Boiling Point	1860^oC
Specific Gravity	1.51 g/cm^3 at 20^oC
Molecular Weight	61.83 g/mole
pH	5.2 (%1 solution)

Table 3.2 Chemical specifications of boric acid (Eti Mine, 2012)

Chemical Specifications (H_3BO_3, Normal Sulphate)	
Component	**Content**
B_2O_3	56.25 % (min.)
Purity	99.90 % (min.)
SO_4	500 ppm (max.)
Cl	10 ppm (max.)
Fe	7 ppm (max.)

Table 3.3 Solubility of boric acid in water (Eti Mine, 2012)

Solubility in Water (H_3BO_3)	
Temperature (^oC)	**g/L of Water**
0	25.2
10	37.8
20	50.8
30	67.2
40	88.7
50	112.6
60	146.5
70	182.8
80	228.8
90	292.8
100	364.1
103.3*	395.6

*Boiling Point

Table 3.4 Particle size distribution of commercially available boric acid (Eti Mine, 2012)

Particle Size Distribution (H_3BO_3)	
Size (mm)	**Content**
+ 1.000	4 % (max.)
- 1.000 +0.063	92 % (min.)
-0.063	4 % (max.)

3.1.1.2 Borax Pentahydrate ($Na_2B_4O_7.5H_2O$)

Borax pentahydrate is the refined form of natural sodium borate and has the chemical formula $Na_2B_4O_7.5H_2O$. Composed of boron oxide (B_2O_3), sodium oxide, and water, it is a mild, alkaline salt, white and crystalline, with excellent buffering and fluxing properties. It is available in crystalline (granular) form and is an important multifunctional source of B_2O_3, particularly for processes in which the simultaneous presence of sodium is beneficial. Borax pentahydrate used at the correct equivalent rate gives solution or melts identical in composition with those of borax decahydrate, it may therefore be substituted at a saving in all applications where borax is used; among present applications of borax pentahydrate are wire drawing baths, corrosion inhibitor solutions, starches, starches, adhesives and the manufacture of other boron compounds (Eti Mine, 2003).

The commercially available borax pentahydrate bag as a product of Eti Mine Works is represented in Figure 3.4 with structure, XRD analysis (Figure 3.5 and 3.6), chemical specifications, physical and chemical properties, particle size distribution and solubility chart (Tables 3.5, 3.6, 3.7 and 3.8).

Figure 3.4 Commercially available Eti Mine Works borax pentahydrate bag (25 kg)

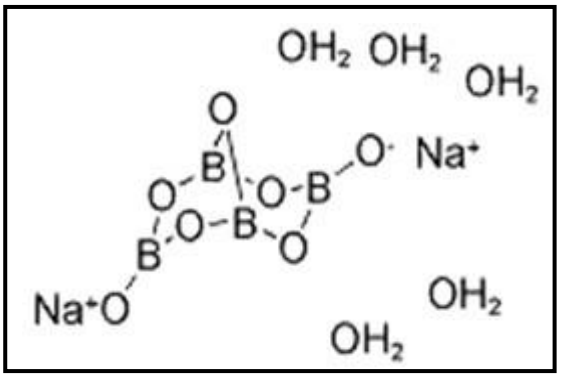

Figure 3.5 Structure of borax pentahydrate

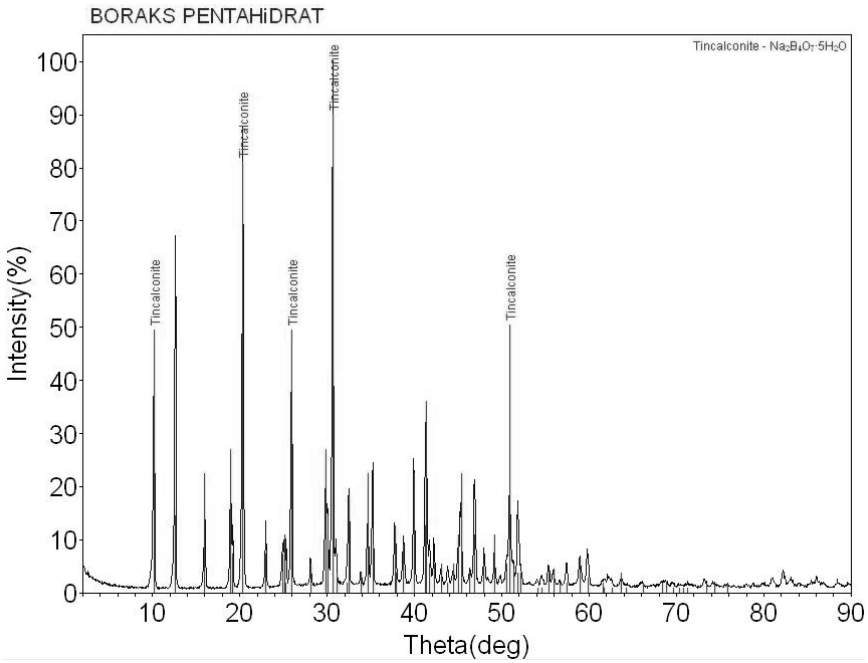

Figure 3.6 XRD analysis of commercial borax pentahydrate (Eti Mine, 2012)

Table 3.5 Physical and chemical properties of borax pentahydrate (Eti Mine,2012)

Physical & Chemical Properties ($Na_2B_4O_7.5H_2O$)	
Physical State	White crystals
Melting Point	741^oC
Boiling Point	1575^oC
Specific Gravity	1.81 g/cm^3 at 20^oC
Molecular Weight	291.35 g/mole
pH	9.3 (%3 solution)

Table 3.6 Chemical specifications of borax pentahydrate (Eti Mine, 2012)

Chemical Specifications ($Na_2B_4O_7.5H_2O$)	
Component	**Content**
B_2O_3	47.76 % (min.)
Purity	99.90 % (min.)
Na_2O	21.25 % (min.)
SO_4	135 ppm (max.)
Cl	70 ppm (max.)
Fe	5 ppm (max.)
Insolubles in Water	150 ppm (max.)

Table 3.7 Particle size distribution of commercially available borax pentahydrate (Eti Mine, 2012)

Particle Size Distribution ($Na_2B_4O_7.5H_2O$)	
Size (mm)	**Content**
+1.000	6 % (max.)
-1.000 +0.063	90 % (min.)
-0.063	4 % (max.)

Table 3.8 Solubility of borax pentahydrate in water (Eti Mine, 2012)

Solubility in Water ($Na_2B_4O_7.5H_2O$)	
Temperature (^oC)	**g/L of Water**
0	17.1
10	25.7
20	39.6
30	60.4
40	96.1
50	138.0
60	241.0
70	282.1
80	338.4
90	410.6
100	501.2

3.1.1.3 Borax Decahydrate ($Na_2B_4O_7.10H_2O$)

Borax decahydrate is the refined form of natural sodium borate. Composed of boric oxide (B_2O_3), sodium oxide, and water, it is a mild, alkaline salt, white and crystalline, with excellent buffering and fluxing properties. Available in powder or granular form, borax decahydrate is an important multifunctional source of B_2O_3, particularly for processes in which the simultaneous presence of sodium is beneficial. Borax Decahydrate is chemically stable under normal storage conditions. It will slowly lose water of crystallization if exposed to a warm, dry atmosphere. Conversely, exposure to a humid atmosphere can cause recrystallization at particle contact points, resulting in caking. Dissolved in water, borax decahydrate hydrolyzes to give a mildly alkaline solution. It is thus capable of neutralizing acids. It also combines with strong alkalis to form compounds of lower pH. The relatively constant pH of borax decahydrate solutions makes it an excellent buffering agent.

The commercially available borax decahydrate bag as a product of Eti Mine Works is represented in Figure 3.7 with structure, XRD analysis (Figures 3.8 and

3.9), physical and chemical properties, chemical specifications, particle size distribution and solubility chart (Tables 3.9, 3.10, 3.11 and 3.12).

Figure 3.7 Commercially available Eti Mine Works borax decahydrate bag (25 kg)

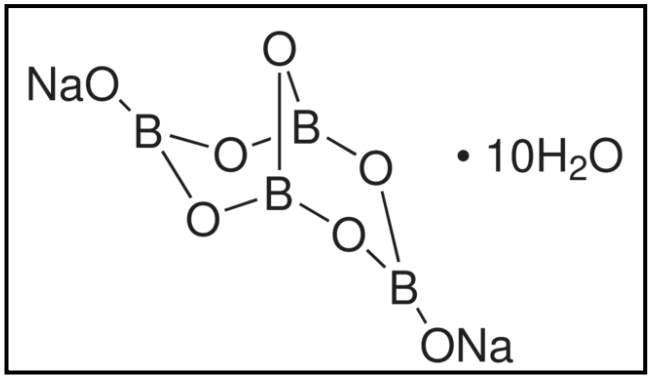

Figure 3.8 Structure of borax decahydrate

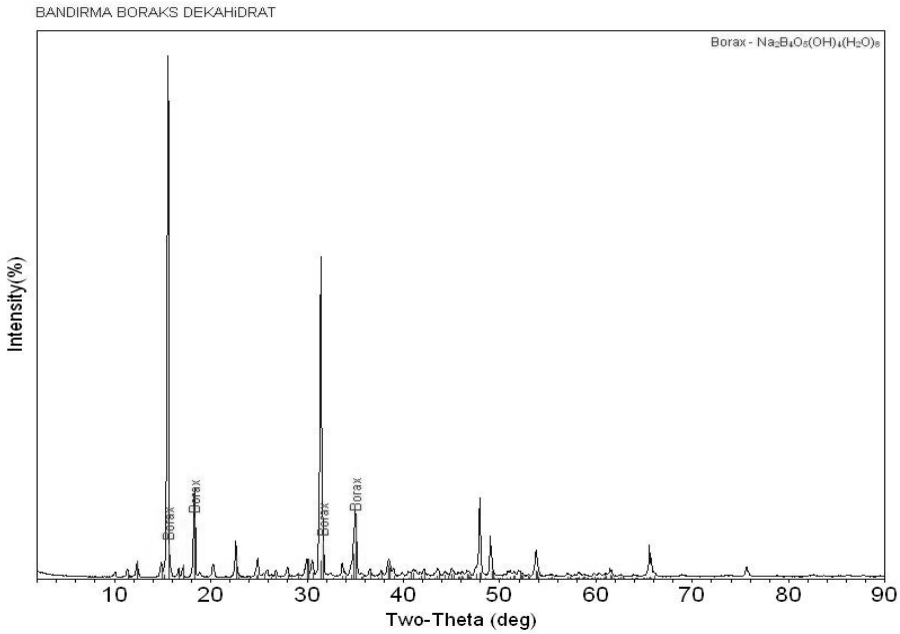

Figure 3.9 XRD analysis of commercial borax decahydrate (Eti Mine, 2012)

Table 3.9 Physical and chemical properties of borax decahydrate (Eti Mine, 2012)

Physical & Chemical Properties ($Na_2B_4O_7.10H_2O$)	
Physical State	White or colorless crystals or powder
Melting Point	741^oC
Boiling Point	1575^oC
Specific Gravity	1.72 g/cm^3 at 20^oC
Molecular Weight	381.37 g/mole
pH	9.2 (%1 solution)

Table 3.10 Chemical specifications of borax decahydrate, granular (Eti Mine, 2012)

Chemical Specifications ($Na_2B_4O_7.10H_2O$)	
Component	**Content**
B_2O_3	36.47 % (min.)
Purity	99.90 % (min.)
Na_2O	16.24 % (min.)
SO_4	70 ppm (max.)
Cl	50 ppm (max.)
Fe	10 ppm (max.)

Table 3.11 Particle size distribution of commercially available borax decahydrate (Eti Mine, 2012)

Particle Size Distribution ($Na_2B_4O_7.10H_2O$)	
Size (mm)	**Content**
+ 1.000	1 % (max.)
- 1.000 +0.063	95 % (min.)
-0.063	4 % (max.)

Table 3.12 Solubility in water as borax decahydrate (Eti Mine, 2012)

Solubility in Water ($Na_2B_4O_7.10H_2O$, Granular)	
Temperature (^oC)	**g/L of Water**
0	19.9
10	31.1
20	49.8
30	79.2
40	127.8
50	179.1
60	303.3
70	369.4
80	443.1
90	531.8
100	656.4

3.1.1.4 Anhydrous Borax – Etibor 68 ($Na_2B_4O_7$)

Etibor-68 is obtained by gradually heating of borax at high temperatures. It has white, odorless and crystalline solid structure at the temperature of 20^{o}C and the pressure of 101.3 kPa. Once $Na_2B_4O_7$ (anhydrous sodium tetraborate) is cooled quickly, it has a glassy amorphous structure. Anhydrous borax dissolves more slowly in water and gives higher heat than the other hydrated borax. In an oxygen-free environment, B_4C_3 and Na_2C_2 are formed via reaction of anhydrous borax with carbon at 1200^{o}C. Also, elemental boron is formed by the reaction of anhydrous borax with metallic sodium (Eti Mine, 2012).

Etibor-68 is used in the production of high quality glass and ceramics. It is used as the source of B_2O_3 in the manufacture of many types of borosilicate glass. Heat and chemical resistant glass, optical lenses, medical and cosmetic containers and glass beads can be given as an example. Properties, high bulk density and fast melting with less energy, of Etibor-68 are superior when it compared with other borax products. Etibor-68 is the source of sodium so it can be used with boric acid and boron oxide to

control the ratio of sodium oxide/boron oxide. The aim of using Etibor-68 in glass is providing a stable structure. Because of the detrimental effect of lead compounds on human health, borates which provide same property for glaze (transparency, melting) are preferred to especially tableware nowadays. Boron compounds like anhydrous borax is preferred to production of glaze for this aim (Eti Mine, 2012).

Etibor-68 is used as a melting agent. Due to the melting property, impurities of metal oxide are dissolved in production of iron-steel and non-ferrous metals by lowering the melting temperature. Removing these impurities from slag is made easier by this property. Etibor-68 is very good solvent for metal oxides at high temperature. The oxidation of metals with air is prevented by covering the surface. Etibor-68 increases the hardness of steel whenever small amounts are added. Properties and processing behavior of steel materials can be changed by Etibor-68 (Eti Mine, 2012).

The commercially available anhydrous borax bag as a product of Eti Mine Works is represented in Figure 3.10 with structure, XRD analysis (Figures 3.11 and 3.12), chemical specifications, particle size distribution, physical and chemical properties and solubility chart (Tables 3.13, 3.14, 3.15 and 3.16).

Figure 3.10 Commercially available Eti Mine Works anhydrous borax bag

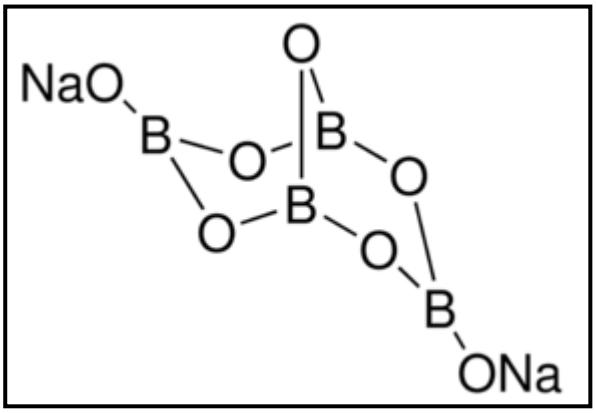

Figure 3.11 Structure of anhydrous borax

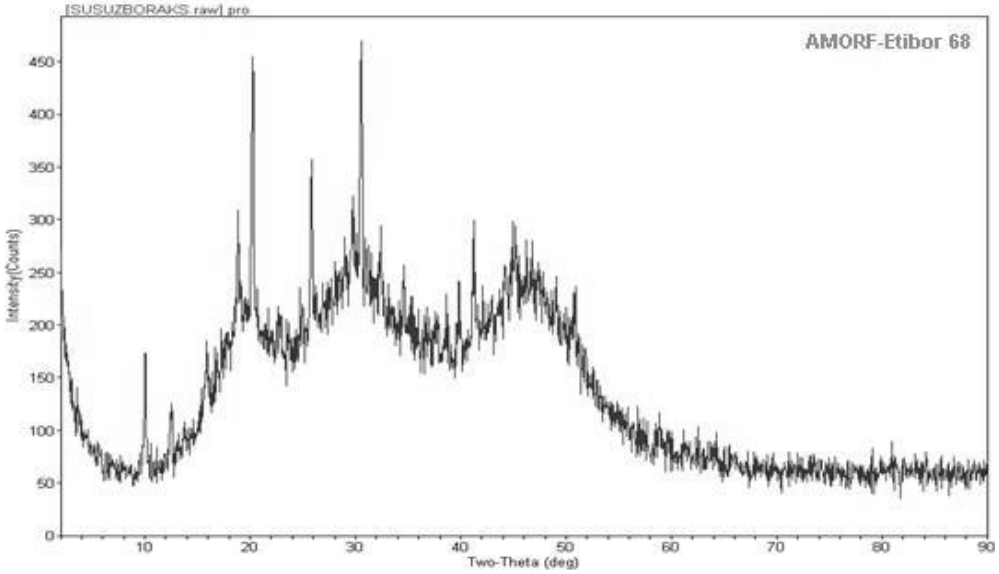

Figure 3.12 XRD analysis of commercial anhydrous borax (Eti Mine,2012)

Table 3.13 Chemical specifications of borax decahydrate, granular (Eti Mine,2012)

Chemical Specifications ($Na_2B_4O_7$)	
Component	**Content**
B_2O_3	68.00 % (min.)
Na_2O	30.27 % (min.)
SO_4	200 ppm (max.)
Cl	105 ppm (max.)
Fe	150 ppm (max.)
Insolubles in Water	920 ppm (max.)

Table 3.14 Particle size distribution of commercially available anhydrous borax (Eti Mine, 2012)

Particle Size Distribution ($Na_2B_4O_7$)	
Size (mm)	**Content**
+ 1.600	1 % (max.)
- 1.600 +0.075	94 % (min.)
-0.075	5 % (max.)

Table 3.15 Physical and chemical properties of anhydrous borax (Eti Mine 2012)

Physical & Chemical Properties ($Na_2B_4O_7$)	
Melting Point	741^oC
Boiling Point	1575^oC
Specific Gravity	3.37 g/cm^3 at 20^oC
Molecular Weight	201.22 g/mole
pH	9.2 (%1 solution)

Table 3.16 Solubility of anhydrous borax in water (Eti Mine, 2012)

Solubility in Water ($Na_2B_4O_7$)	
Temperature (^oC)	**g/L of Water**
0	1.21
10	1.76
20	2.69
30	4.02
40	6.19
50	9.74
60	17.01
70	19.91
80	23.88
90	28.98
100	35.37

3.1.2 Solution Properties

The electrolyte properties formed by different solutes in water were detected by limiting the bath temperature at approximately 80^{o}C (Table 3.17).

Table 3.17 Properties of electrolyte solution formed in laboratory experiments in comparison with theoretical data

Properties of Electrolyte Solution				
Solute	**pH (exp.)**	**pH (theor.)**	**Solubility (g/L, 80^{o}C, exp.)**	**Solubility (g/L, 80^{o}C, theor.)**
Boric Acid	4.5	5.2	190	228.8
Borax Pentahydrate	9.4	9.3	175	338.4
Borax Decahydrate	9.5	9.2	200	443.1
Anhydrous Borax	9.8	9.2	17	23.88

3.2 Electrode Selection

Several different substrates were used in electro-deposition studies as electrodes. These substrates can be listed as copper, titanium, iron, aluminum, lead and stainless steel (Figure 3.13). The substrates were ready to be cut in desired dimensions. Two different sets of metal plates were used during experiments for two different experimental setups for final experimental setup. The first set was used for electro-deposition in beakers (1 L). The dimensions of these metal substrates were adjusted generally as 100x20 mm with a thickness of 0.2 mm. The second set was used for electro-deposition in polypropylene bath with dimensions of 250x150x180 mm. The dimensions of these metal substrates were adjusted generally as 150x150 mm with a thickness of 2 mm. The resistivity values of Cu, Fe, Pb, Ti, Al and stainless steel are $1.7x10^{-8}$, $1.0x10^{-7}$, $2.2x10^{-7}$, $4.2x10^{-7}$, $2.8x10^{-8}$ and $6.9x10^{-7}$ Ω.m, respectively. Graphite anode bars were also used as electrodes in some experiments. These types of electrodes are resistant to higher currents. The general height of graphite electrodes varies between 300 to 350 mm. Their diameters may vary such as 3.25, 5, 6.5, 8 and 10 mm. There are 3 types of carbon based electrodes. These are amorphous, graphite and electro-graphite electrodes. The graphite electrodes are

mainly used in electrical arc furnaces to melt steel in a recycling process. The contents of pure graphite electrode used are; fixed carbon: 99.86 %, sulphur: 0.02 %, ash: 0.12 %.

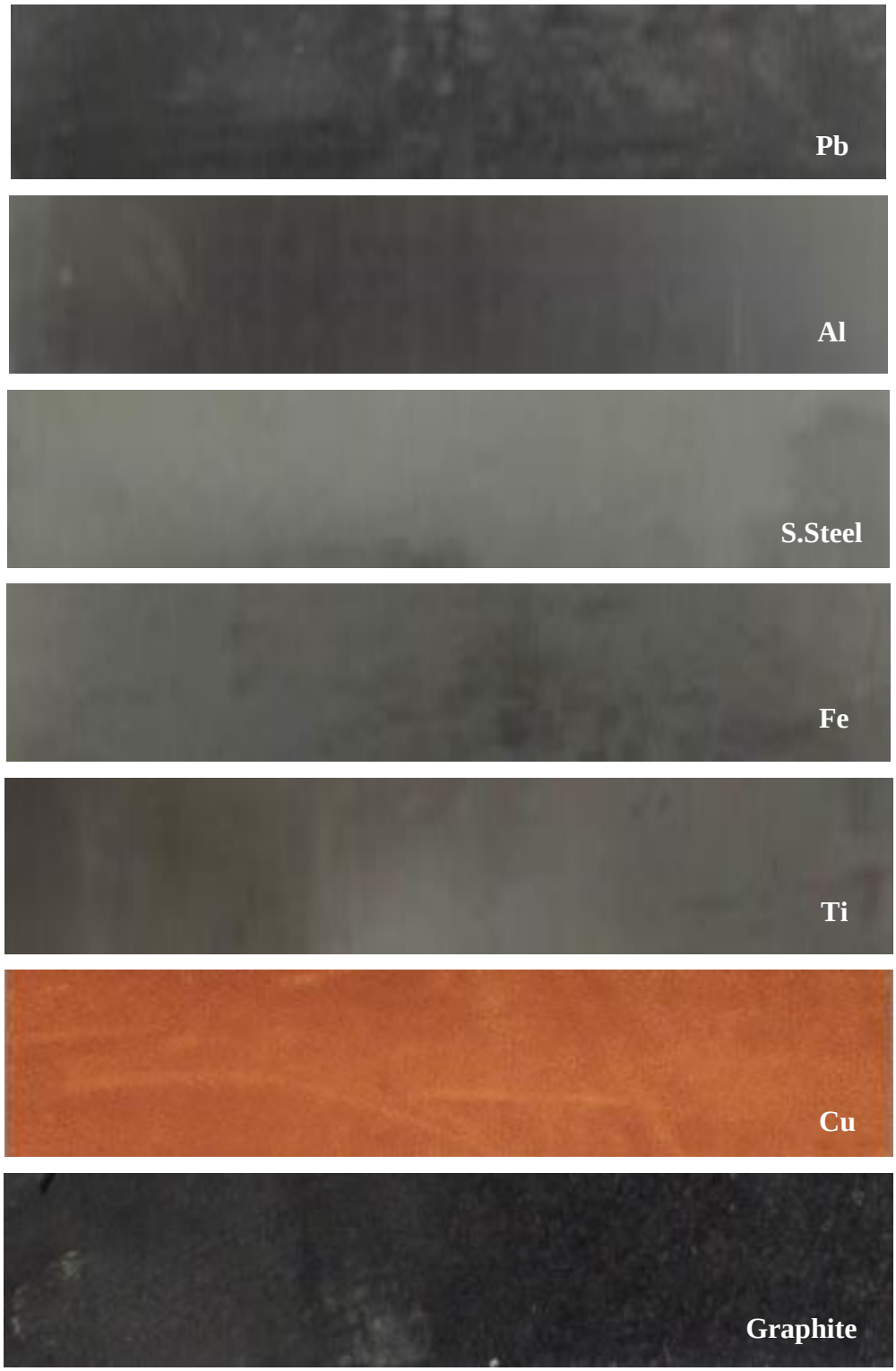

Figure 3.13 Substrates used in electro-deposition studies

3.3 Electro-deposition and Experimental Setup

In 1833, the English scientist, Michael Faraday, developed Faraday's laws of electrolysis. Faraday's first law of electrolysis and Faraday's second law of electrolysis state that the amount of a material deposited on an electrode is proportional to the amount of electricity used. The amount of different substances liberated by a given quantity of electricity is proportional to their electrochemical equivalent (Lou & Huang, 2006).

An electrolytic cell essentially consists of two or more electrodes dipping into an electrolyte. These electrodes are connected to an external electric power source. When the current is switched on, the anode becomes positively charged, while the cathode becomes negatively charged. Thus, during electrolysis the cations or the positively charged ions move towards the cathode and the anions or the negatively charged ions migrate towards the anode (Gupta, 2003).

When a direct electric current passes through an electrolyte, chemical reactions take place at the contacts between the circuit and the solution. This process is called electrolysis. Electrolysis takes place in an electrolytic cell. Electroplating is one specific type of electrolysis. Besides electroplating, electrolysis has also been widely used for preparation of halogens and notably chlorine, and refining of metals, such as copper and zinc. Understanding the electrochemical principles of electro-deposition is essential to the development of electroplating technologies (Bosso & Gaseca, 1971; Lou & Huang, 2006).

In a wider sense, all electron-transfer reactions are considered oxidation = reduction. The substance gaining electrons (oxidizing agent, or oxidant) oxidizes the substance that is losing electrons (reducing agent, or reductant). In the process, the oxidizing agent is itself reduced by the reducing agent. Because a cathode is attached to the negative pole of the electric source, it supplies electrons to the electrolyte. On the contrary, an anode is connected to the positive pole of the electric source; therefore, it accepts electrons from the electrolyte. Various reactions take place at the

electrodes during electrolysis. In general, reduction takes place at the cathode, and oxidation takes place at the anode (Lou & Huang, 2006).

Electro-deposition or electrochemical deposition involves the reduction of metal ions from electrolytes. At the cathode, electrons are supplied to cations, which migrate to the anode. In its simplest form, the reaction in aqueous medium at the cathode follows the equation with a corresponding anode reaction:

$$M^{n+} + ne^- \rightarrow M \quad (3.1)$$

At the anode, electrons are supplied to the anions, which migrate to the anode. The anode material can be either a sacrificial anode or an inert anode. For the sacrificial anode, the anode reaction is:

$$M \rightarrow M^{n+} + ne^- \quad (3.2)$$

In electroplating, sufficient voltage should be provided by the power source. The voltage–current relationship follows Ohm's law. The concepts of electrode potentials, equilibrium electrode potential, over potential and overvoltage are of fundamental importance. The current is driven by a potential difference, or voltage through the conducting medium, either electrolytic or metallic. The voltage necessary to force a given current through a conductor is given by Ohm's law:

$$E = I R \quad (3.3)$$

where E is the voltage (V), I is the current (A) and R the resistance of the conductor (Ω).

Direct current (DC) electrolysis is represented in Figure 3.14. Two electrodes, immersed in solution, are connected to the output of a DC current source. The cathode, onto which the deposition forms, may itself be a metal or a semiconductor or a non-metallic conductor such as graphite. Anode is necessary to complete the

electrical circuit to remove anions and thereby maintain overall charge neutrality in solution. Sacrificial anodes are made of the same metal that is being deposited, e.g. copper where permanent anode, e.g. titanium, are used to complete the circuit and force depletion of solution.

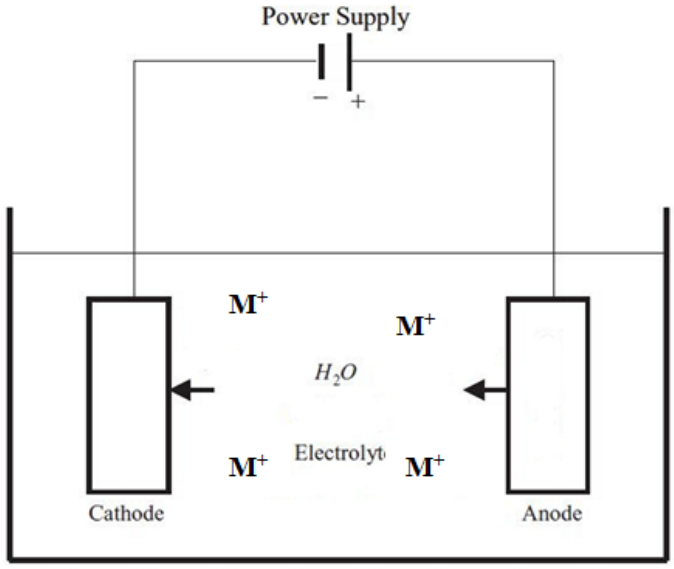

Figure 3.14 Electrolysis schematic, migrations of metal ions to cathode

3.3.1 Stern-Graham Model Electrolyte Double Layer Concept

The concepts embodied in the Stern-Graham model of the electrolyte double layer are illustrated in Figure 3.15. The plane of mean charge of specifically adsorbed anions is defined as the inner Helmholtz layer, and thus encloses an adsorbed layer of water molecules, electrostatically attracted to the cathode surface and there oriented, as well as certain surface active species present in solution. The spatial extent of this region is known as the inner Helmholtz layer. In the same way, the mean geometric location of charge centers due to metal ions adsorbed at the cathode is known as the outer Helmholtz layer and so defines the outer limit of the rigid Helmholtz layer. Beyond this lies the so-called diffuse layer in which metal ions are fully mobile, and whose spacing from one another is a function of total ionic concentration in bulk solution. The concentration of positively charged ions in this layer is governed by the need to maintain overall charge neutrality, including those charged species adsorbed at the electrode surface (Kanani, 2004).

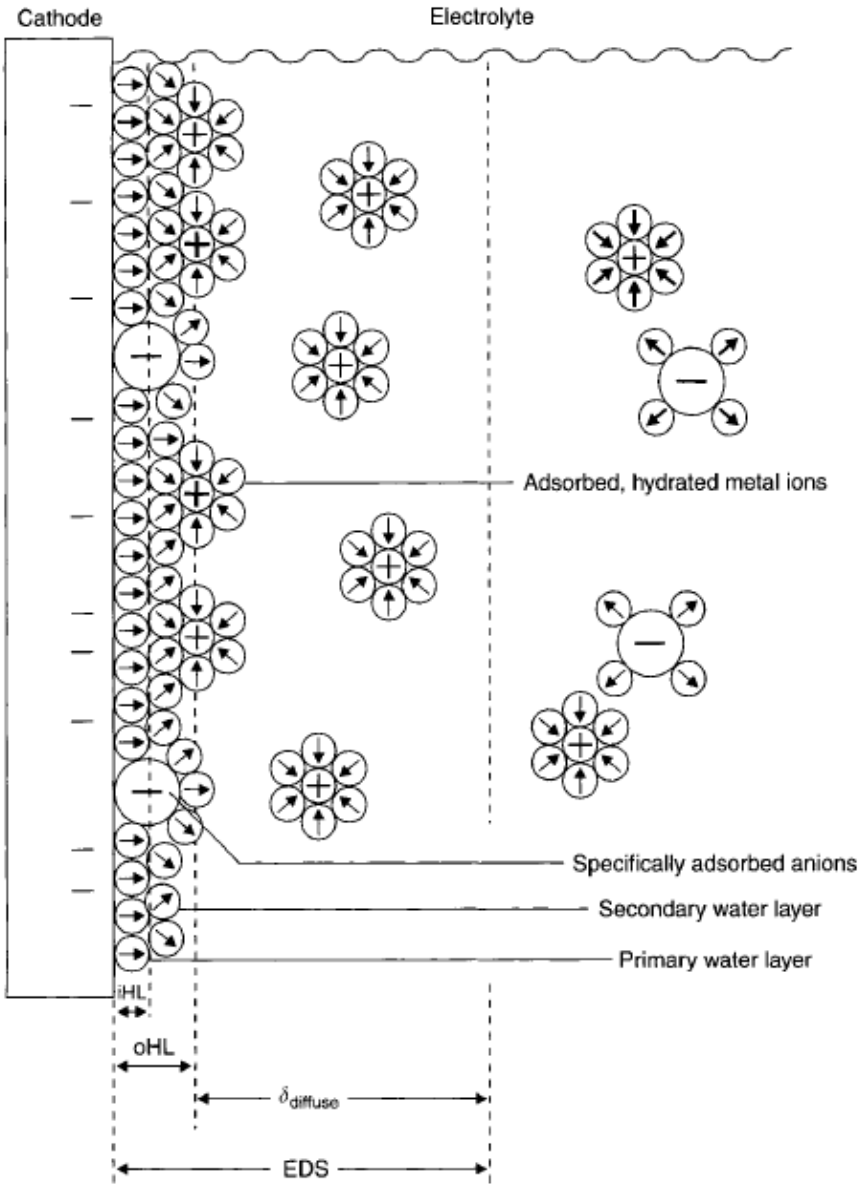

Figure 3.15 Stern-Graham model of the electrolyte double layer (Kanani, 2004)

3.3.2 Cleaning

Cleaning methods should be able to minimize substrate damage while removing the contaminants, dust, film or debris. Cleaning processes are based on two approaches which are chemical and mechanical approach. A chemical approach usually includes solvent degreasing, alkaline cleaning and acid cleaning. Contaminants consist of oils and grease of various types, waxes, and miscellaneous organic materials. These contaminants can be removed by appropriate organic solvents, either by dipping the work pieces in the solvent or by vapor decreasing. In

alkaline cleaning, work pieces are immersed in tanks of hot alkaline cleaning solutions to remove dirt and solid soil. Acid cleaning can move heavy scale. The most commonly used acids include sulfuric and hydrochloric.

The cleaning of substrates was performed by using hydrochloric, nitric and chromic acid. Ultrasonic cleaning was also applied to clean substrates prior to electro-deposition experiments (Figure 3.16) with Everest brand ultrasonic bath present in EMUM, DEU.

Figure 3.16 Everest brand ultrasonic bath in EMUM, DEU

3.3.3 Experimental Setup

There were four different experimental setups benefited during this research. These four setups are going to be entitled as “preliminary setup”, “first laboratory setup”, “second laboratory setup” and “final laboratory setup”. The preliminary studies were conducted by Soyberg brand redressor with operating ranges of 0-25 amperes and 5-48 volts in laboratories of Department of Technical Programs in Dokuz Eylül University Vocational School of Higher Education. Studies of boron nitride and carbide production were conducted with this setup at first (Figure 3.17). The first laboratory setup included a Platin brand, pilot scale redressor in laboratories of EMUM, DEU (Figure 3.18). The second laboratory setup involved a magnetic stirrer with heating feature and Quassar 500 brand redressor (Figure 3.19).

Figure 3.17 Redressor and preliminary experimental setup in IMYO, DEU

Figure 3.18 Redressor and first laboratory experimental setup in EMUM, DEU

Figure 3.19 Redressor and second laboratory experimental setup in EMUM, DEU

The final laboratory setup was a bit professional. This setup was used in experimental electro-deposition studies for the last two years of the research. This setup involved a polypropylene bath, a thermo-couple, a magnetic stirrer with heating feature and Alpha-Tech brand redressor with operating ranges of 0-200 amperes and 0-600 volts. The redressor also has touchscreen control and pulse feature (Figure 3.20).

Figure 3.20 Redressor and final laboratory experimental setup in EMUM, DEU

Some additional laboratory equipment was also used during the studies for bath, sample, electrolyte preparation and safety. These can be listed as high-energy ball mill, agate mortar, pH meter, analytical balance, water purifier, mechanical stirrer, magnetic stirrer and heater, polypropylene bath, water circulator, wire stand and clamps (Figure 3.21)


(a)
(b)
(c)
(d)
(e)
(f)

Figure 3.21 Auxiliary laboratory equipment in electro-deposition experimental setup (a) high-energy ball mill, (b) agate mortar, (c) pH meter, (d) analytical balance, (e) water purifier, (f) mechanical stirrer, (g) magnetic stirrer and heater, (h) polypropylene bath, (j) water circulator, (k) wire stand and clamps

3.4 Characterization Studies

The chemical, surface and phase characterizations of electrolytes and deposited electrode bars were performed by X-Ray Diffractometer (XRD), X-ray Photoelectron Spectrometer (XPS), Inductively Coupled Plasma Optical Emission Spectrometer (ICP-OES), Atomic Absorption Spectrophotometer (AAS) and Scanning Electron

Microscope (SEM). The particle size distribution analysis of electrolyte and deposited products were performed by Laser Particle Size Analyzer, Zeta Sizer and Scanning Electron Microscope. The devices used in characterization studies belong to Dokuz Eylül University Department of Mining Engineering and Center for Production and Application of Electronic Materials (EMUM).

Thermo Scientific brand, Cu-Kα type XRD device (Figure 3.22); Thermo Scientific brand, Kα Surface Analysis type XPS device (Figure 3.23); Coxem brand, EM-30 type SEM (Figure 3.24); Malvern brand, Zetasizer Nano Z type nano particle size analyzer with measurement range of 3.8 nm to 100 microns (Figure 3.25); Horiba brand, Partica LA-950 V2 type laser diffraction particle size distribution analyzer (Figure 3.26); Analytik Jena brand, Nova 300 type atomic absorption spectrophotometer (Figure 3.27) and Varian brand, 710-ES type ICP-OES (Figure 3.28) are illustrated in order below.

Figure 3.22 Thermo Scientific, Cu-Kα type XRD device in EMUM, DEU

Figure 3.23 Thermo Scientific, Kα Surface Analysis type XPS device in EMUM, DEU

Figure 3.24 Coxem, EM-30 SEM with ion coater in EMUM, DEU

Figure 3.25 Malvern, Zetasizer Nano Z type nano particle size analyzer in EMUM, DEU

Figure 3.26 Horiba, LA-950 V2 type particle size analyzer in Mining Eng., DEU

Figure 3.27 Analytik Jena atomic absorption spectrophotometer in Mining Eng., DEU

Figure 3.28 Varian, 710-ES type ICP-OES in Mining Eng., DEU

3.4.1 Analysis Procedure of Boron

The boron analysis is a bit complex in many points of view. To summarize, 5 grams of finely ground boron sample, 15-20 ml HCl and equal amount of purified water are put into a flask and boiled about 20-25 minutes by condenser. After boiling, the flask is left for cooling and another 75 ml of purified water is added. The mixture is rinsed and boiled for another 10-15 minutes. The flask is left for cooling again. 50 ml of purified water is poured through condenser into the flask. The solution is taken to a 250 ml volumetric flask and filled with water. The residue is waited to precipitate and then filtered. 50 ml of solution is taken to a 400 ml beaker. Two or three drops of indicator (P-nitrophenol) are dropped and NaOH is added when the color turns to yellow. $Fe(OH)_3$ and $Al(OH)_3$ are precipitated by heating and hydroxides are filtered from the cooled solution. A few drops of HCl is added and then neutralized with NaOH till the color turns to yellow again. 10 drops of indicator (phenolphthalein) and 25-50 ml neutral glycerin is added. Then the solution is titrated with NaOH till the color turns to violet. Each 1 ml of NaOH used in titration represents 0.01741 grams of B_2O_3.

CHAPTER FOUR
EXPERIMENTAL STUDIES

The experimental electro-deposition studies were performed to determine the optimum parameters for production of boron end products from boron derivatives. The boron derivatives used in those experiments can be listed as boric acid, borax pentahydrate, borax decahydrate and anhydrous borax. Due to low solubility of anhydrous borax in water and low B_2O_3 content of tincal concentrate with respect to other solutes, the parameter screening was not successfully achieved. The experimental studies also involve the sample preparation, size reduction and characterization. The results of characterization studies and analysis are discussed in "Chapter Five" in detail.

The experimental studies performed by four different electro-deposition setups should also be examined under different stages. These stages are going to be entitled as "preliminary studies" and "laboratory studies". The preliminary studies were generally conducted by preliminary and first laboratory setup. The laboratory studies were performed by using the second and final laboratory setup.

The preliminary studies revealed that it is possible to produce boron end products as boron carbide and/or boron nitride by electro-deposition method using boron derivatives with temperatures between 60 and 100^{o}C. However, the preliminary setup used could not be operated well due to many reasons such as fluctuations in voltage and current due to redressor, unhindered impurities, surface corrosions of electrodes, etc. Despite all, some promising results were acquired during these experiments. The XRD analysis of a sample experiment conducted by boric acid with experimental conditions of 80^{o}C, 5A, 12V, graphite anode, Fe cathode and NaCl addition is given in Figure 4.1 showing phase formations of BN, B_4C, C_3N_4 and Fe.

The experiment design was conducted according to these results obtained from preliminary studies. Several different parameters as solute type, solute concentration, anode type, cathode type, pH, temperature, duration, voltage, current and current

density were varied. Current density is defined as current in amperes per unit area of the electrode. It is a very important variable in electroplating operations. It affects the character of the deposit and its distribution. The solvent was fixed as purified water and solute concentrations were defined according to their solubilities in relevant temperature to obtain a saturated solution in water. The changes in concentration, bath temperature and pH with time were also investigated to evaluate the reaction mechanism. In some cases, a buffer solution or additional solutes were benefited to initiate or enhance deposition.

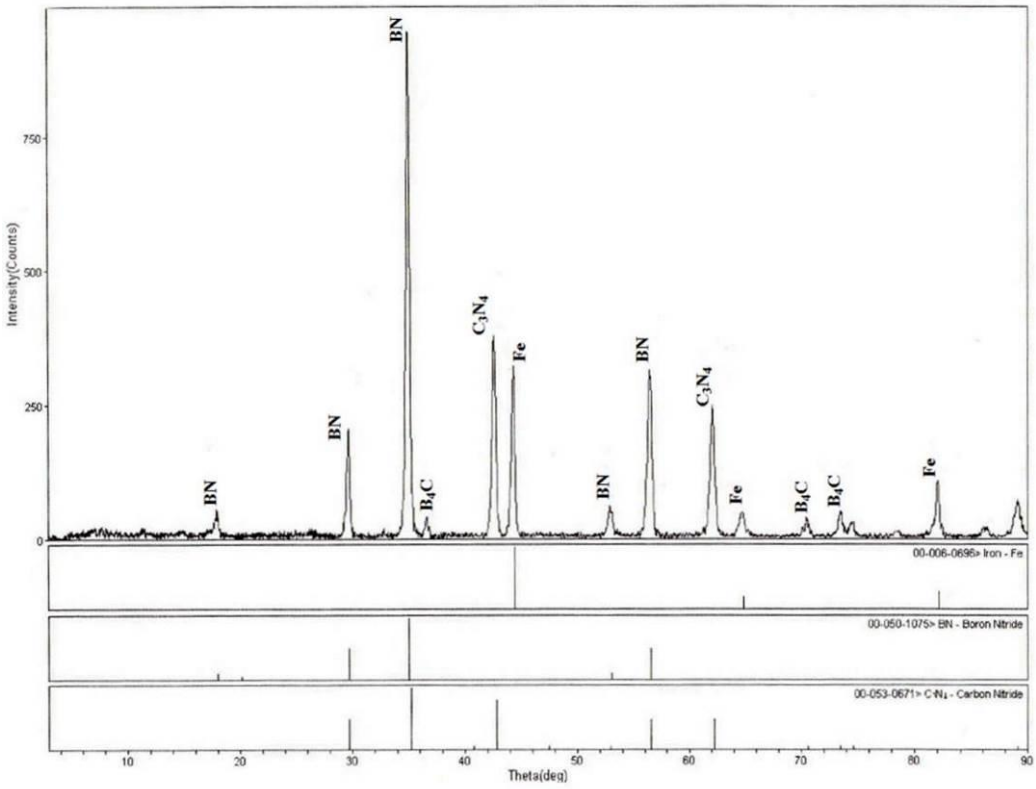

Figure 4.1 A sample XRD analysis of preliminary studies

The experimental studies were grouped according to the solute type used. The most successful and pure results were gathered from the studies conducted with borax pentahydrate. The formation of boron nitride and boron carbide were observed in many successful deposition trials. In addition, formation of elemental boron in some parameters was observed. The final laboratory setup proved many advantages in by providing full control on redressor and bath parameters.

A simplified flowsheet of the doctoral research is given in Figure 4.2.

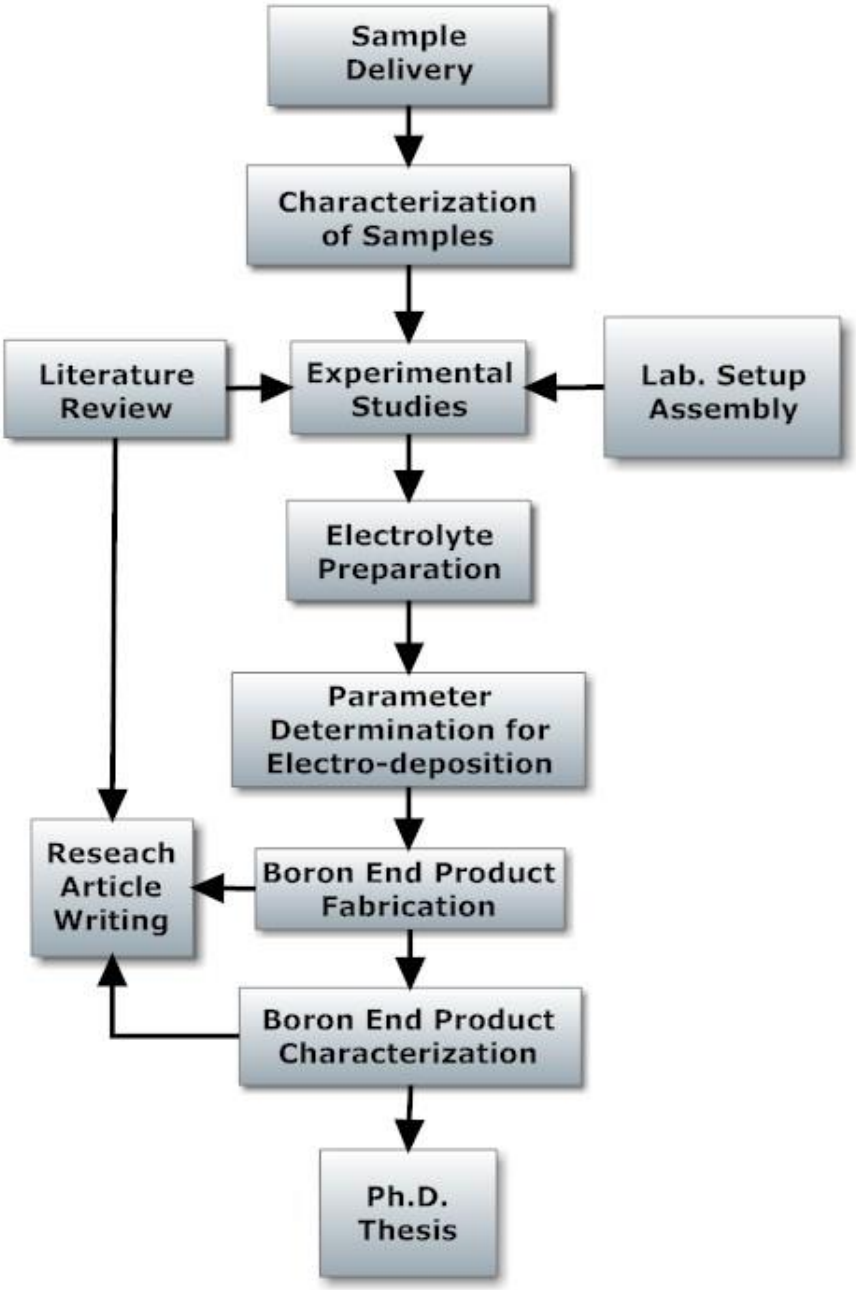

Figure 4.2 Flowsheet of doctoral research progress

4.1 Boron End Product Fabrication from Boric Acid

The simplified design of electro-deposition experiments conducted by using H_3BO_3 as solute is listed in Table 4.1. Many other unsuccessful experiments are screened out. The table represents the experiment code, type of anode and cathode, pH of the solution, additions such as buffer solution or catalyst, voltage set (V), current acquired (A), current density (A/dm^2) and duration of the experiment (min.).

Table 4.1 Simplified electro-deposition experiments conducted by boric acid (H_3BO_3) as solute (190 g/L initial solute concentration, 80°C initial bath temperature, purified water as solvent)

Code	Anode	Cathode	pH	Addition	V	A	A/dm^2	Duration (min.)
BA01	Graphite	Fe	3.5-5.0	$NH_4.Cl$	4	1	0.45	30
BA02	Graphite	Fe	3.5-5.0	$NH_4.Cl$	8	1	0.45	10
BA03	Graphite	Fe	3.5-5.0	$NH_4.NO_3$	12	2	0.90	10
BA04	Graphite	Fe	3.5-5.0	$NH_4.NO_3$	16	4	1.80	10
BA05	Graphite	Fe	3.5-5.0	-	20	5	2.25	10
BA06	Graphite	Fe	3.5-5.0	-	24	5	2.25	10
BA07	Ti	Fe	3.5-5.0	$NH_4.Cl$	20	1	0.45	30
BA08	Ti	Fe	3.5-5.0	-	40	1	0.45	10
BA09	Ti	Fe	3.5-5.0	-	60	2	0.90	10
BA10	Graphite	Cu	3.5-5.0	$NH_4.NO_3$	4	0	0	2
BA11	Graphite	Cu	3.5-5.0	$NH_4.NO_3$	8	2	10	30
BA12	Graphite	Cu	3.5-5.0	$NH_4.NO_3$	12	2	10	10
BA13	Graphite	Cu	3.5-5.0	$NH_4.NO_3$	16	3	15	10
BA14	Graphite	Cu	3.5-5.0	$NH_4.NO_3$	20	4	20	10
BA15	Graphite	Cu	3.5-5.0	$NH_4.NO_3$	24	5	25	10
BA16	Graphite	Fe	3.5	CH_3COOH	24	5	2.25	10
BA17	Ti	Fe	3.5	CH_3COOH	60	3	1.35	10
BA18	Graphite	Cu	3.5	CH_3COOH	24	5	25	10
BA19	Graphite	Fe	3.5-5.0	$NH_4.NO_3$	24	5	2.25	10
BA20	Graphite	Cu	3.5-5.0	$NH_4.NO_3$	30	5	25	10
BA21	Graphite	Cu	3.5-5.0	$NH_4.Cl$	24	5	25	10
BA22	Graphite	Cu	3.5-5.0	$NH_4.Cl$	24	5	25	10

The initial concentration of boric acid was set at 190 g/L which corresponds to its maximum solubility values to achieve a saturated solution at 80°C. The bath temperature was varied between 60 and 100°C and it was determined due to rapid crystallization of boric acid in low temperatures and safety issues in high temperatures. The bath volume and accordingly the electrode surface area changed among experiments, thus the current densities changed. The electrode dimensions for

800 ml glass bath were 100x20x0.2 mm where these dimensions were 150x150x2 mm for 4 liters polypropylene bath.

In addition to those listed tests, hundreds of other experiments were performed to achieve a stable and reproducible experimental data. The determination pH, solute concentration and bath temperature changes were performed during the experiments with duration of 30 minutes which are BA01, BA07 and BA11. The measurements of pH, $\%B_2O_3$ and temperature with respect to time were taken (Tables 4.2, 4.3 and 4.4). The B_2O_3 content of initial samples were varied between 51.78 and 53.89. Bath temperature changed with time and this trend differs with respect to electrodes selected. Titanium electrodes with high electrical resistivity provided high voltage levels in electro-deposition experiments, therefore the bath temperature increased to 78^oC from initial temperature of 98^oC due to excess heating of titanium electrodes.

Table 4.2 Measurements of pH, $\%B_2O_3$ and bath temperature with respect to time for BA01

Time (min.)	% B_2O_3	Bath Temp. (^oC)	pH
0	52.65	75	3.5
2	51.78	76	3.5
4	50.07	78	3.6
6	48.65	81	3.7
8	36.98	81	4.1
10	24.04	82	4.2
15	23.78	84	4.5
20	23.05	85	4.6
25	23.18	87	5.0
30	22.98	88	4.9

The pH levels also changed with time due to reaction mechanisms and removal of solute from the solution by achieving deposition. During the experiment BA07, no reaction was observed thus the B_2O_3 content remained close to initial concentration at the end of 30 minutes.

Table 4.3 Measurements of pH, $\%B_2O_3$ and bath temperature with respect to time for BA07

Time (min.)	% B_2O_3	Bath Temp. (^oC)	pH
0	53.89	78	3.4
2	52.01	81	3.5
4	50.14	82	3.5
6	50.07	83	3.6
8	49.86	86	3.7
10	49.87	88	3.8
15	49.82	94	3.8
20	49.72	95	3.8
25	48.98	97	3.9
30	48.68	98	3.9

Table 4.4 Measurements of pH, $\%B_2O_3$ and bath temperature with respect to time for BA11

Time (min.)	% B_2O_3	Bath Temp. (^oC)	pH
0	51.78	75	3.4
2	51.36	76	3.3
4	42.31	76	3.4
6	33.74	78	3.5
8	32.45	77	3.8
10	31.96	78	3.9
15	29.54	82	4.2
20	29.52	85	4.4
25	28.93	84	4.8
30	28.90	83	4.5

A buffer solution of acetic acid (CH_3COOH) to keep a low pH level and an additional catalyst of ammonium nitrate ($NH_4.NO_3$) or ammonium chloride ($NH_4.Cl$) as N source were applied in some experiments.

The XRD analyses of experiments which a deposition is observed and effects of parameters are going to be discussed in “Chapter Five”. Samples of deposited

substrates and images illustrating the progress of deposition for several successful and unsuccessful trials are listed below.

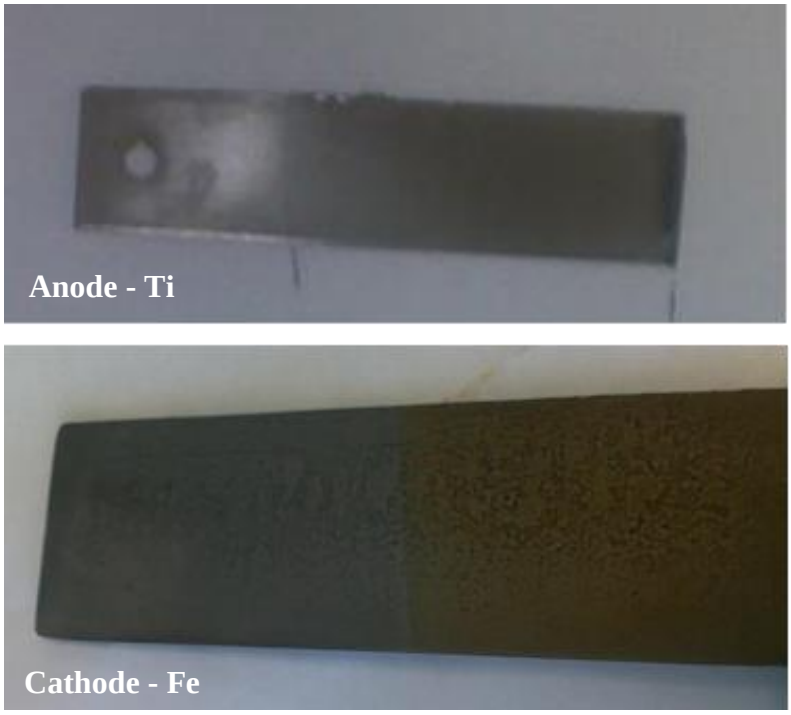

Figure 4.3 Anode and cathode electrodes of BA07 after deposition

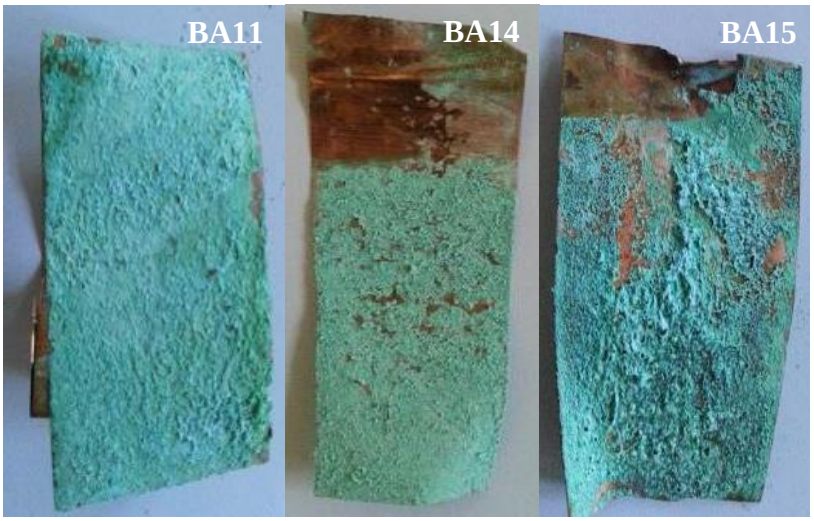

Figure 4.4 Cu cathode electrodes of BA11, BA14 and BA15 after deposition

4.2 Boron End Product Fabrication from Borax Pentahydrate

The summarized design of electro-deposition experiments conducted by using $Na_2B_4O_7.5H_2O$ as solute is listed in Table 4.5. The table represents the experiment code, type of anode and cathode, pH of the solution, additions such as buffer solution or catalyst, voltage set (V), current acquired (A), current density (A/dm^2) and duration of the experiment (min.).

Table 4.5 Electro-deposition experiments conducted by borax pentahydrate ($Na_2B_4O_7.5H_2O$) as solute (175 g/L initial solute concentration, 80^oC initial bath temperature, purified water as solvent)

Code	Anode	Cathode	pH	Addition	V	A	A/dm^2	Duration (min.)
BPH01	Cu	Cu	9-10	-	4	0	0	2
BPH02	Cu	Cu	9-10	-	6	3	15	10
BPH03	Cu	Cu	9-10	-	8	3	15	10
BPH04	Cu	Cu	9-10	-	10	3	15	10
BPH05	Cu	Cu	9-10	-	12	3	15	10
BPH06	Cu	Cu	9-10	-	14	3	15	10
BPH07	Cu	Cu	9-10	-	16	4	20	10
BPH08	Cu	Cu	9-10	-	18	5	25	10
BPH09	Cu	Cu	9-10	-	20	5	25	10
BPH10	Cu	Cu	9-10	-	22	5	25	10
BPH11	Cu	Cu	9-10	-	24	7	35	10&30
BPH12	Cu	Cu	9-10	-	26	7	35	10
BPH13	Cu	Cu	9-10	-	28	8	40	10
BPH14	Cu	Cu	9-10	-	30	7	35	10
BPH15	Cu	Cu	9-10	-	14	3	15	10
BPH16	Cu	Cu	9-10	-	14	5	25	10
BPH17	Cu	Cu	9-10	-	14	7	35	10
BPH18	Cu	Cu	9-10	-	14	9	45	10
BPH19	Cu	Cu	9-10	-	14	11	55	10
BPH20	Cu	Cu	9-10	-	18	13	65	10
BPH21	Cu	Cu	9-10	-	20	15	75	10
BPH22	Cu	Cu	9-10	-	20	17	85	2

BPH23	Graphite	Fe	9-10	-	4	1	0.45	30
BPH24	Graphite	Fe	9-10	-	6	1	0.45	10
BPH25	Graphite	Fe	9-10	-	8	1	0.45	10
BPH26	Graphite	Fe	9-10	-	18	4	1.80	10
BPH27	Graphite	Fe	9-10	-	20	5	2.25	10
BPH28	Fe	Fe	9-10	-	20	1	0.45	10
BPH29	Ti	Ti	9-10	-	60	1	5	10
BPH30	Ti	Ti	9-10	-	160	2	10	10
BPH31	Ti	Ti	9-10	-	170	4	20	10
BPH32	Ti	Fe	9-10	-	100	1	0.45	10
BPH33	Ti	Fe	9-10	-	130	2	0.45	10
BPH34	Ti	Fe	9-10	-	150	4	1.80	10
BPH35	Cu	Cu	9-10	-	70	15	6.75	10
BPH36	Cu	Cu	9-10	-	70	18	8.10	10
BPH37	Cu	Cu	9-10	-	70	18	8.10	10
BPH38	Graphite	Cu	9-10	-	12	3	1.35	10
BPH39	Graphite	Cu	4.5	$C_6H_8O_7$	24	9	45	10
BPH40	Cu	Cu	9-10	Active C	24	7	35	10
BPH41	Cu	Cu	9-10	NaSCN	24	7	35	10
BPH42	Graphite	Cu	4	CH_3COOH	24	10	50	10
BPH43	Cu	Cu	9-10	CO_2	24	10	50	10
BPH44	Al	Al	9-10	-	20	0	0	2
BPH45	Graphite	Al	9-10	-	20	0	0	2
BPH46	Al	Cu	9-10	-	20	0	0	2
BPH47	Pb	Pb	9-10	-	20	1	0.45	10
BPH48	Graphite	Pb	9-10	-	20	1	0.45	10
BPH49	Pb	Cu	9-10	-	20	1	0.45	2
BPH50	S.S.	S.S.	9-10	-	170	1	0.45	2
BPH51	Graphite	S.S.	9-10	-	150	1	0.45	2
BPH52	S.S.	Cu	9-10	-	170	1	0.45	2

The initial concentration of borax pentahydrate was set at 175 g/L which corresponds to its maximum solubility values to achieve a saturated solution at 80^{o}C. The bath temperature was varied between 60 and 100^{o}C and it was determined due to

rapid crystallization and precipitation of borax pentahydrate in low temperatures and safety issues in high temperatures. The bath volume and accordingly the electrode surface area changed among experiments, thus the current densities changed. The electrode dimensions for 800 ml glass bath were 100x20x0.2 mm where these dimensions were 150x150x2 mm for 4 liters polypropylene bath.

The experiments listed in Table 4.5 only represent the stable and reproducible experimental data apart from additional many other experiments. The determination pH, solute concentration and bath temperature changes were performed during the experiments with duration of 30 minutes which are BPH11 and BPH23. The measurements of pH, $\%B_2O_3$ and temperature with respect to time were taken (Table 4.6 and 4.7).

The B_2O_3 content of initial samples of BPH11 and BPH23 were 49.63 and 47.65, respectively. Bath temperature changed with time and this trend differs with respect to electrodes selected. The pH levels remained natural except experiments that a buffer solution of catalyst was used.

Table 4.6 Measurements of pH, $\%B_2O_3$ and bath temperature with respect to time for BPH11

Time (min.)	**% B_2O_3**	**Bath Temp. (^oC)**	**pH**
0	49.63	78	9.3
2	47.63	80	9.3
4	47.32	80	9.4
6	39.67	81	9.4
8	22.35	82	9.3
10	22.14	82	9.2
15	22.25	84	9.2
20	21.96	87	9.1
25	21.02	88	9.2
30	19.85	88	9.1

Table 4.7 Measurements of pH, %B_2O_3 and bath temperature with respect to time for BPH23

Time (min.)	% B_2O_3	Bath Temp. (^oC)	pH
0	47.65	79	9.4
2	47.01	79	9.3
4	45.98	81	9.3
6	44.12	81	9.1
8	40.54	81	9.0
10	40.12	82	8.8
15	40.10	81	8.5
20	39.58	81	8.6
25	39.01	83	8.5
30	38.65	84	8.5

The XRD analyses of experiments which a deposition is observed and effects of parameters are going to be discussed in "Chapter Five". Samples of deposited substrates and images illustrating the progress of deposition for several successful and unsuccessful trials are listed below (Figures 4.5 to 4.13).

Figure 4.5 Cu cathode electrode of BPH04 after deposition

Figure 4.6 Cu cathode electrode of BPH09 after deposition

Figure 4.7 Cu cathode electrode of BPH10 after deposition

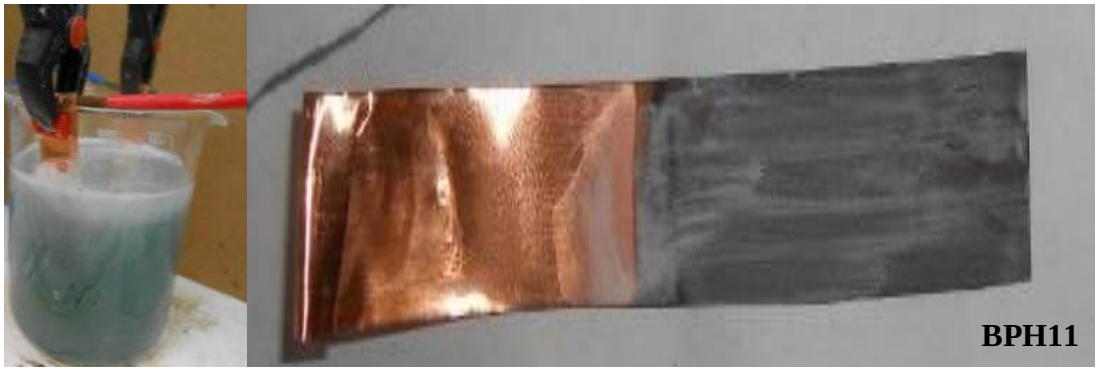

Figure 4.8 Cu cathode electrode of BPH11 after deposition

Figure 4.9 Cu cathode electrode of BPH13 after deposition

Figure 4.10 Cu cathode electrode of BPH14 after deposition

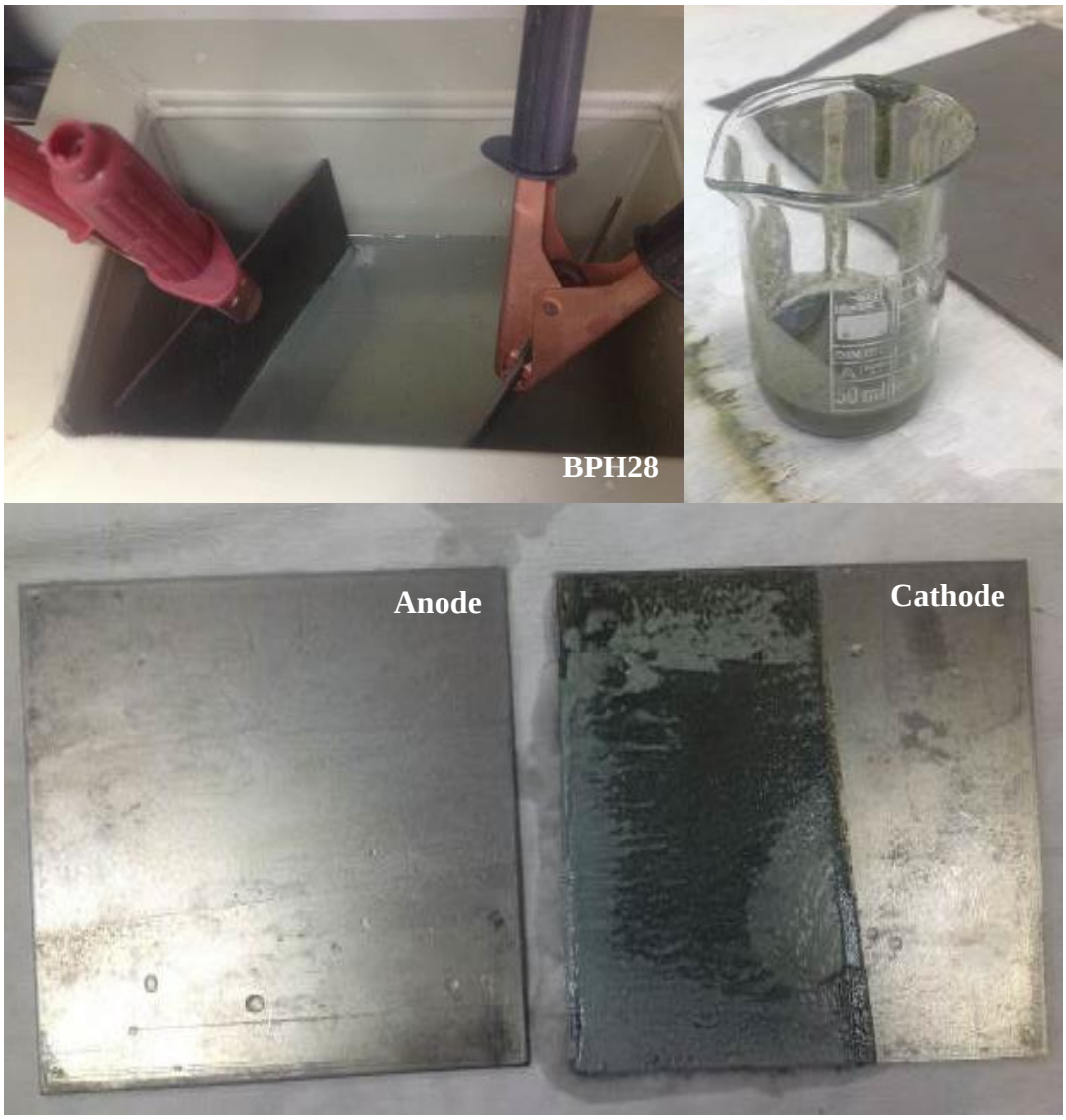

Figure 4.11 Fe electrodes of BPH28 after deposition

Figure 4.12 Cu cathode electrodes of BPH35, BPH36 and BPH37 after deposition

Figure 4.13 Ti anode and cathode electrodes of BPH31 after deposition

The touchscreen on the redressor has many capabilities. The touchscreen panel of redressor displays the voltage, current, temperature measured by thermocouple and duration of the experiment. The adjustment buttons for voltage and ampere are shown in yellow. The blue and red buttons are for start and stop functions. The voltage to be experimented can be entered in the touchscreen digitally. When the experiment is ready, start button is pressed and the main control screen indicates the voltage and current. Several images are given below (Figures 4.14) indicating the experimental parameters on the touchscreen and fluctuations in V and A.

Figure 4.14 Touchscreen images of several experiments

4.3 Boron End Product Fabrication from Borax Decahydrate

The simplified design of electro-deposition experiments conducted by using $Na_2B_4O_7.10H_2O$ as solute is listed in Table 4.8. The table represents the experiment code, type of anode and cathode, pH of the solution, additions such as buffer solution or catalyst, voltage set (V), current acquired (A), current density (A/dm^2) and duration of the experiment (min.).

Table 4.8 Electro-deposition experiments conducted by borax decahydrate ($Na_2B_4O_7.10H_2O$) as solute (200 g/L initial solute concentration, 80^oC initial bath temperature, purified water as solvent)

Code	Anode	Cathode	pH	Addition	V	A	A/dm^2	Duration (min.)
BDH01	Cu	Cu	9-10	-	4	1	5	10
BDH02	Cu	Cu	9-10	-	6	1	5	10
BDH03	Cu	Cu	9-10	-	8	2	10	10
BDH04	Cu	Cu	9-10	NaSCN	10	2	10	10
BDH05	Cu	Cu	9-10	NaSCN	12	2	10	10
BDH06	Cu	Cu	9-10	NaSCN	14	2	10	30
BDH07	Cu	Cu	9-10	NaSCN	16	3	15	10
BDH08	Cu	Cu	9-10	NaSCN	18	4	20	10
BDH09	Cu	Cu	9-10	NaSCN	20	5	25	10
BDH10	Cu	Cu	9-10	-	12	1	5	10
BDH11	Cu	Cu	9-10	-	12	2	10	10
BDH12	Cu	Cu	9-10	-	12	3	15	10
BDH13	Cu	Cu	9-10	-	12	4	20	10
BDH14	Cu	Cu	9-10	-	13	5	25	30
BDH15	Cu	Cu	9-10	-	13	6	30	10

The initial concentration of borax decahydrate was set at 200 g/L which corresponds to its maximum solubility values to achieve a saturated solution at 80^oC. The bath temperature was varied between 60 and 100^oC and it was determined due to rapid crystallization and precipitation of borax decahydrate in low temperatures and safety issues in high temperatures. The bath volume and accordingly the electrode surface area changed among experiments, thus the current densities changed. The

electrode dimensions for 800 ml glass bath were 100x20x0.2 mm where these dimensions were 150x150x2 mm for 4 liters polypropylene bath.

The experiments listed in Table 4.15 only represent the stable and reproducible experimental data apart from additional many other experiments. The determination pH, solute concentration and bath temperature changes were performed during the experiments with duration of 30 minutes which are BDH06 and BDH14. The measurements of pH, $\%B_2O_3$ and temperature with respect to time were taken (Table 4.9 and 4.10).

The B_2O_3 content of initial samples of BDH06 and BDH14 were 39.23 and 38.45, respectively. Bath temperature changes with time and the pH levels remained natural through all experiments.

The XRD analyses of experiments which a deposition is observed and effects of parameters are going to be discussed in "Chapter Five". Samples of deposited substrates and images illustrating the progress of deposition for several successful and unsuccessful trials are listed below (Figures 4.15 to 4.19).

Table 4.9 Measurements of pH, $\%B_2O_3$ and bath temperature with respect to time for BDH06

Time (min.)	% B_2O_3	Bath Temp. (^oC)	pH
0	39.23	79	9.3
2	37.52	80	9.2
4	32.99	80	9.2
6	28.54	82	9.2
8	22.45	84	9.3
10	20.14	84	9.2
15	19.98	84	9.1
20	19.55	83	9.1
25	19.02	84	9.0
30	18.45	85	9.1

Table 4.10 Measurements of pH, %B_2O_3 and bath temperature with respect to time for BDH14

Time (min.)	% B_2O_3	Bath Temp. (^oC)	pH
0	38.45	80	9.2
2	36.41	81	9.2
4	34.14	81	9.2
6	32.45	82	9.3
8	30.21	82	9.3
10	30.11	84	9.4
15	30.14	85	9.4
20	29.92	89	9.3
25	29.83	90	9.4
30	29.85	90	9.3

Figure 4.15 Cu cathode electrode of BDH05 after deposition

Figure 4.16 Cu cathode electrode of BDH06 after deposition

Figure 4.17 Cu cathode electrode of BDH09 after deposition

Figure 4.18 Cu cathode electrode of BDH11 after deposition

Figure 4.19 Cu cathode electrode of BDH14 after deposition

CHAPTER FIVE
RESULTS AND DISCUSSION

The results of hundreds of electro-deposition experiments with different parameters were performed. Chemical analyses, pH and bath temperature tracing, XRD analyses, removal of B_2O_3 from the solution, SEM analysis and eventually particle size distribution evaluations were applied to obtain the optimum parameters of boron end product fabrication from boron derivatives. Mainly, the phases of B_4C, $B_{13}C_2$, BC_5, B_{28} and BN were determined in addition to impurities from substrates such as Fe and Cu phases. The results of the experiments which a deposition could not be achieved were also evaluated. The evaluations of experimental results are categorized according to the solutes used. The constant parameters in all experiments were purified water as solvent and initial bath temperature of approximately 80^oC. The bath temperature was set at 80^oC and the initial concentrations of solutes were determined accordingly with respect to their solubilities at that temperature. The bath temperatures of 25, 40 and 60^oC were also investigated through electro-deposition experiments; however a stable solution could not be achieved at lower temperatures than 80^oC due to rapid crystallization and precipitation issues. The dissolved B_2O_3 amounts were investigated for both boric acid and borax pentahydrate with respect to bath temperature to achieve the most stable and saturated solution (Figure 5.1).

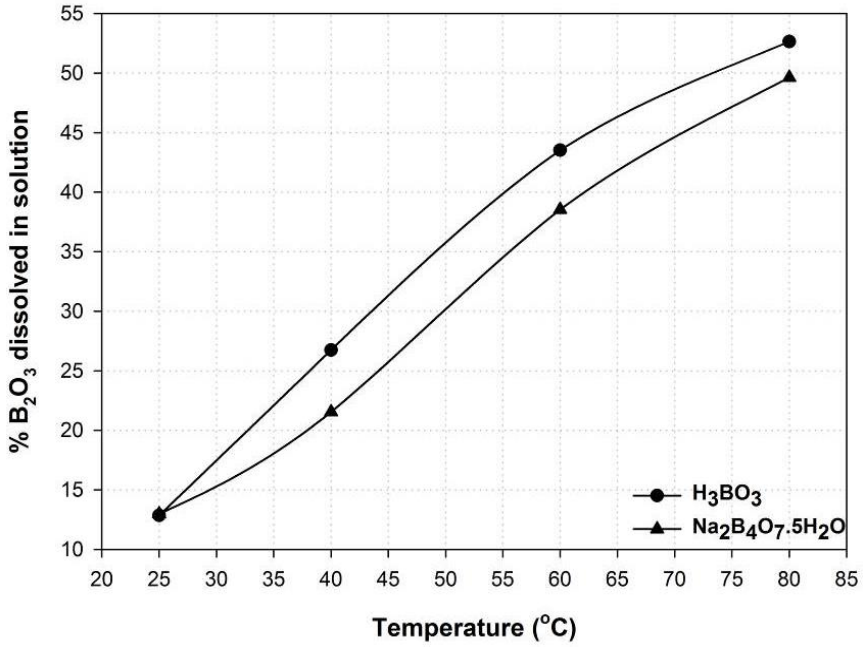

Figure 5.1 Dissolved B_2O_3 contents of boric acid and borax pentahydrate in water

5.1 Evaluation of Experiments Conducted with H_3BO_3 as Solute

Initial boric acid concentration of 190 g/L in water was set to achieve a saturated solution regardless of crystallized and/or precipitated solid particles. The determination of pH, solute concentration and bath temperature changes were performed during the experiments with duration of 30 minutes which are BA01, BA07 and BA11. The experimental parameters of these three experiments are listed in Table 5.1 for a reminder.

Table 5.1 Experimental parameters of BA01, BA07 and BA11

Code	Anode	Cathode	pH	Addition	V	A	A/dm^2	Duration (min.)
BA01	Graphite	Fe	3.5-5.0	NH_4.Cl	4	1	0.45	30
BA07	Ti	Fe	3.5-5.0	NH_4.Cl	20	1	0.45	30
BA11	Graphite	Cu	3.5-5.0	$NH_4.NO_3$	8	2	10	30

The B_2O_3 content of initial samples were varied between 51.78 and 53.89. However, the B_2O_3 concentration of solutions changed significantly with time in BA01 and BA11 (Figure 5.2).

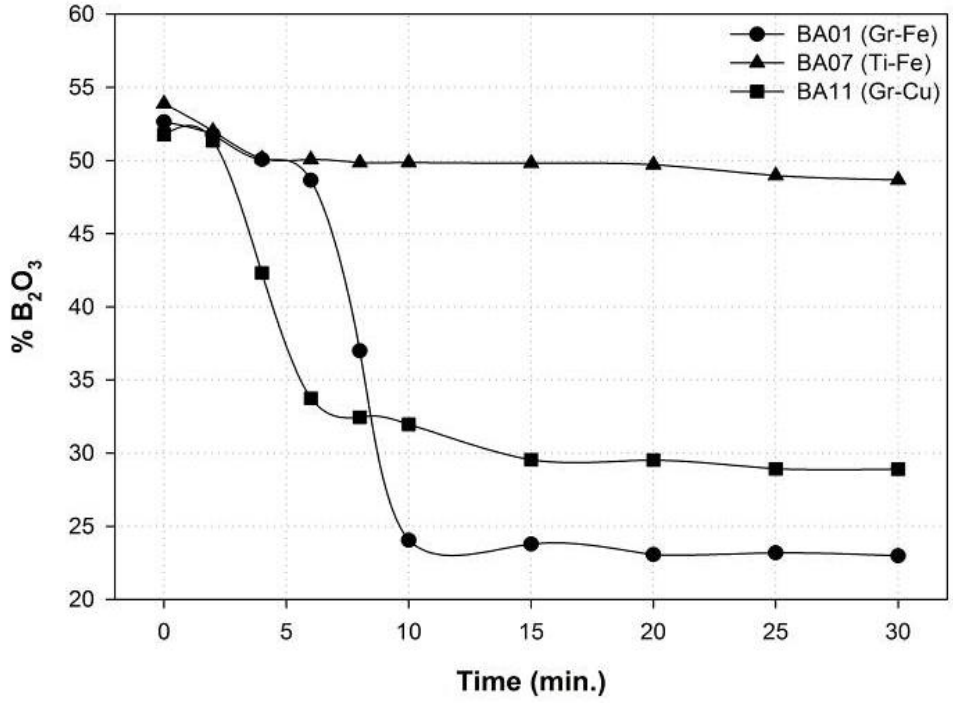

Figure 5.2 B_2O_3 removal trend in electrolytes of BA01, BA07 and BA11 with time

According to chemical analyses of liquid samples taken during experiments in definite intervals, B_2O_3 content of electrolytes in BA01 and BA11 decreased between 2 and 10 minutes. Moreover, deposition was also observed between those intervals during 30 minutes of experiments. The deposition of boron products was proved with significant amount of B_2O_3 removal from the solution.

The change in bath temperature was also traced since the bath temperature level directly affects solubility and indirectly affects pH level. The trend in temperature change differed with respect to electrodes selected (Figure 5.3). Titanium electrode with high electrical resistivity provided high voltage levels in electro-deposition experiments, therefore the bath temperature increased to 78°C from initial temperature of 98°C in BA07. In experiments BA01 and BA11, slight increase and fluctuations were observed in bath temperatures during 30 minutes.

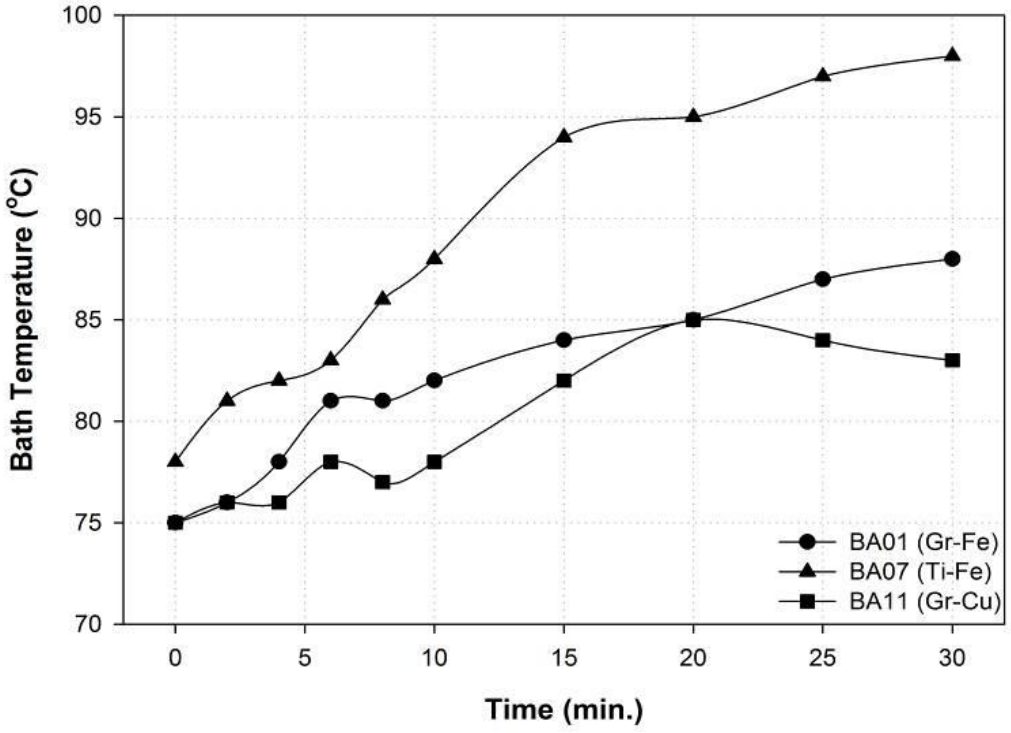

Figure 5.3 Change in bath temperature with respect to time for BA01, BA07 and BA11

The pH levels also changed with time due to reaction mechanisms and removal of solute from the solution by achieving deposition (Figure 5.4). The removal and decomposition of boric acid from the solution also affected the bath pH level. As experiments proceeded the pH level of bath tended to rise to neutral “salt” level.

During the experiment BA07, no reaction was observed thus the B_2O_3 content remained close to initial concentration at the end of 30 minutes as well as pH level.

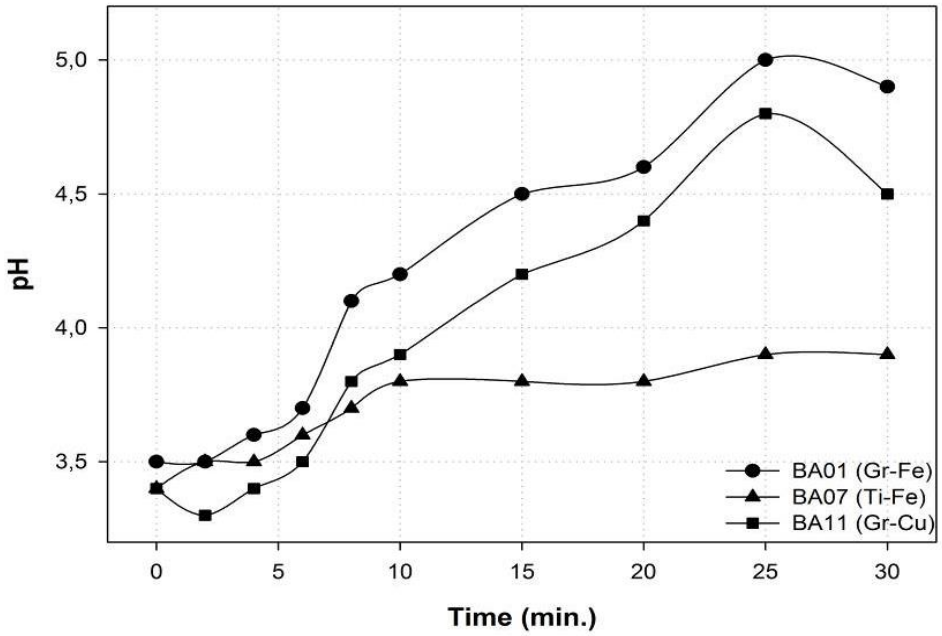

Figure 5.4 Change in pH level with respect to time for BA01, BA07 and BA11

The natural pH levels detected and remained as so in many experiments. Although due to some fluctuations in bath pH level during experiments, a buffer solution of acetic acid (CH_3COOH) was used in BA16, BA17 and BA18 to keep pH level at 3.5. As a result, no deposition was achieved in those experiments. Addition of nitrogen (N) source as ammonium nitrate ($NH_4.NO_3$) and ammonium chloride ($NH_4.Cl$) provided positive results in BN formation. The sample results of experiment set BA are given below.

To begin with, in experiment BA01 with parameters listed in Table 5.2, a successful deposition on Fe cathode was achieved with addition of ammonium chloride and the coated substrate was analyzed by XRD to determine the phases formed (Figure 5.5).

Table 5.2 Experimental parameters of BA01

Code	Anode	Cathode	pH	Addition	V	A	A/dm^2	Duration (min.)
BA01	Graphite	Fe	3.5-5.0	$NH_4.Cl$	4	1	0.45	30

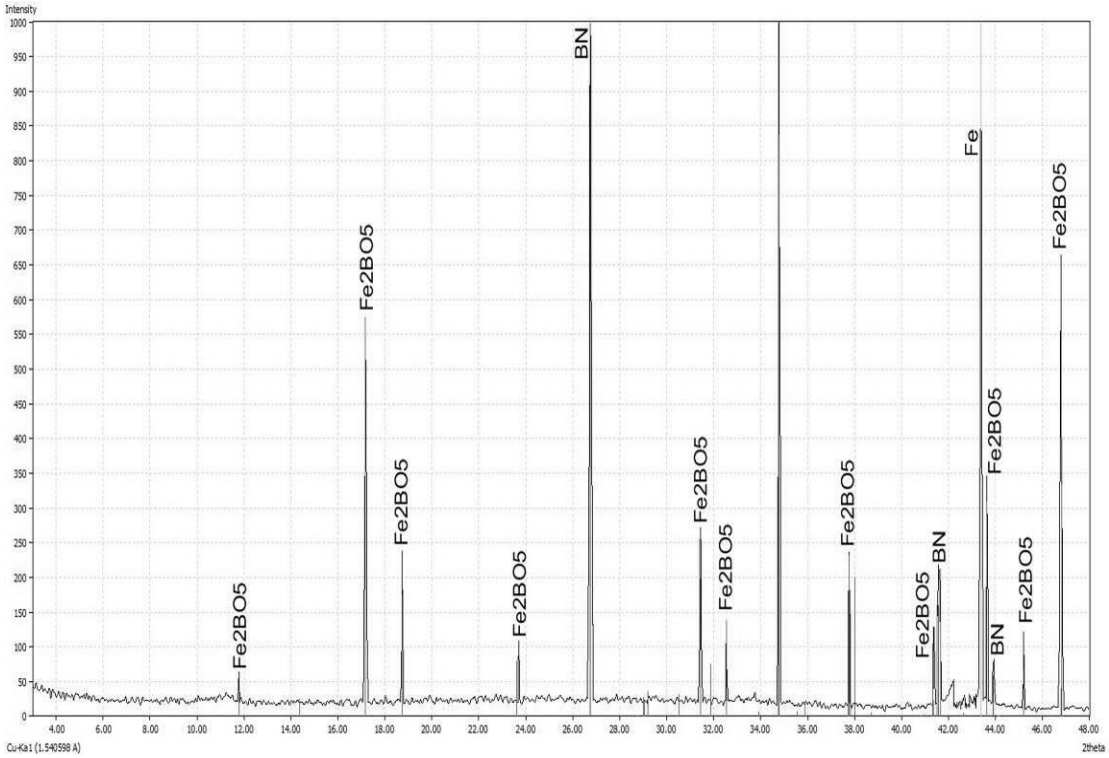

Figure 5.5 XRD analysis of deposited Fe cathode of BA01

The formation of BN, Fe_2BO_5 and Fe phases were determined as a result of XRD analysis. The impurities from the substrate and not fully deposited parts of the electrode revealed Fe_2BO_5 and Fe phases. The formation of BN with three main peaks was proved and the removal of B_2O_3 from the solution was supported by formation of BN and Fe_2BO_5.

The SEM analysis of the substrate revealed that the size of particles deposited reached micron and nano levels (Figure 5.6).

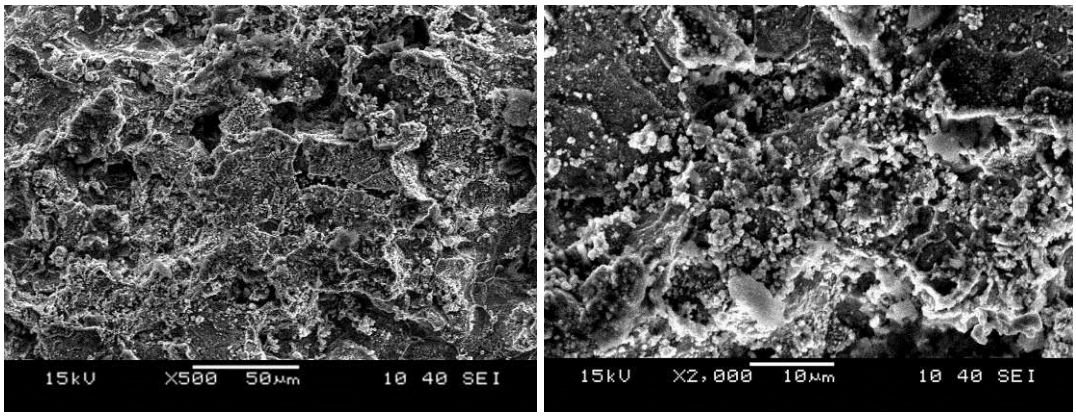

Figure 5.6 SEM analysis of deposited Fe cathode of BA01 (x500 & x2000)

In experiment BA11 with parameters listed in Table 5.3, a successful deposition on Cu cathode was achieved with addition of ammonium nitride and the coated substrate was analyzed by XRD to determine the phases formed (Figure 5.7).

Table 5.3 Experimental parameters of BA11

Code	Anode	Cathode	pH	Addition	V	A	A/dm^2	Duration (min.)
BA11	Graphite	Cu	3.5-5.0	$NH_4.NO_3$	8	2	10	30

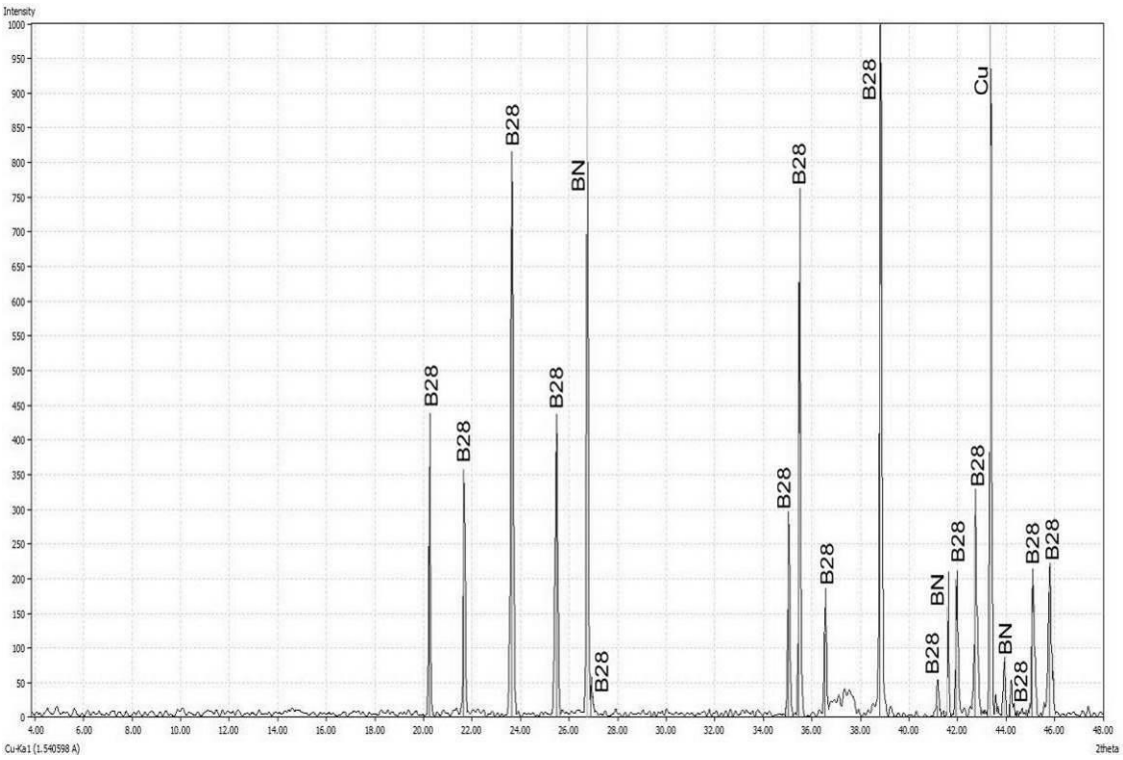

Figure 5.7 XRD analysis of deposited Cu cathode of BA11

The formation of BN, B_{28} and Cu phases were determined as a result of XRD analysis. The impurities from the substrate and not fully deposited parts of the electrode revealed Cu phases. The formation of BN with three main peaks was proved and the removal of B_2O_3 from the solution was supported by formation of BN and B_{28}.

The SEM analysis of the substrate revealed that the size of particles deposited were at micron levels (Figure 5.8).

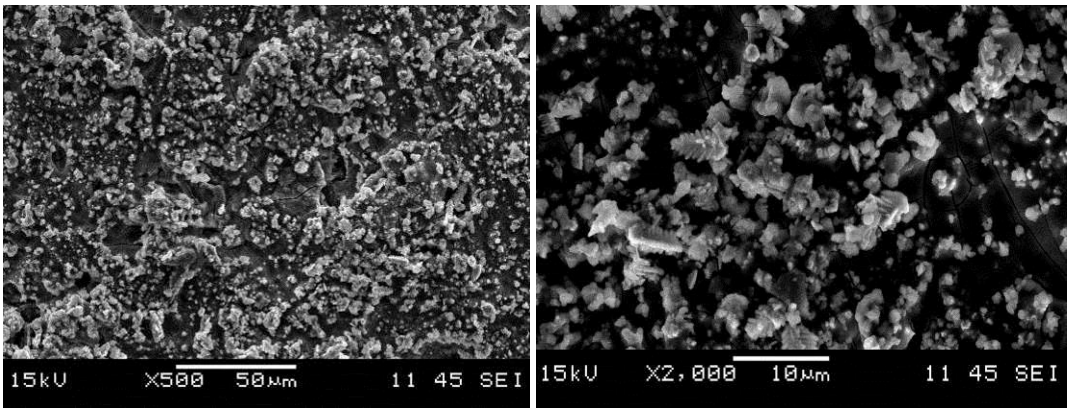

Figure 5.8 SEM analysis of deposited Cu cathode of BA11 (x500 & x2000)

In experiment BA14 with parameters listed in Table 5.4, a successful deposition on Cu cathode was achieved with addition of ammonium nitride and the coated substrate was analyzed by XRD to determine the phases formed (Figure 5.9).

Table 5.4 Experimental parameters of BA14

Code	Anode	Cathode	pH	Addition	V	A	A/dm^2	Duration (min.)
BA14	Graphite	Cu	3.5-5.0	$NH_4.NO_3$	20	4	20	10

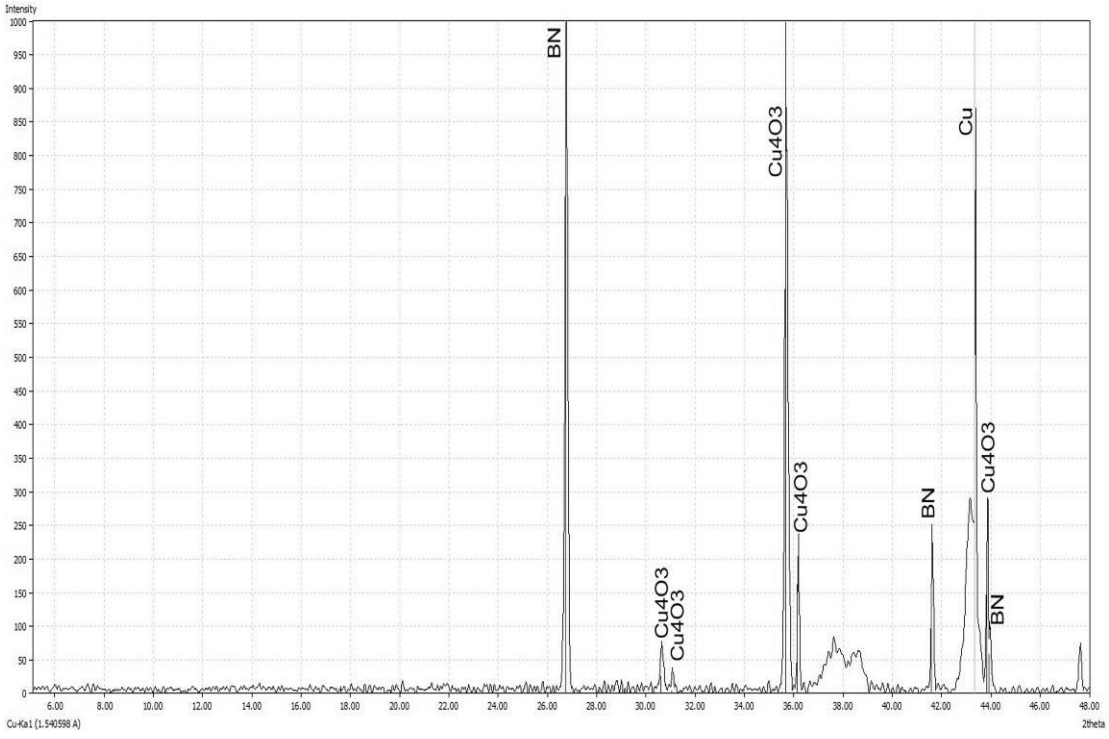

Figure 5.9 XRD analysis of deposited Cu cathode of BA14

The formation of BN, Cu_4O_3 and Cu phases were determined as a result of XRD analysis. The impurities from the substrate and not fully deposited parts of the electrode revealed Cu_4O_3 and Cu phases. The formation of BN with three main peaks was proved.

The SEM analysis of the substrate revealed that the sizes of particles deposited were at micron and nano levels (Figure 5.10).

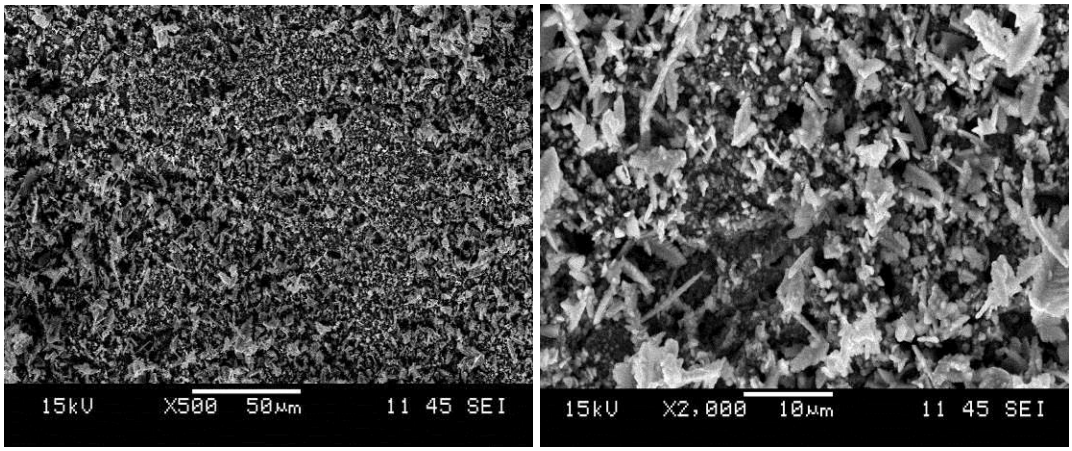

Figure 5.10 SEM analysis of deposited Cu cathode of BA14 (x500 & x2000)

In experiment BA15 with parameters listed in Table 5.5, a successful deposition on Cu cathode was achieved with addition of ammonium nitride and the coated substrate was analyzed by XRD to determine the phases formed (Figure 5.11).

Table 5.5 Experimental parameters of BA15

Code	Anode	Cathode	pH	Addition	V	A	A/dm^2	Duration (min.)
BA15	Graphite	Cu	3.5-5.0	$NH_4.NO_3$	24	5	25	10

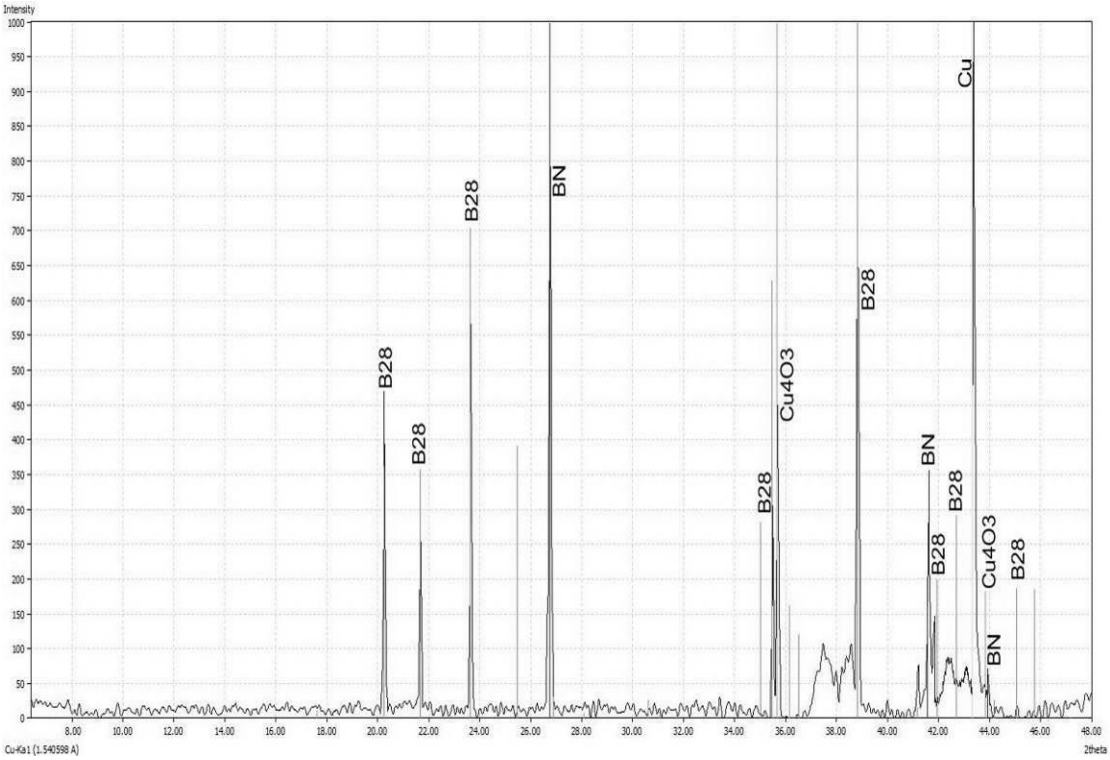

Figure 5.11 XRD analysis of deposited Cu cathode of BA15

The formation of BN, Cu_4O_3, B_{28} and Cu phases were determined as a result of XRD analysis. The impurities from the substrate and not fully deposited parts of the electrode revealed Cu_4O_3 and Cu phases. The formation of BN with three main peaks and B_{28} with several matching main peaks was proved.

In experiment BA20 with parameters listed in Table 5.6, a deposition on Cu cathode was achieved with addition of ammonium nitride and the coated substrate was analyzed by XRD and XPS to determine the phases formed elemental quantification (Figure 5.12 and 5.13).

Table 5.6 Experimental parameters of BA20

Code	Anode	Cathode	pH	Addition	V	A	A/dm^2	Duration (min.)
BA20	Graphite	Cu	3.5-5.0	$NH_4.NO_3$	30	5	25	10

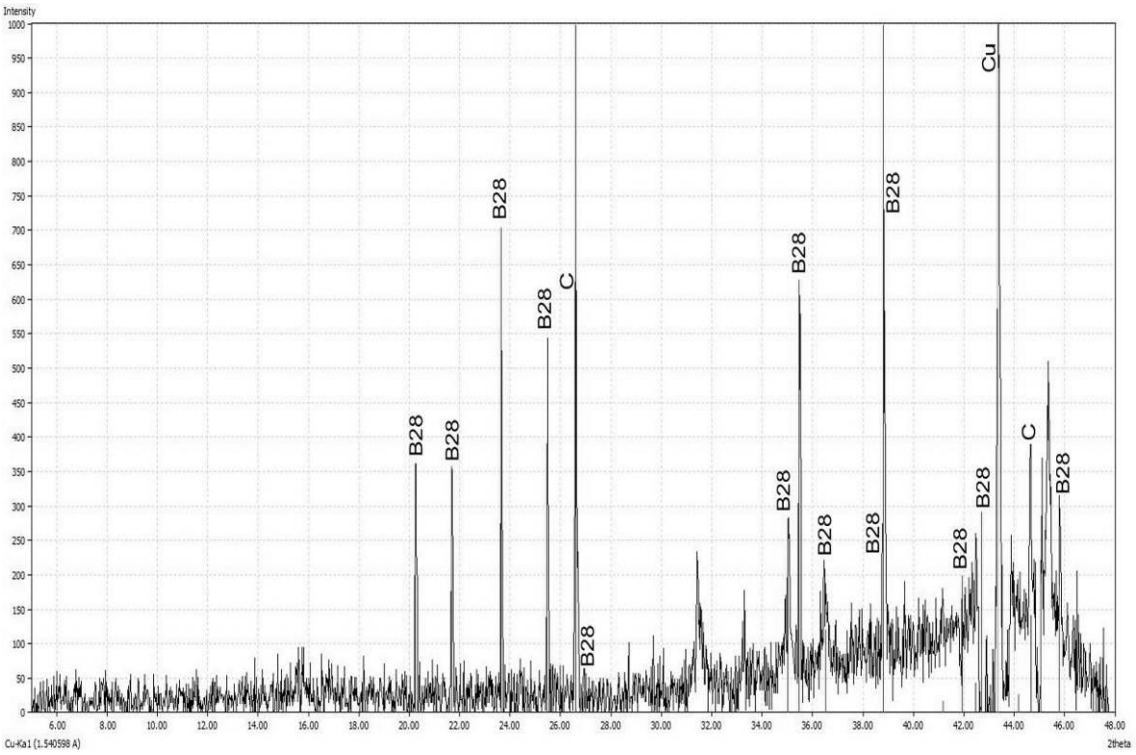

Figure 5.12 XRD analysis of deposited Cu cathode of BA20

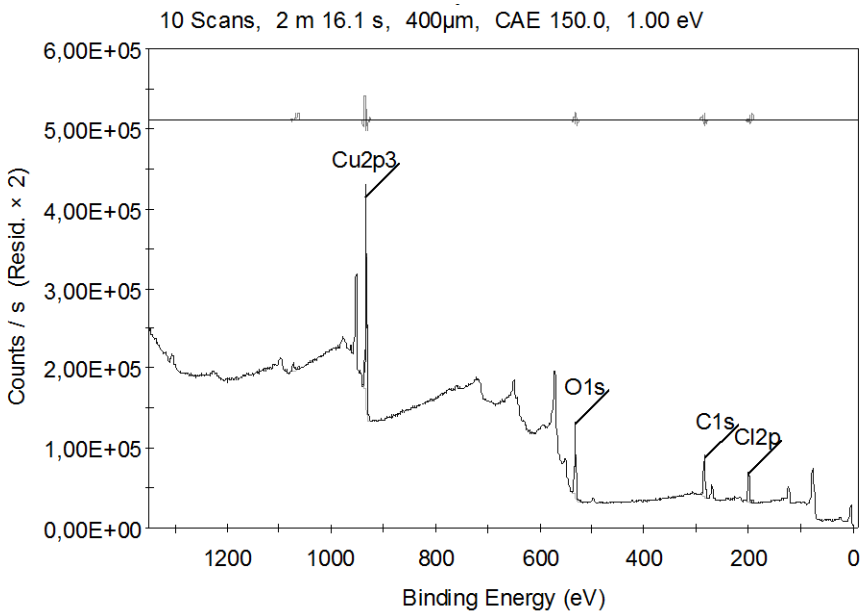

Name	Peak BE	FWHM eV	Area (P) CPS.eV	At. %
C1s	284.64	3.040	182759.49	38.81
O1s	531.47	3.147	351725.34	29.26
Cu2p3	932.73	2.646	820552.11	16.58
Cl2p	199.32	3.397	151317.66	13.50
Na1s	1071.99	3.450	39367.71	1.86

Figure 5.13 XPS analysis of deposited Cu cathode of BA20

The formation of B_{28}, C and Cu phases were determined as a result of XRD analysis. The deposited C and Cu phases were result of electrode corrosion in high voltages. Although formation of B_{28} was determined, XPS analysis did not detect any boron minerals on the substrates. In addition, the low amount of B_2O_3 removal from the solution in BA20 supported the XPS results.

5.2 Evaluation of Experiments Conducted with $Na_2B_4O_7.5H_2O$ as Solute

Initial borax pentahydrate concentration of 175 g/L in water was set to achieve a saturated solution without crystallized and/or precipitated solid particles. The determination of pH, solute concentration and bath temperature changes were performed during the experiments with duration of 30 minutes which are BPH11 and BPH23. The experimental parameters of these two experiments are listed in Table 5.7 for a reminder.

Table 5.7 Experimental parameters of BPH11 and BPH23

Code	Anode	Cathode	pH	Addition	V	A	A/dm^2	Duration (min.)
BPH11	Cu	Cu	9-10	-	24	7	35	30
BPH23	Graphite	Fe	9-10	-	4	1	0.45	30

The B_2O_3 content of initial samples were varied between 49.63 and 47.65. However, the B_2O_3 concentration of BPH11 changed significantly with time. According to chemical analyses of liquid samples taken during experiments in definite intervals, B_2O_3 content of electrolyte in BPH11 decreased between 0 and 8 minutes. The deposition of boron products was proved with significant amount of B_2O_3 removal from the solution. On the contrary, the B_2O_3 content of electrolyte in BPH23 did not undergo such a decrease and dropped to 40.54% at the end of 8 minutes (Figure 5.14).

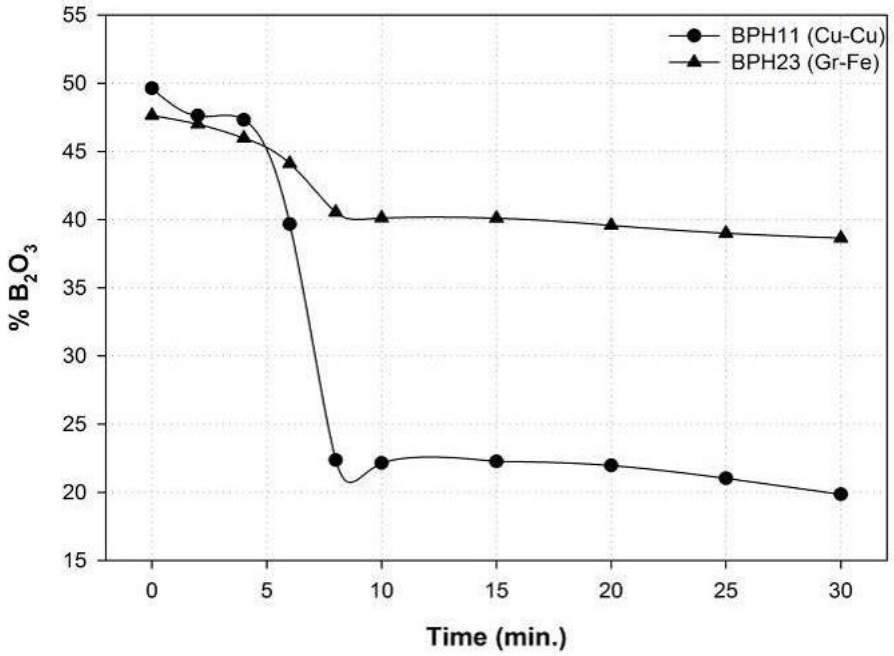

Figure 5.14 B_2O_3 removal trend in electrolytes of BPH11 and BPH23 with time

The trends in temperature change were nearly similar although the electrical resistivity of Cu and Fe differed (Figure 5.15). Iron electrode with high electrical resistivity provided similar voltage levels with copper electrode in electro-deposition experiments, therefore the bath temperature varied between 78°C and 84°C for BPH23 and between 78°C and 88°C for BPH11 regardless of electrode type.

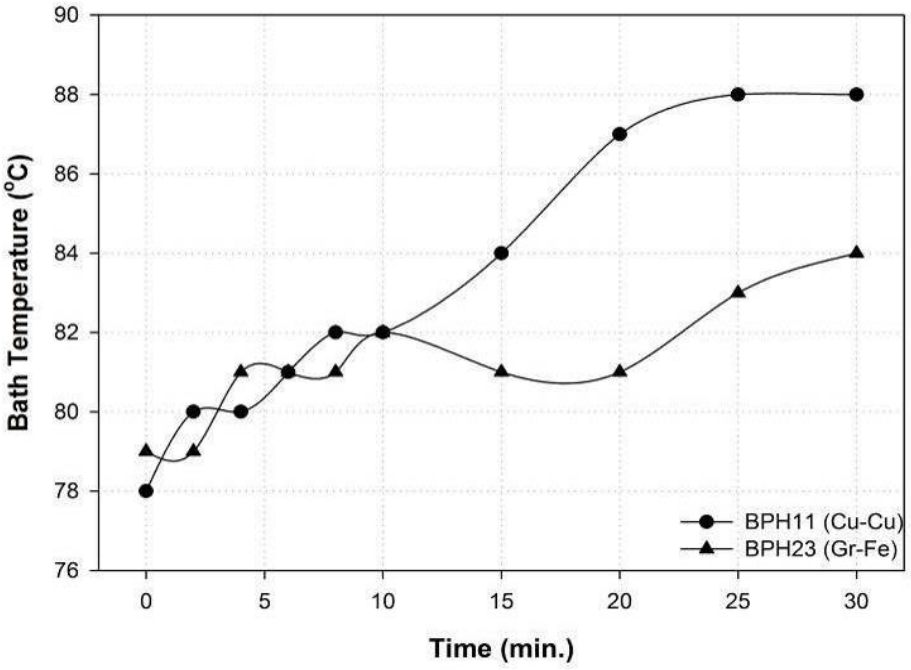

Figure 5.15 Change in bath temperature with respect to time for BPH11 and BPH23

The change in pH levels was also traced for BPH11 and BPH23 during 30 minutes (Figure 5.16). The formation boric acid due to free boron, hydrogen and oxygen ions also affects the bath pH level. As experiments proceeded the pH level of baths tended to decrease to acidic level.

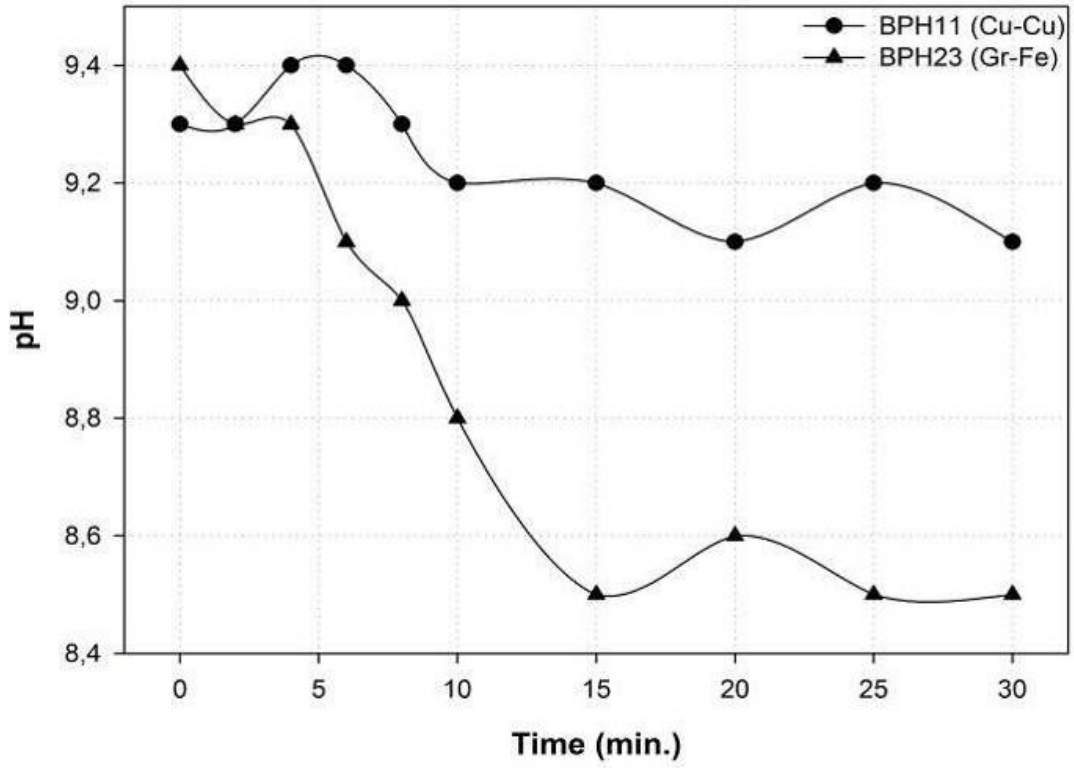

Figure 5.16 Change in pH level with respect to time for BPH11 and BPH23

Buffer solutions of citric acid ($C_6H_8O_7$) and acetic acid (CH_3COOH) were used in BPH39 and BPH42 to provide an acidic electrolyte for electro-deposition. Also, addition of active carbon, carbon dioxide (CO_2) and sodium thiocyanate (NaSCN) were investigated. It was revealed that, addition NaSCN provided positive results as both carbon and nitrogen source.

In experiment BPH04 with parameters listed in Table 5.8, a deposition trial on Cu cathode was performed and the substrate was analyzed by XRD to determine the phases formed (Figure 5.17).

Table 5.8 Experimental parameters of BPH04

Code	Anode	Cathode	pH	Addition	V	A	A/dm^2	Duration (min.)
BPH04	Cu	Cu	9-10	-	10	3	15	10

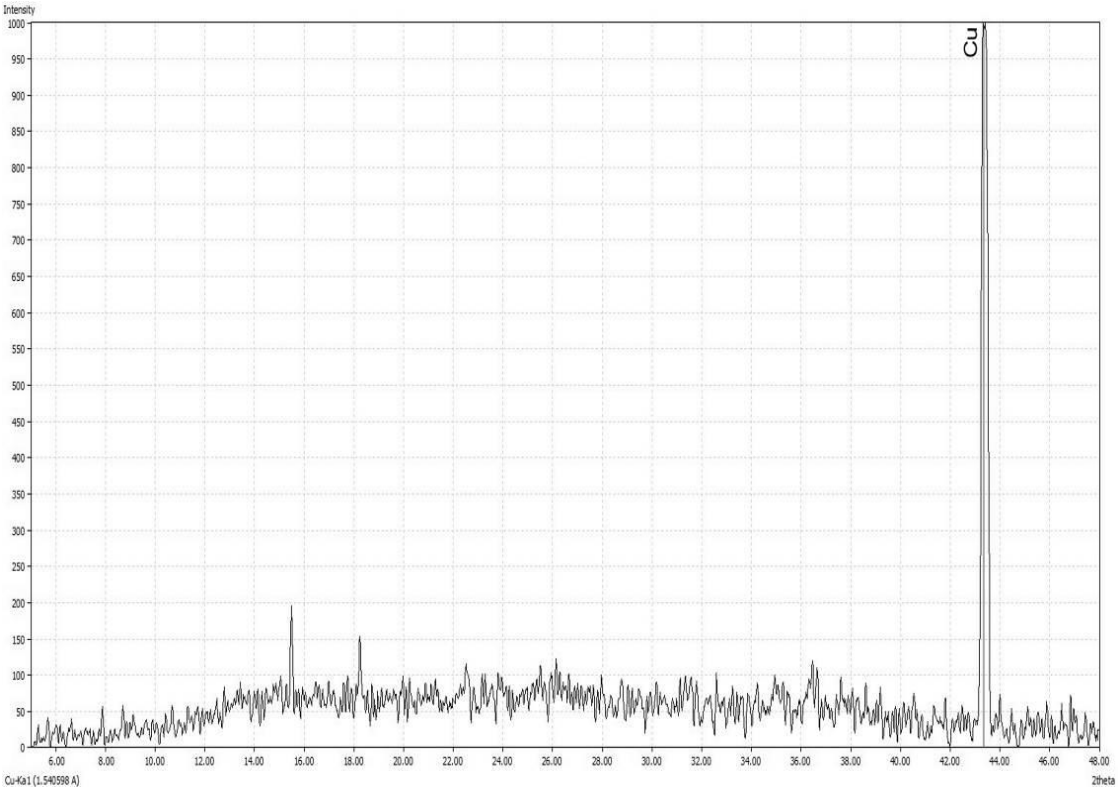

Figure 5.17 XRD analysis of deposited Cu cathode of BPH04

The formation of only Cu phase was detected as a result of XRD analysis. It was revealed that, the deposition of BPH04 was not successful.

In experiment BPH09 with parameters listed in Table 5.9, a successful deposition on Cu cathode was achieved and the coated substrate was analyzed by XRD to determine the phases formed (Figure 5.18).

Table 5.9 Experimental parameters of BPH09

Code	Anode	Cathode	pH	Addition	V	A	A/dm^2	Duration (min.)
BPH09	Cu	Cu	9-10	-	20	5	25	10

The formation of B_{28}, $Na_2B_4O_7$, Cu_2O and Cu phases were determined as a result of XRD analysis. As seen on the XRD, the deposition involved many impurities from substrates and solute. The formation of B_{28} with several matching peaks was detected imprecisely.

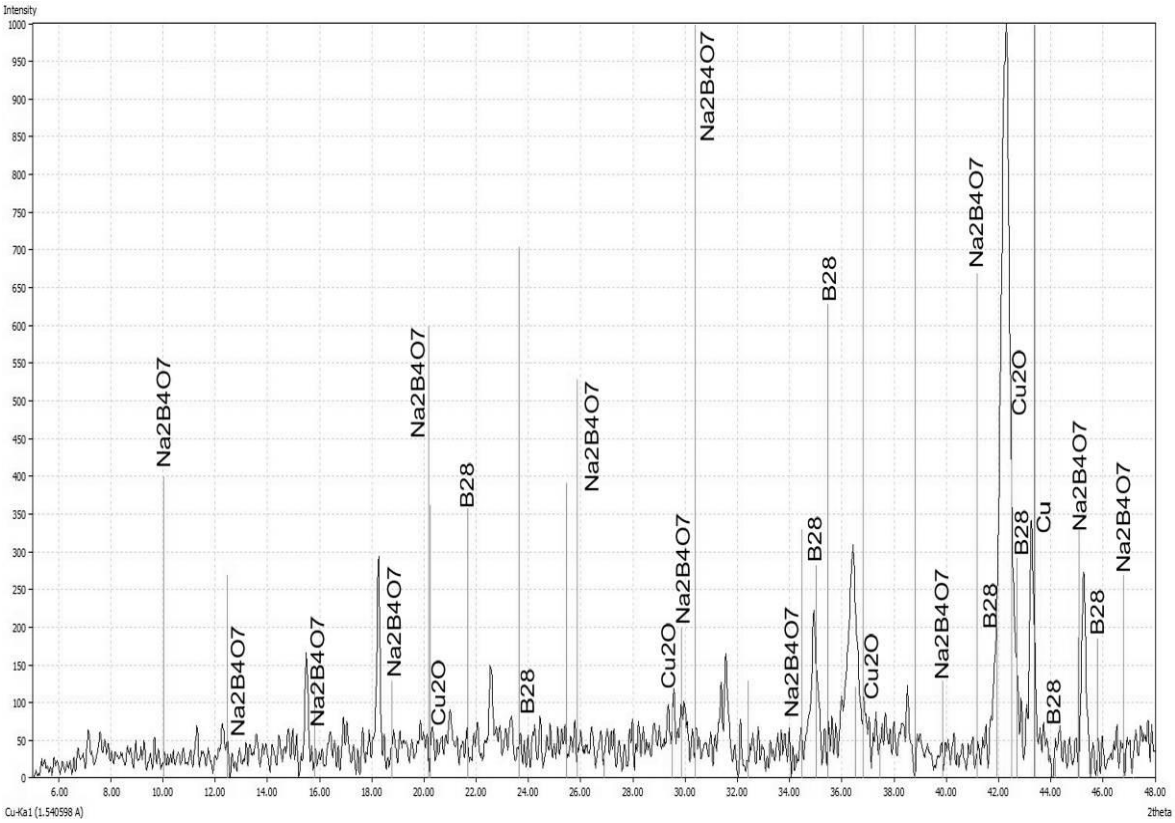

Figure 5.18 XRD analysis of deposited Cu cathode of BPH09

In experiment BPH10 with parameters listed in Table 5.10, a successful deposition on Cu cathode was achieved and the coated substrate was analyzed by XRD to determine the phases formed (Figure 5.19).

Table 5.10 Experimental parameters of BPH10

Code	Anode	Cathode	pH	Addition	V	A	A/dm^2	Duration (min.)
BPH10	Cu	Cu	9-10	-	22	5	25	10

The formation of BC_5, Cu_4O_3 and Cu phases were determined as a result of XRD analysis. The impurities from the substrate and not fully deposited parts of the

electrode revealed Cu_4O_3 and Cu phases. The formation of BC_5 with three main peaks was proved.

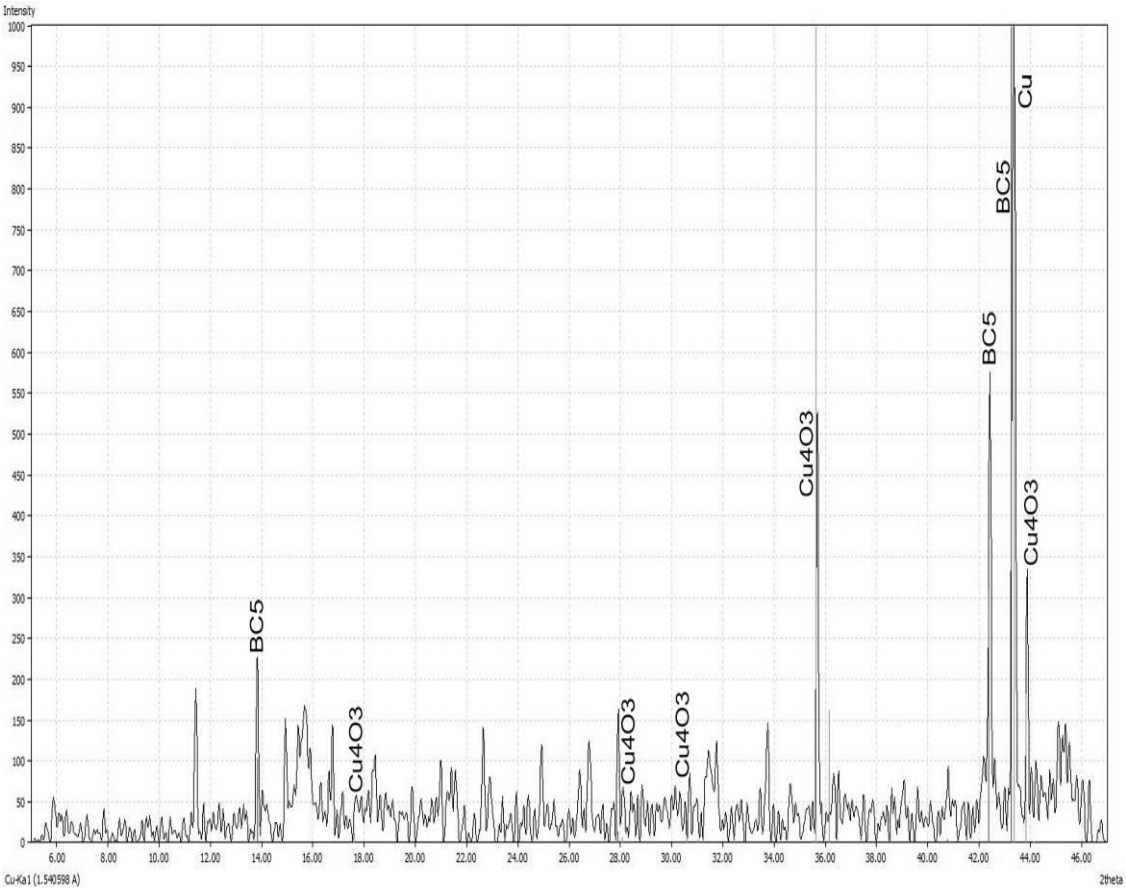

Figure 5.19 XRD analysis of deposited Cu cathode of BPH10

In experiment BPH11 with parameters listed in Table 5.11, a successful deposition on Cu cathode was achieved and the coated substrate was analyzed by XRD to determine the phases formed (Figure 5.20).

Table 5.11 Experimental parameters of BPH11

Code	Anode	Cathode	pH	Addition	V	A	A/dm^2	Duration (min.)
BPH11	Cu	Cu	9-10	-	24	7	35	10

The formation of BC_5 and $CuCO_3$ phases were determined as a result of XRD analysis. The impurities from the substrate, solute and dissolved compounds caused the formation of $CuCO_3$ phase. The formation of BC_5 with several matching peaks

was proved. The analyzed B_2O_3 removal from the electrolyte during deposition also supported formation of boron products on substrates.

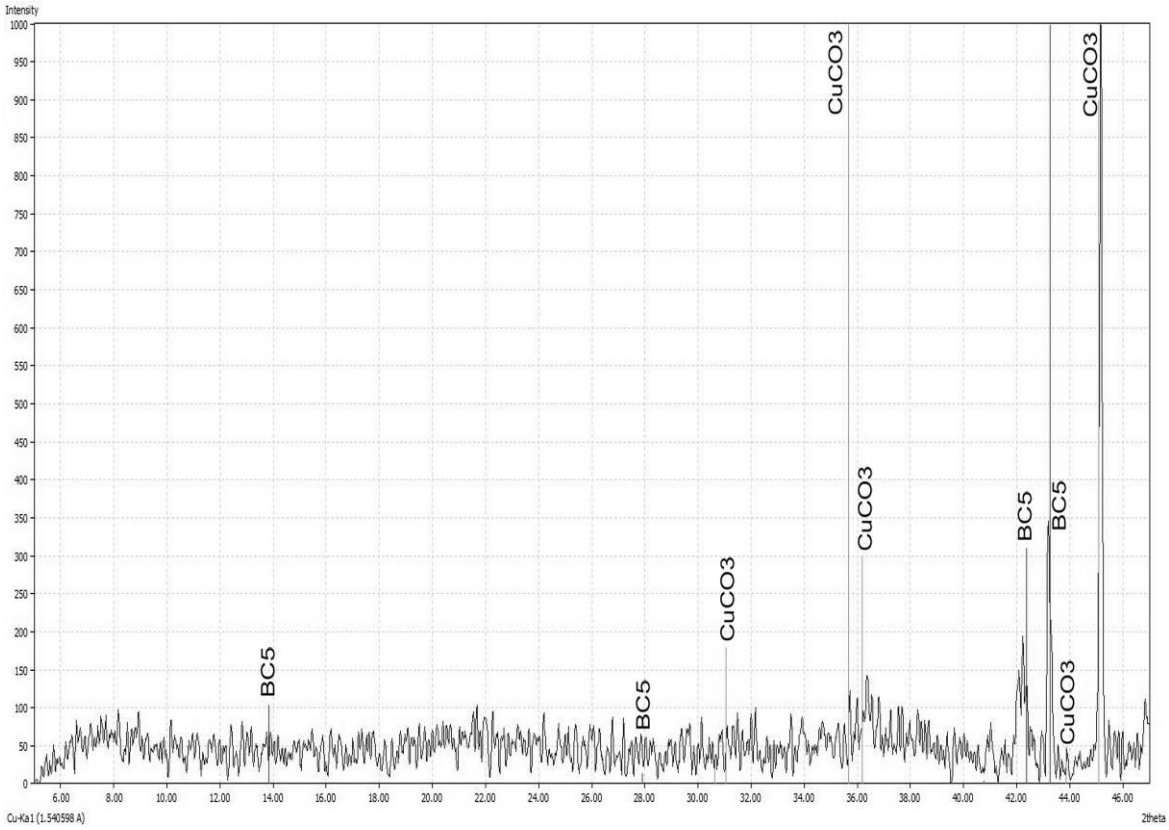

Figure 5.20 XRD analysis of deposited Cu cathode of BPH11

In experiment BPH13 with parameters listed in Table 5.12, a successful deposition on Cu cathode was achieved and the coated substrate was analyzed by XRD to determine the phases formed (Figure 5.21).

Table 5.12 Experimental parameters of BPH13

Code	Anode	Cathode	pH	Addition	V	A	A/dm^2	Duration (min.)
BPH13	Cu	Cu	9-10	-	28	8	40	10

The formation of B4C and Cu phases were determined as a result of XRD analysis. B_4C phases with precisely matching peaks proved the formation of boron carbide.

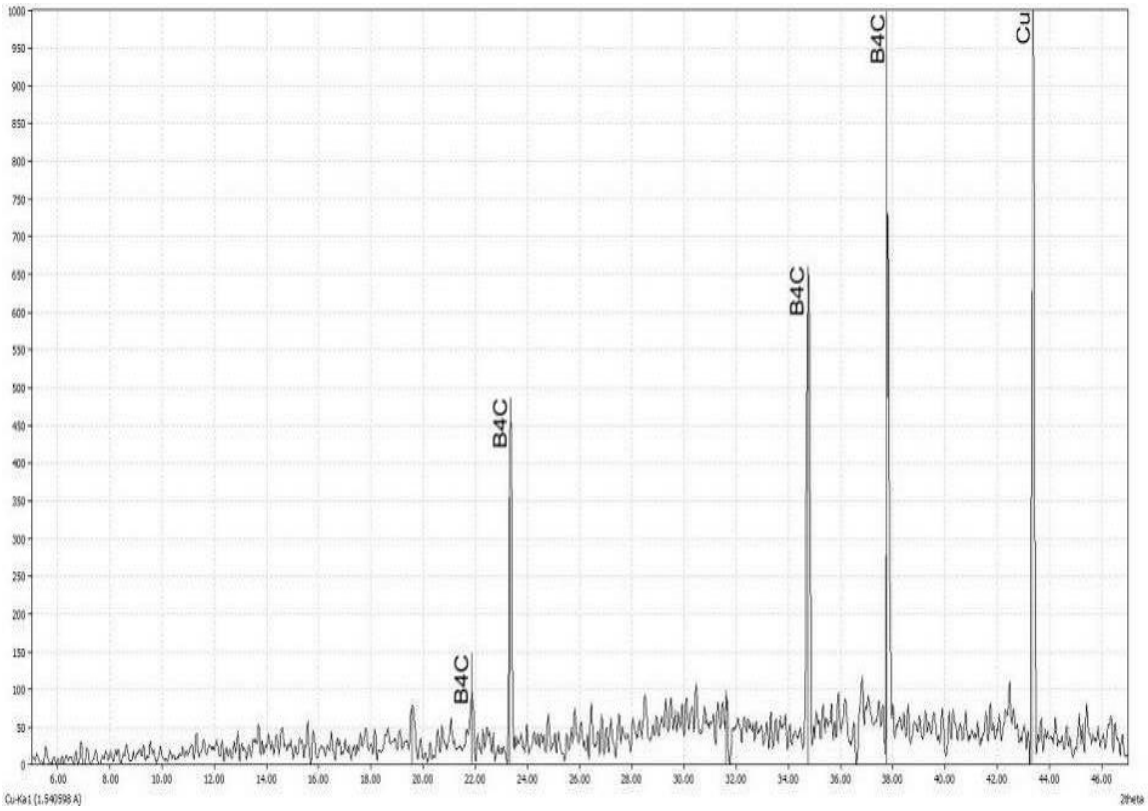

Figure 5.21 XRD analysis of deposited Cu cathode of BPH13

The SEM analysis of the substrate in BPH13 revealed that the sizes of particles deposited were at micron and sub-micron levels (Figure 5.22).

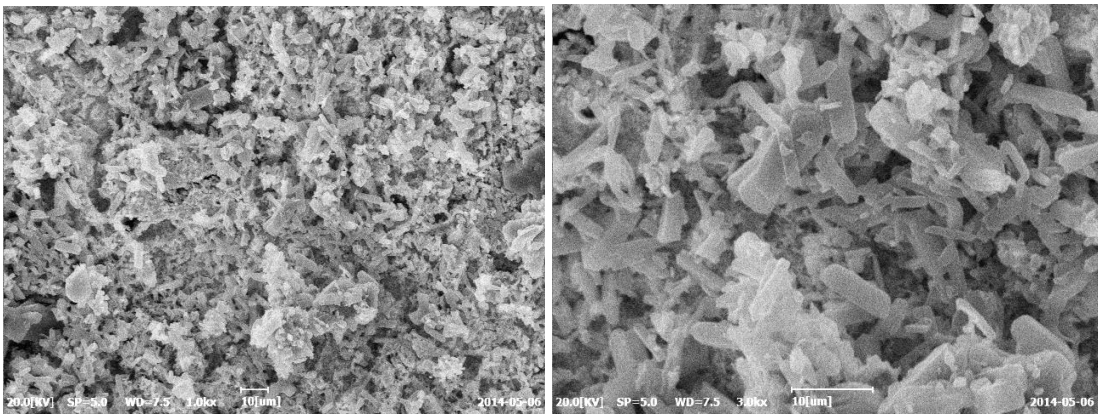

Figure 5.22 SEM analysis of deposited Cu cathode of BPH13 (x1000 & x3000)

As a result of experiment BPH14 with parameters listed in Table 5.13, a successful deposition on Cu cathode was achieved and the coated substrate was analyzed by XRD to determine the phases formed (Figure 5.23).

Table 5.13 Experimental parameters of BPH14

Code	Anode	Cathode	pH	Addition	V	A	A/dm^2	Duration (min.)
BPH14	Cu	Cu	9-10	-	30	7	35	10

The formation of BC_5, B_{28}, Cu_2O and Cu phases were determined as a result of XRD analysis. The formation of BC_5 with exactly matching peaks was proved. In addition several matching peaks of B_{28} revealed its formation besides impurities of Cu and Cu oxides. The XPS analysis supported the content of B, C, O and Cu on the deposited substrate (Figure 5.24).

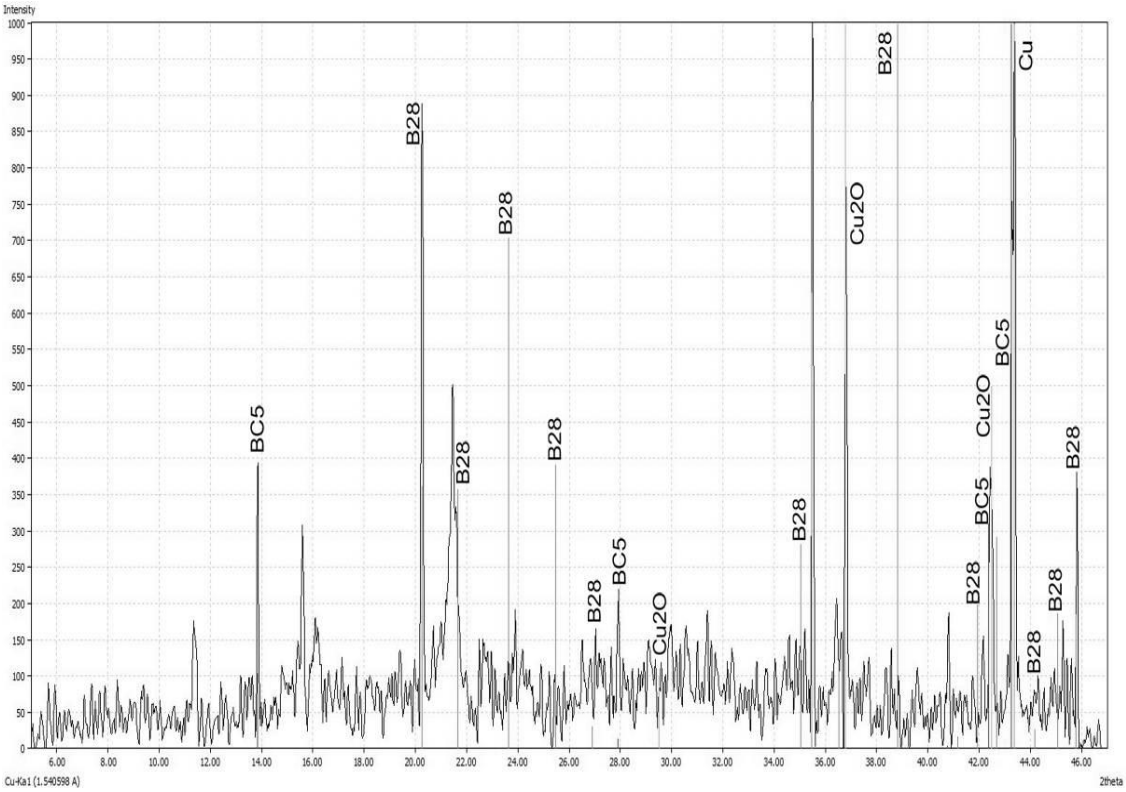

Figure 5.23 XRD analysis of deposited Cu cathode of BPH14

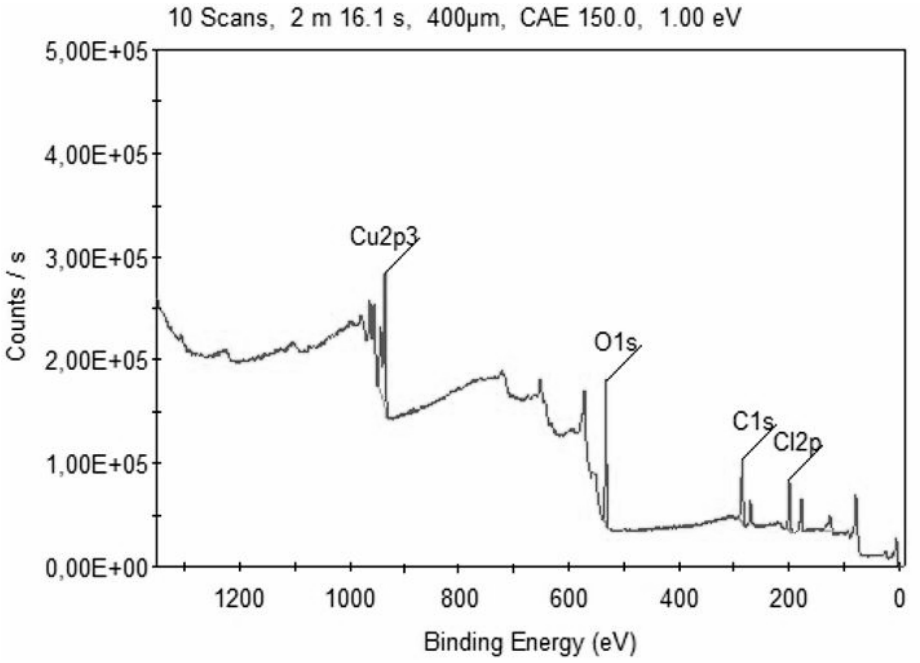

Name	Peak BE	FWHM eV	Area (P) CPS.eV	At. %
C1s	285.72	3.099	229929.11	35.86
O1s	532.67	2.871	491581.75	30.05
Cl2p	200.01	3.143	181753.39	11.90
B1s	187.29	2.133	47457.02	10.98
Cu2p3	936.01	3.449	580757.73	8.64

Figure 5.24 XPS analysis of deposited Cu cathode of BPH14

In experiment BPH23 with parameters listed in Table 5.14, a small amount of deposition on Fe cathode was achieved and the coated substrate was analyzed by XRD to determine the phases formed (Figure 5.25).

Table 5.14 Experimental parameters of BPH23

Code	Anode	Cathode	pH	Addition	V	A	A/dm^2	Duration (min.)
BPH23	Graphite	Fe	9-10	-	4	1	0.45	30

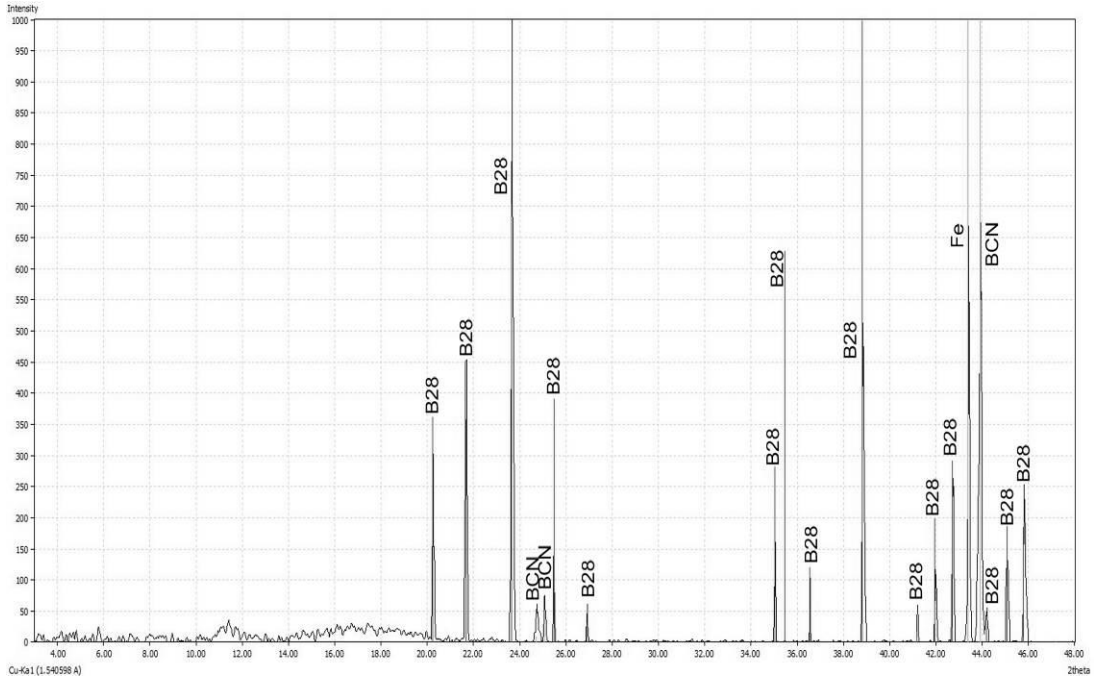

Figure 5.25 XRD analysis of deposited Fe cathode of BPH23

The formation of BCN, B_{28} and Fe phases were determined as a result of XRD analysis. The formation of B_{28} and BCN peaks was proved with exactly matching, however the B_2O_3 removal from the electrolyte during the experiment was low. Therefore, it was determined that a sufficient amount of B_2O_3 should be bounded and removed from solution to form boron carbide. Otherwise, elemental boron or other boron products were deposited.

In experiment BPH28 with parameters listed in Table 5.15, a large amount of deposition on Fe cathode was achieved and the coated substrate was analyzed by XRD to determine the phases formed (Figure 5.26).

Table 5.15 Experimental parameters of BPH28

Code	Anode	Cathode	pH	Addition	V	A	A/dm^2	Duration (min.)
BPH28	Fe	Fe	9-10	-	20	1	0.45	10

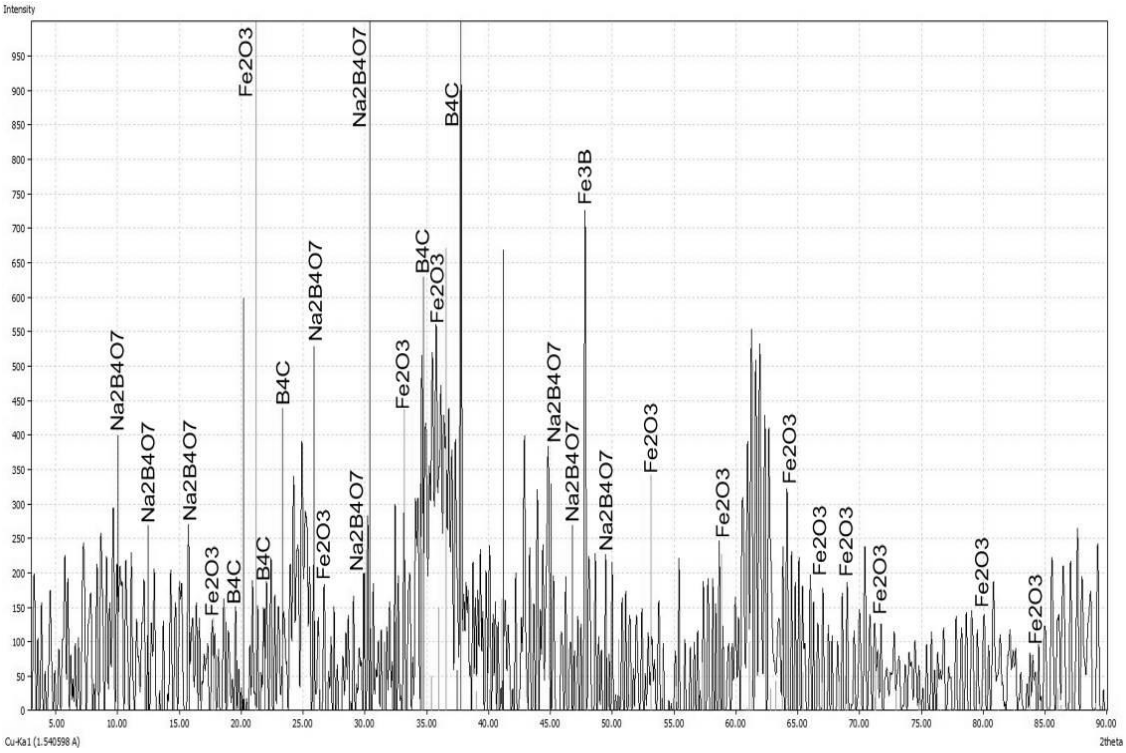

Figure 5.26 XRD analysis of deposited Cu cathode of BPH28

As it was revealed by the XRD analysis, the deposition performed in BPH28 involved many impurities due to oxidation of Fe as Fe_2O_3, deposition of solute as $Na_2B_4O_7$ and formation Fe_3B. Although, the formation of B_4C with exactly matching peaks was proved. The SEM analysis of the substrate in BPH28 presented an amorphous structure (Figure 5.27). In addition, the XPS analysis also supported the high amount of oxide formation, boron and carbon deposition (Figure 5.28).

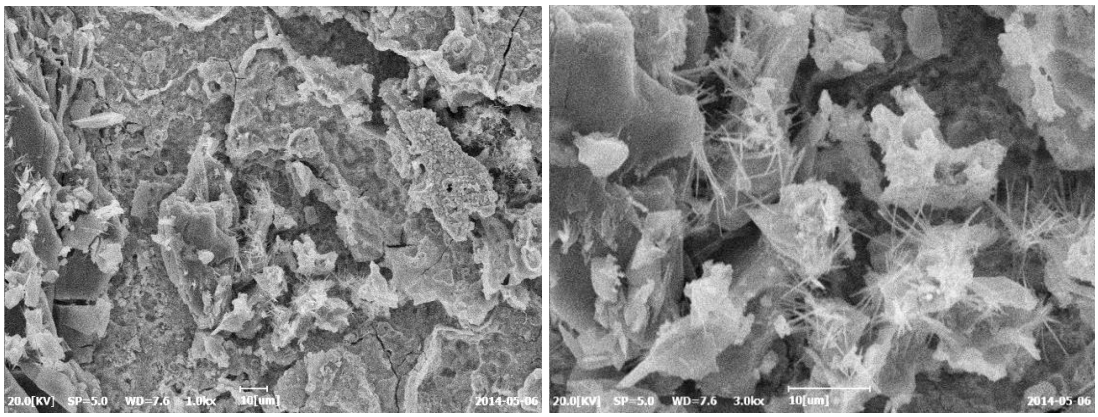

Figure 5.27 SEM analysis of deposited Cu cathode of BPH28 (x1000 & x3000)

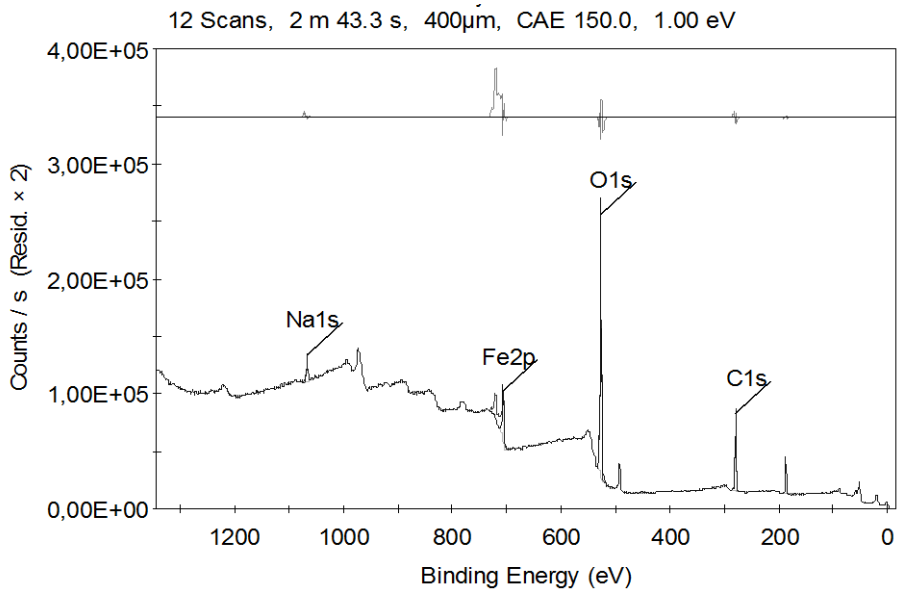

Name	Peak BE	FWHM eV	Area (P) CPS.eV	At. %
O1s	526.38	2.905	808871.68	46.88
C1s	279.30	2.200	174480.06	25.82
B1s	187.09	2.133	78578.38	22.90
Fe2p	706.54	3.529	198544.01	2.33
Na1s	1066.31	2.331	63462.48	2.08

Figure 5.28 XPS analysis of deposited Fe cathode of BPH28

As a result of experiment BPH31 with parameters listed in Table 5.16, a deposition trial on Ti cathode was performed and the substrate was analyzed by XRD to determine the phases formed (Figure 5.29). According to XRD analysis of BPH31 and observed conditions during the experiment no deposition of boron products was achieved. The clear peaks of Ti represented the clear surface of the titanium electrode.

Table 5.16 Experimental parameters of BPH31

Code	Anode	Cathode	pH	Addition	V	A	A/dm^2	Duration (min.)
BPH31	Ti	Ti	9-10	-	170	4	20	10

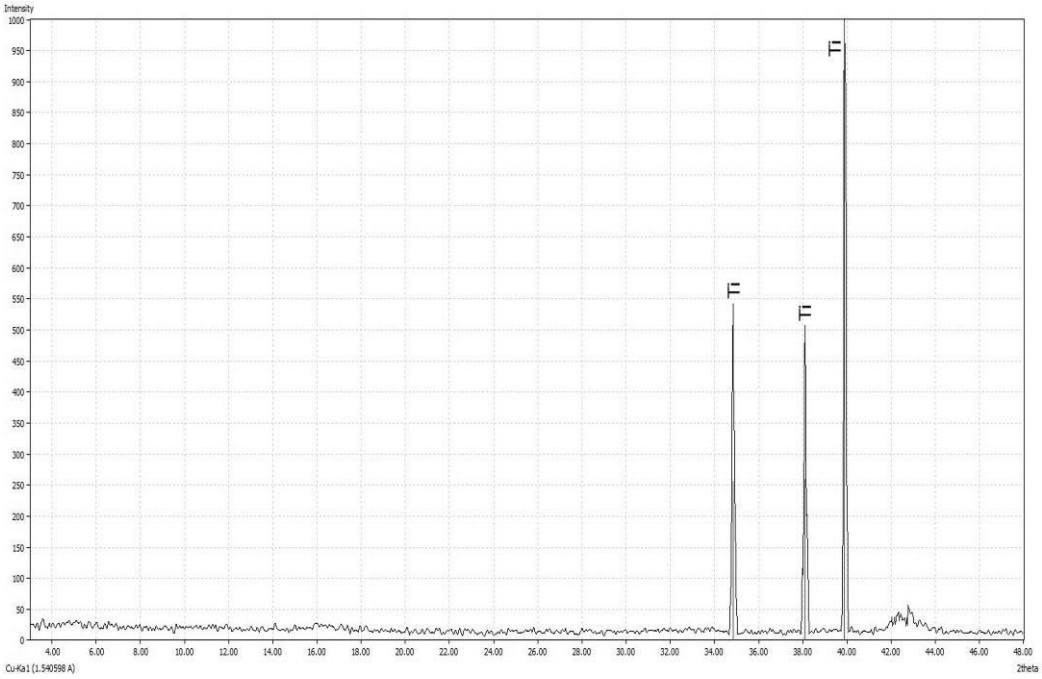

Figure 5.29 XRD analysis of deposited Ti cathode of BPH31

As a result of experiment BPH36 with parameters listed in Table 5.17, a successful deposition on Cu cathode was achieved and the coated substrate was analyzed by XRD to determine the phases formed (Figure 5.30). The formation of B_4C, BC_5 and B_{28} phases are determined by many exactly matching peaks. The current was set constant in this experiment and a high voltage level of 70V was achieved. The SEM analysis of the substrate in BPH36 revealed that the average particle size of deposited particles were about 1 micron or below (Figure 5.31).

Table 5.17 Experimental parameters of BPH36

Code	Anode	Cathode	pH	Addition	V	A	A/dm^2	Duration (min.)
BPH36	Cu	Cu	9-10	-	70	18	8.10	10

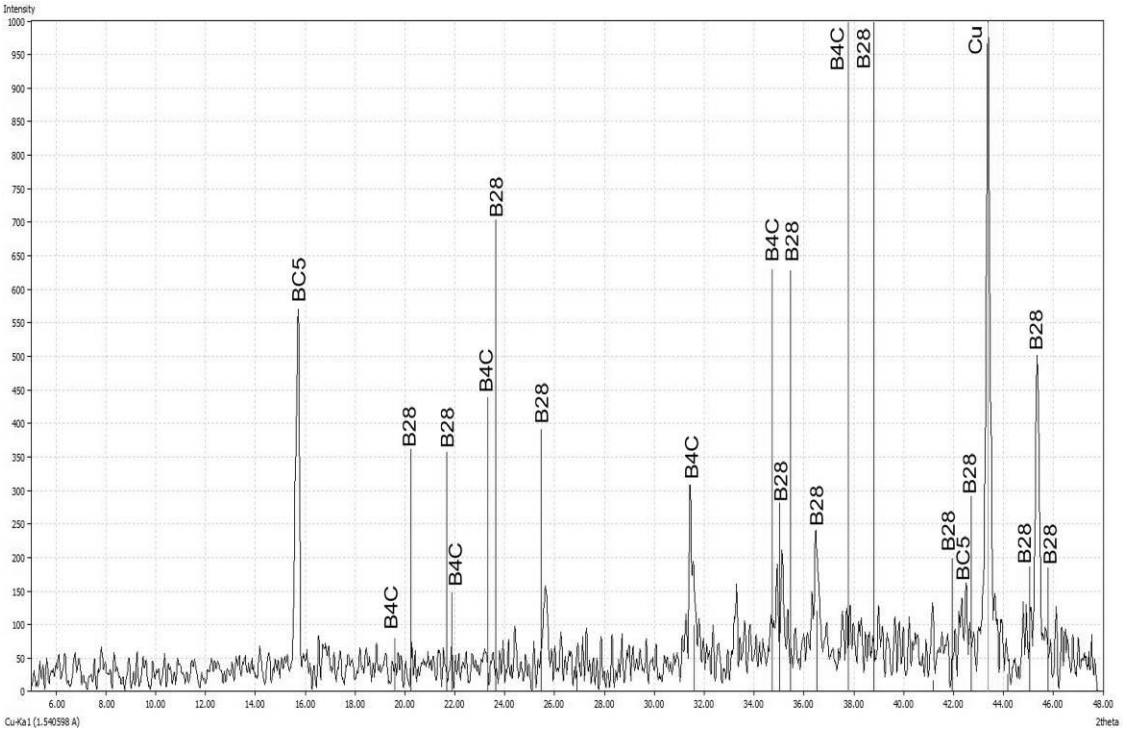

Figure 5.30 XRD analysis of deposited Cu cathode of BPH36

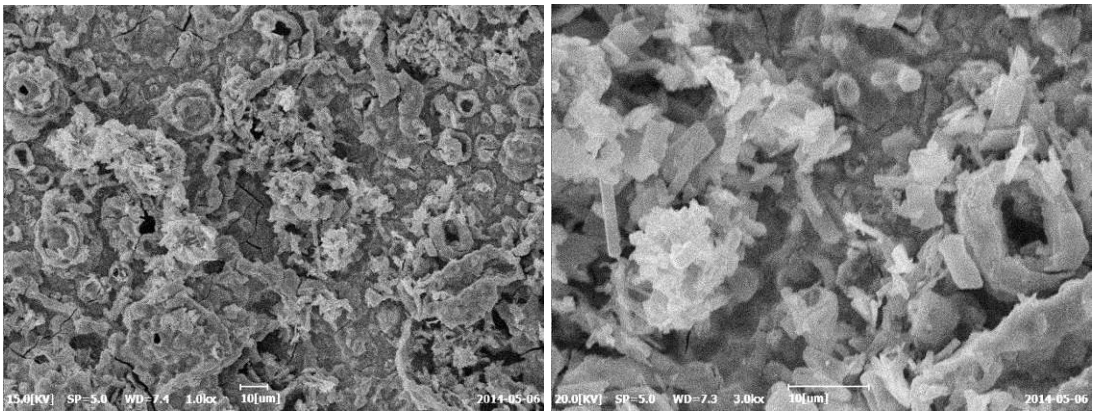

Figure 5.31 SEM analysis of deposited Cu cathode of BPH36 (x1000 & x3000)

In experiment BPH37 with parameters listed in Table 5.18, the reproducibility of experiment BPH36 was tested. As a result, the phases of BC5 and B28 were successfully determined as in BPH36 according to XRD analysis (Figure 5.32).

Table 5.18 Experimental parameters of BPH37

Code	Anode	Cathode	pH	Addition	V	A	A/dm^2	Duration (min.)
BPH37	Cu	Cu	9-10	-	70	18	8.10	10

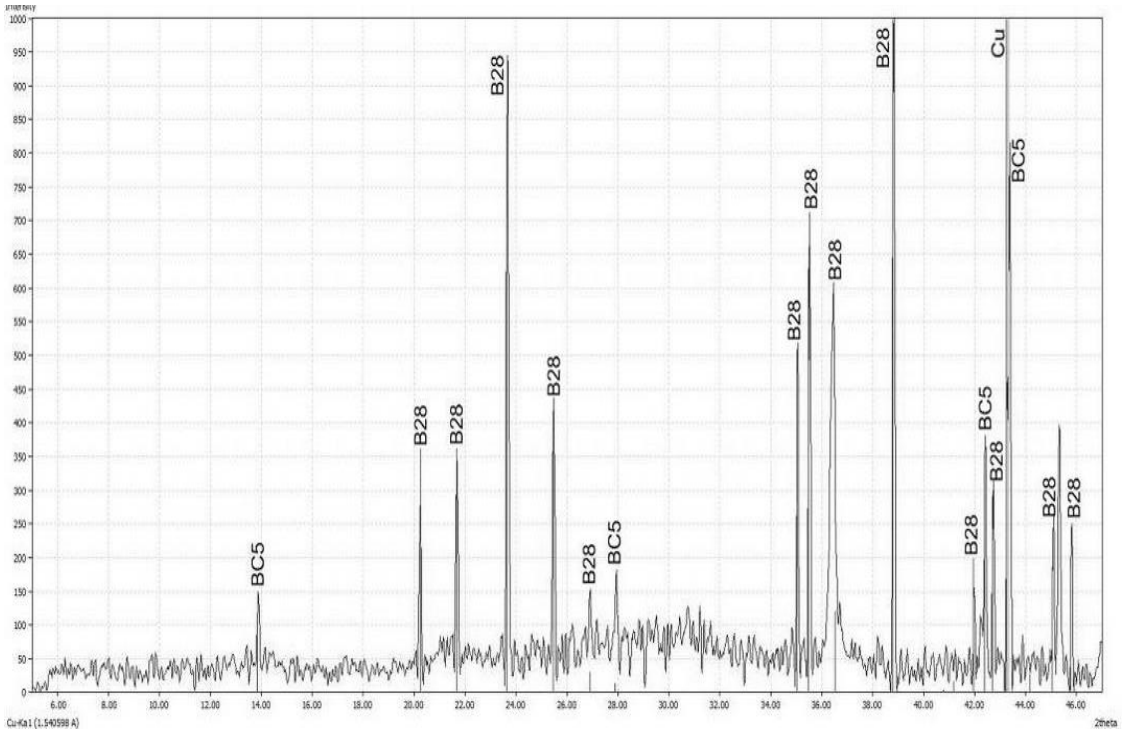

Figure 5.32 XRD analysis of deposited Cu cathode of BPH37

As a result of experiment BPH41 with parameters listed in Table 5.19, a successful deposition on Cu cathode was achieved and the coated substrate was analyzed by XRD to determine the phases formed (Figure 5.33). According to XRD analysis, addition of NaSCN enhanced the formation nitrogen and carbon based boron products such as BC_5 and BCN. The oxides of copper and free carbon peaks were also determined.

Table 5.19 Experimental parameters of BPH41

Code	Anode	Cathode	pH	Addition	V	A	A/dm^2	Duration (min.)
BPH41	Cu	Cu	9-10	NaSCN	24	7	35	10

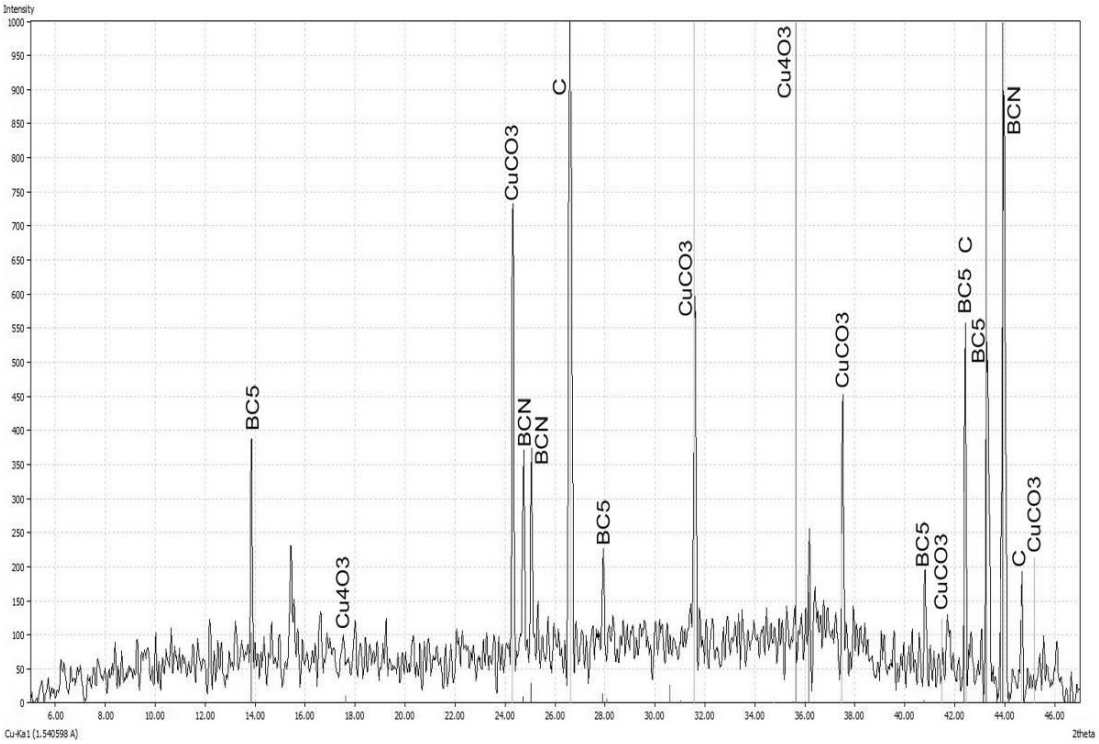

Figure 5.33 XRD analysis of deposited Cu cathode of BPH41

5.3 Evaluation of Experiments Conducted with $Na_2B_4O_7.10H_2O$ as Solute

Initial borax decahydrate concentration of 200 g/L in water was set to achieve a saturated solution without crystallized and/or precipitated solid particles. The determination of pH, solute concentration and bath temperature changes were performed during the experiments with duration of 30 minutes which are BDH06 and BDH14. The experimental parameters of these two experiments are listed in Table 5.20 for a reminder.

Table 5.20 Experimental parameters of BDH06 and BDH14

Code	Anode	Cathode	pH	Addition	V	A	A/dm^2	Duration (min.)
BDH06	Cu	Cu	9-10	NaSCN	14	2	10	30
BDH14	Cu	Cu	9-10	-	13	5	25	30

The B_2O_3 content of initial samples were varied between 39.23 and 38.45. According to chemical analyses of liquid samples taken during experiments in

definite intervals, B_2O_3 content of electrolyte in BDH06 decreased rapidly with respect to BDH14 between 0 and 8 minutes. The deposition of boron products was proved with significant amount of B_2O_3 removal from the solution in BDH06. On the contrary, the B_2O_3 content of electrolyte in BDH14 did not undergo such a decrease and dropped to 30.21% at the end of 8 minutes (Figure 5.34).

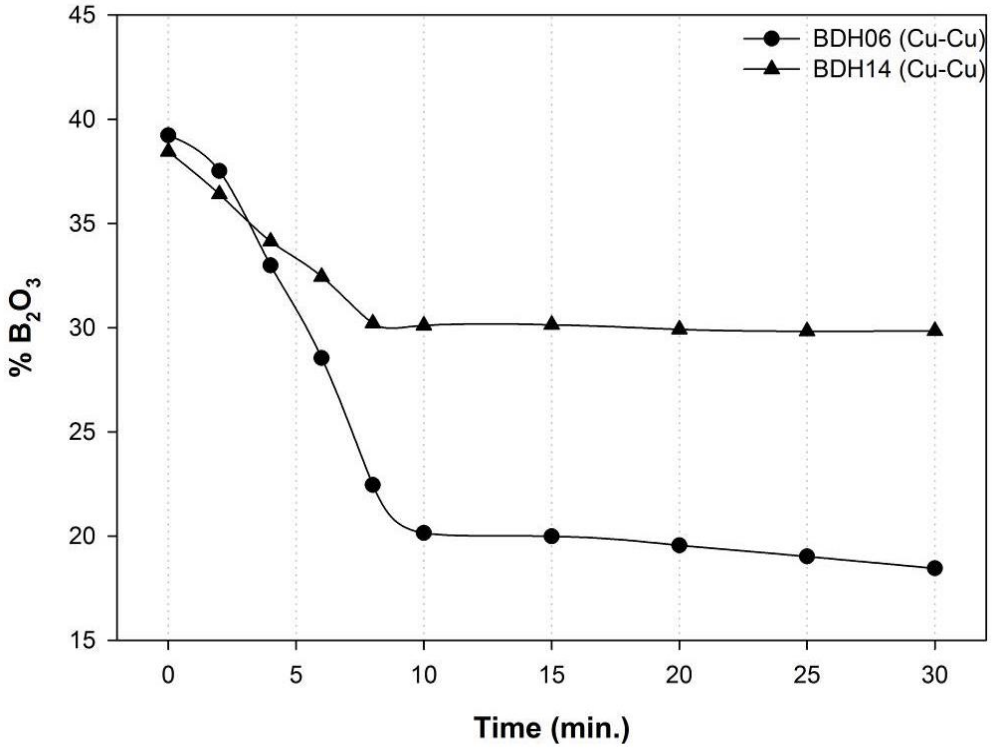

Figure 5.34 B_2O_3 removal trend in electrolytes of BDH06 and BDH14 with time

The bath temperature changed nearly similar to about 15 minutes; however the bath temperature of BDH14 increased rapidly to 90^oC after 15 minutes (Figure 5.35). Nevertheless, the deposition of BDH14 was unsuccessful and only oxides of copper were observed on Cu cathode.

The change in pH levels was also traced for BDH06 and BDH14 during 30 minutes (Figure 5.36). The formation boric acid due to free boron, hydrogen and oxygen ions didn't affect the bath pH level as in borax pentahydrate experiments. There was only a slight decrease in pH level of BDH06 when the reactions commenced.

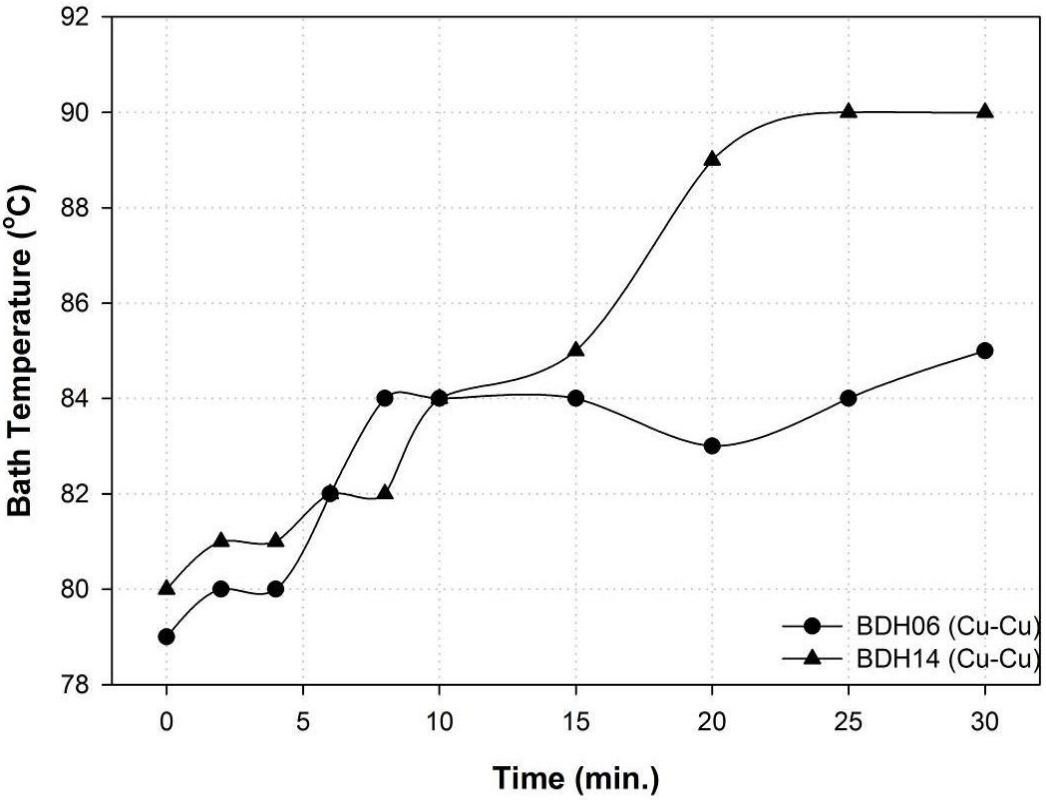

Figure 5.35 Change in bath temperature with respect to time for BDH06 and BDH14

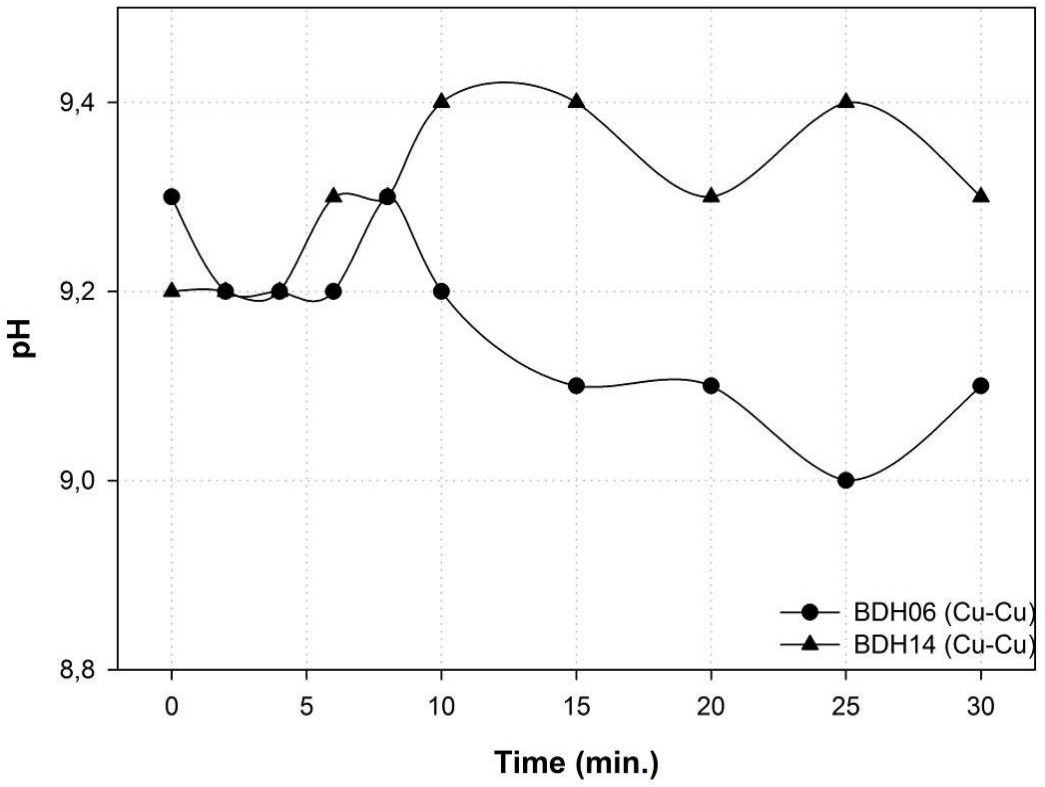

Figure 5.36 Change in pH level with respect to time for BDH06 and BDH14

In experiment BDH05 with parameters listed in Table 5.8, a deposition trial on Cu cathode was performed and the substrate was analyzed by XRD to determine the phases formed (Figure 5.37). According to XRD analysis, despite the addition of NaSCN, only formation of Cu, $CuCo_3$ and Cu_2O phases were achieved. Thus, an unsuccessful deposition was performed in BDH05.

Table 5.21 Experimental parameters of BDH05

Code	Anode	Cathode	pH	Addition	V	A	A/dm^2	Duration (min.)
BDH05	Cu	Cu	9-10	NaSCN	12	2	10	10

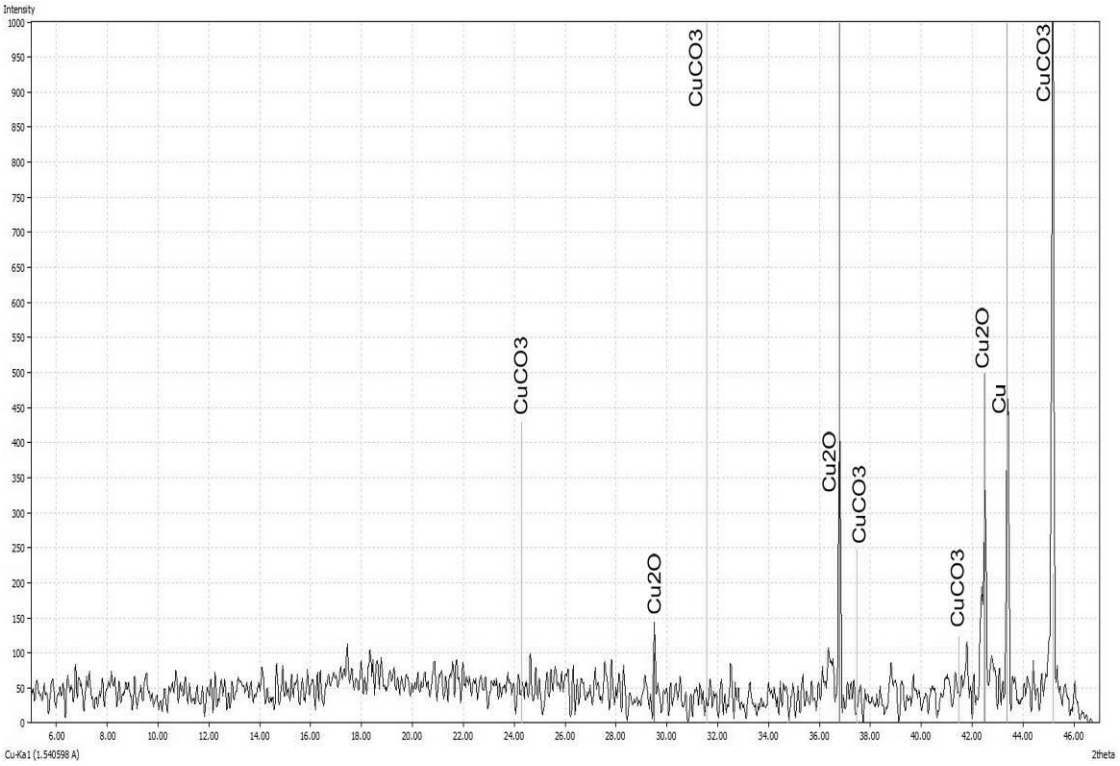

Figure 5.37 XRD analysis of deposited Cu cathode of BDH05

However, a successful deposition was performed in experiment BDH06 with very similar experimental parameters. As the voltage increased, current and current density increased as well for advancing experiments and successful depositions were achieved. In experiment BDH09 (Table 5.22), the formation of boron products and their particle size determination were performed by XRD analysis (Figures 5.38)

Table 5.22 Experimental parameters of BDH09

Code	Anode	Cathode	pH	Addition	V	A	A/dm^2	Duration (min.)
BDH09	Cu	Cu	9-10	NaSCN	20	5	25	10

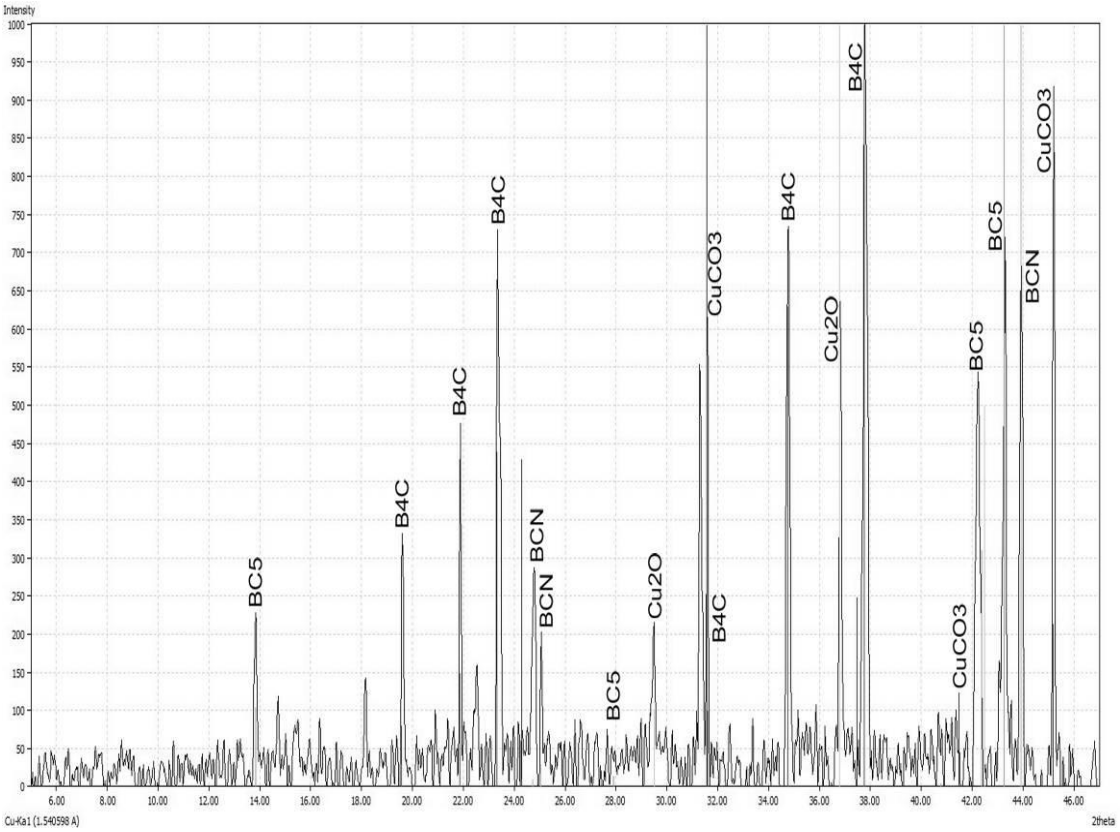

Figure 5.38 XRD analysis of deposited Cu cathode of BDH09

According to XRD analysis, the formation of B4C, BC5, BCN, $CuCo_3$ and Cu_2O with many matching peaks were determined. The SEM analysis stated that, the particles deposited were at sub-micron, nano levels.

5.4 Optimum Experimental Parameters for Electro-deposition

The experimental studies conducted with boric acid, borax pentahydrate and borax decahydrate as solutes finalized by the determination of optimum intervals for production of boron carbide, boron nitride, boron carbonitride and elemental boron.

The maximum optimum deposition time was determined as 8 to 10 minutes by both observation and B_2O_3 removal amount from the electrolyte. In most of the experiments, the reaction slowed and B_2O_3 removal stopped after 10 minutes.

The titanium electrodes generally caused the deposition of solute in different forms or oxides of cathode although stable high voltage levels were reached due to high electrical resistivity. In the experiments conducted with aluminum, stainless steel and lead; deposition failed due to high voltage generated, rapidly increasing bath temperature and fluctuating current values.

The interference trials on bath pH level resulted unsuccessfully since natural pH of bath formed by saturated solute at suitable temperature worked well in most of the experiments. Deposition was hindered due to addition of buffer solutions to decrease the pH level.

Addition of ammonium chloride, ammonium nitride and sodium thiocyanate as nitrogen source; acetic acid, active carbon, dissolved carbon dioxide and sodium thiocyanate as carbon source resulted in success in most of the experiments. The additives were prepared at equal molarity of solutes. The addition of a nitrogen source was revealed to be compulsory in acidic media to form boron nitride. Addition of sodium thiocyanate resulted in formation of boron carbonitride while most of the boron carbide formations were due to graphite anode and dissolved carbon dioxide in water.

Different type of anode and cathode were benefited in formation of electrical potential difference to enhance deposition. In experiments conducted with graphite as anode and Fe as cathode, depositions were achieved at low potential and current densities which corresponds to lower energy consumption in larger deposition areas. However, successful depositions were also performed in experiments with copper as anode and cathode. Additional external power was needed to initiate the deposition reactions in those experiments, thus high voltage levels with high current densities were reached.

The optimum experimental conditions as intervals and the resultant phases detected by XRD analysis are listed in Table 5.22 with respect to solute types.

Table 5.23 Optimum experimental parameters and resultant products

Boric Acid as Solute (saturated, 190 g/L)					
Fixed Parameters					
Solvent	***pH***	***Temperature***	***Duration (min.)***	***Anode***	
Purified Water	Natural 3.5 - 5.0	75 - 85^{o}C	8 - 10	Graphite	
Variables					
Cathode	***V***	***A***	***Addition***	***Deposited Products***	
Fe	4 - 16	1 - 4	$NH_4.Cl$ / $NH_4.NO_3$	BN, Fe_2BO_5	
Cu	8 - 30	2 - 5	$NH_4.Cl$ / $NH_4.NO_3$	BN, B_{28}	
Borax Pentahydrate as Solute (saturated, 175 g/L)					
Fixed Parameters					
Solvent	***pH***	***Temperature***	***Duration (min.)***		
Purified Water	Natural 9.0 - 10.0	75 - 85^{o}C	8 - 10		
Variables					
Anode	***Cathode***	***V***	***A***	***Addition***	***Deposited Products***
Cu	Cu	18 - 70	5 - 18	-	B_4C, BC_5, B_{28}
Cu	Cu	18 - 30	5 - 7	NaSCN	BC_5, BCN
Gr	Fe	4 - 20	1 - 5	-	BCN, B_{28}
Fe	Fe	1 - 20	1 - 5	-	B_4C, Fe_3B
Borax Decahydrate as Solute (saturated, 200 g/L)					
Fixed Parameters					
Solvent	***pH***	***Duration (min.)***	***Anode & Cathode***	***Temperature***	
Purified Water	Natural 9.0 - 10.0	8 - 10	Cu	75 - 85^{o}C	
V	***A***	***Addition***	***Deposited Products***		
4 - 20	1 - 5	NaSCN	B_4C, BC_5, BCN		

The stable solubility and pH level of borax pentahydrate solutions were generally the main solute in successful depositions. Copper, graphite and iron electrodes were used in most of the experiments due to stable temperature levels suitable for atmospheric deposition bath and ease of characterization.

The optimum conditions for electro-deposition vary due to solute type, anode and cathode type, additional chemical compounds, voltage set and current acquired. Therefore, the deposited products differ with respect to dissolved elements in electrolyte during electro-deposition.

CHAPTER SIX
CONCLUSIONS

6.1 General Conclusions

Effective ways to utilize boron ores, concentrates or derivatives are the main discussion topics of boron mining industry in Turkey for several decades. The current boron technology in Turkey only allows the export of raw boron compounds and their concentrates. Therefore, manufacturing of boron end products is a well-known and well-discussed topic of interest in Turkish boron production industry. The fabrication of boron end products from boron derivatives is applied in many countries for many years. Eti Mine has also attempted the establishment of boron carbide and boron nitride production plants and carried out pre-feasibility studies in 2003 to establish the economic feasibility of boron end product fabrication. Nevertheless, no production plant for boron end products has emerged from these studiesdespite the proven profitability of this value added products.

The production of such boron end products as boron carbide, boron nitride, boron carbonitride and elemental boron are possible in industrial scale. However these procedures require large amounts of energy and possess environmental limitations. The literature review revealed that the minimum temperature of thermal reactions to produce boron carbide or boron nitride is 1500^{o}C and may go up to 2000^{o}C. This research proves the possibility of boron end product fabrication by an environmental friendly, low energy consuming modified electro-deposition method in lower temperature levels (60-80^{o}C) unlike the traditional production methods. Boron carbide, boron nitride, boron carbonitride and elemental boron were produced by electro-deposition at low temperatures regardless of sintering and thermal treatment. Boron derivatives of boric acid, borax decahydrate and borax pentahydrate were the main inputs in production nano-sized boron end products by electro-deposition as powders or coating products. pH intervals, bath temperature, solute concentration, voltage set, current acquired and experiment duration were among the experimental variables tested. Different phase formations with different anode and cathode

electrodes and different chemical compound additions were achieved. Successful depositions of B_4C, BC_5, BN, BCN and B_{28} were performed after a deep parameter screening process. The samples were characterized by XRD, XPS and SEM to determine the phases, contents and particle sizes of the deposited materials.

In optimum experimental studies conducted by boric acid as solute, a saturated solution was prepared at 80^{o}C at a pH level of 3.5 with an electrolyte concentration of 190 g/L. The addition of ammonium nitride and ammonium chloride had positive affects in formation of nitrogen based phases. Graphite as anode, iron and copper as cathode were singled out as electrodes. BN and B_{28} formations were achieved in low voltage (max. 30V) and current (max. 5A) levels. Borax pentahydrate was used as solute in most of the experiments. A saturated solution was prepared at 80^{o}C at a pH level of 9.3 with an electrolyte concentration of 175 g/L. Higher voltage and current levels were reached in experiments conducted with copper as the electrode. Formation of B_4C, BC_5, BCN and B_{28} were accomplished in these experiments. The depositions of same phases were also achieved using borax decahydrate as the solute. It was revealed that, a graphite anode or additional compounds enhances the formation of boron end products.

6.2 Future Plans

The extensive usage of boron in this modified electro-deposition method for boron end product fabrication is expected to reduce the deficit of Turkey in end product export. The suitability of products should be determined and evaluated with respect to fabrication of nano-composites and advanced materials afterwards. Moreover, the economical analysis of this method should be investigated through a pilot scale setup to determine the capital and operational costs as well as raw material requirements. Hence, a further study with a multidisciplinary research team should be carried out in order to assess the potential of using these boron end products in a daily use or military purposes. In addition, the production of advanced materials with this environmental friendly and low energy consuming method will fulfill the gap in the literature regarding boron end products.

REFERENCES

Acarkan, N., Bulut, G., Kangal, O. & Önal, G. (2005). A new process for upgrading boron content and recovery of borax concentrate. *Minerals Engineering, 18*, 739-741.

Ahn, H., Klimek, K.S. & Rie, K.T. (2003). BCN coatings by RF PACVD at low temperature. *Surface and Coatings Technology*, *174-175*, 1225-1228.

Alizadeha, A., Taheri-Nassaja, A.E. & Ehsanib, E. (2004). Synthesis of boron carbide powder by a carbothermic reduction method. *Journal of the European Ceramic Society, 24*, 3227-3234.

Aoki, H., Tokuyama, S., Sasada, T., Watanabe, D., Mazumder, M.K., Kimura, C. et al. (2008). Dry etching properties of boron carbon nitride (BCN) films using carbon fluoride gas. *Diamond & Related Materials, 17*, 1800-1804.

Aydogdu, A. & Sevinç, N. (2003). Carbothermic formation of boron nitride. *Journal of the European Ceramic Society, 23*, 3153-3161.

Batar, T., Kahraman, B., Cirit, E. & Çelik, S.B. (1998). Dry processing of borax by calcination as an alternative to wet methods. *International Journal of Mineral Processing, 54*, 99-110.

Batar, T. & Aytekin, Y. (2012). *Mineral processing lecture notes*, Dokuz Eylül University Department of Mining Engineering, 1-14.

Blank, V.D., Seepujak, A., Polyakov, E.V., Batov, D.V., Kulnitskiy, B.A., Parkhomenko et al. (2009). Growth and characterization of BNC nanostructures. *Carbon, 47*, 3167-3174.

Boren National Boron Research Institute (2013). *Report on boron reserves*. Retrieved February 2, 2014, from http://www.boren.gov.tr/en/boron/reserves

Bosso, J.F. & Gaseca, G.R. (1971). Electro-deposition process. *US Patent 3,619,398*.

Buluttekin, M.B. (2008). Bor maden ekonomisi: Türkiye'nin dünya bor piyasasındaki yeri. *II. International Economy Congress, Izmir (In Turkish)*, 1-36.

Burgess, J.S., Acharya, C.K., Lizarazo, J., Yancey, N., Flower, B., Kwon, G. et al. (2008). Boron doped carbon powders formed at 1000^{o}C and one atmosphere. *Carbon, 46*, 1711 -1717.

Camurlu, H.E., Sevinç, N. & Topkaya, Y. (2008). Effect of calcium carbonate addition on carbothermic formation of hexagonal boron nitride. *Journal of the European Ceramic Society, 28*, 679-689.

Camurlu, H.E., Topkaya, Y. & Sevinç, N. (2009). Catalytic effect of alkaline earth oxides on carbothermic formation of hexagonal boron nitride. *Ceramics International, 35*, 2271-2275.

Carlsson, M., Garcia, F.J. & Johnsson, M. (2002). Synthesis and characterization of boron carbide whiskers and thin elongated platelets. *Journal of Crystal Growth, 236*, 466-476.

Celik, M.S., Uzunoglu, H.A. & Arslan, F. (1994). Decrepitation properties of some boron minerals. *Powder Technology, 79*, 167-172.

Chang, B., Gersten, B.L., Szewczyk, S.T. & Adams, J. W. (2007). Characterization of boron carbide nano-particles prepared by a solid state thermal reaction. *Applied Physics A, 86*, 83-87.

Chen, H.Y., Wang, J., Yang, H., Li, W.Z. & Li, H.D. (2000). Synthesis of boron carbide films by ion beam sputtering. *Surface and Coatings Technology, 128-129*, 329-333.

Chen, S., Wang, D.Z., Huang, J.Y. & Ren, Z.F. (2004). Synthesis and characterization of boron carbide nano-particles. *Applied Physics A, 79*, 1757-1759.

Chen, Y., Tong, Z. & Luo, L. (2008). Boron nitride nano-wires produced on commercial stainless steel foil. *Chinese Journal of Chemical Engineering, 16* (3), 485-487.

Chen, C.S., Shih, Y.J., Huang, Y.H. & Huang, G.H. (2011) Recovery of nickel with the addition of boric acid using an electro-deposition reactor. *Desalination and Water Treatment, 32* (1-3), 345-350.

Deepak, F.L., Vinod, C.P., Mukhopadhyay, K., Govindaraj, A. & Rao, C.N.R. (2002). Boron nitride nano-tubes and nano-wires. *Chemical Physics Letters, 353*, 345-352.

Deng, F., Xie, H.Y. & Wang, L. (2006). Synthesis of submicron B_4C by mechanochemical method. *Materials Letters, 60*, 1771-1773.

Deng, J. & Chen, G. (2006). Surface properties of cubic boron nitride thin films. *Applied Surface Science, 252*, 7766-7770.

Dilek, S.N., Özbelge, H.Z., Sezgi, N.A. & Dogu, T. (2001). Kinetic studies for boron carbide formation in a dual impinging jet reactor. *Industrial & Engineering Chemistry Research, 40*, 751-755.

Doménech-Carbó, A., Sánchez-Ramos, S., Yusá-Marco, D.J., Moya-Moreno, M., Gimeno-Adelantado, J.V. & Bosch-Reig, F. (2004). Electrochemical determination of boron in minerals and ceramic materials. *Analytica Chimica Acta, 501*, 103-111.

Ebrahimi, F., Bourne, G.R., Kelly, M.S. & Matthews, T.E. (1999). Mechanical properties of nanocrystalline nickel produced by electro-deposition. *NanoStructured Materials, 11* (3), 343-350.

Ediz, M.N. & Özdag, H. (2002). Direct processing of tincal ores and the wastes of the Etibor Kırka Borax Mine. *Turkish Journal of Engineering & Environmental Sciences, 26*, 107-116.

Emrullahoglu, Ö.F., Emrullahoglu, C.B.& Günaydın, S. (2002). Production of boron nitride. *I. International Boron Symposium, Kütahya (In Turkish)*, 124-128.

Eroglu, Ö.D., Sezgi, N.A., Özbelge, H.Ö. & Durmazuçar, H.H. (2003). Synthesis and characterization of boron carbide films by plasma-enhanced chemical vapor deposition. *Chemical Engineering Communications,190*, 360-372.

Eti Mine (2003). Pre-feasibility report summaries, *Boron Nitride Planning & Data Processing Department*, Ankara.

Eti Mine, Activity report (2012). Retrieved December 12, 2013, from http://www.etimaden.gov.tr

Garrett, D.E. (Ed.). (1998). *Borates: Handbook of deposits, processing, properties, and use*. Academic Press.

Gedikbey, T., Şarda, D. & Birlik, E. (2004a). Boric acid production from colemanite and pandermite minerals. *II. International Boron Symposium, Eskişehir (In Turkish)*, 285-292.

Gedikbey, T., Şarda, D. & Birlik, E. (2004b). Boric acid production from ulexite and tunellite minerals. *II. International Boron Symposium, Eskişehir (In Turkish)*, 291-296.

Golberg, D, Dorozhkin, P.S., Bando, Y., Dong, Z.C., Tang, C.C., Uemura, Y., et al. (2003). Structure, transport and field-emission properties of compound nano-tubes: CN_x vs. BNC_x ($x < 0.1$). *Applied Physics A – Materials, 76*, 499-507.

Gosset, D. & Provot, B. (2001) Boron carbide as a potential inert matrix: an evaluation. *Progress in Nuclear Energy, 38* (3-4), 263-266.

Görgülü, A.O. & Arslan, M. (2003). Alternatif bor bileşikleri. *Journal of Balıkesir University, Institute of Natural Sciences (In Turkish), 5.1*, 42-50.

Grigorev, O.N., Bega, N.D., Lyashenko, V.I., Dubovik, T.V., Panashenko, V.M. & Shcherbina, O.D. (2005). Dependence of the structure of sintered boron carbonitride on the defect level in the starting BN powder. *Powder Metallurgy and Metal Ceramics, 44*, 5-6.

Guojian, J., Jiayue, X., Hanrui, Z. & Wenlan, L. (2009). Combustion of $Na_2B_4O_7$+Mg+C to synthesis B_4C powders. *Journal of Nuclear Materials, 393*, 487-491.

Gupta, C.K. (2003) *Chemical Metallurgy: Principles and Practice.* Weinheim: Wiley-Vch, 670-710.

Han, W.Q., Mickelson, W., Cumings, J. & Zettl, A. (2002). Transformation of $B_xC_yN_z$ nanotubes to pure BN nanotubes. *Applied Physics Letters, 81*, 1110-1112.

Hayun, S., Paris, V., Dariel, M.P., Frage, N. & Zaretzky, E. (2009). Static and dynamic mechanical properties of boron carbide processed by spark plasma sintering. *Journal of the European Ceramic Society, 29*, 3395-3400.

Helvacı, C., & Palmer, M.R. (1997). The boron isotope geochemistry of the neogene borate deposits of Western Turkey. *Geochimica et Cosmochimica Acta, 61* (15), 3161-3169.

Huang, F.L., Cao, C.B., Xiang, X., Lv, R.T. & Zhu, H.S. (2004). Synthesis of hexagonal boron carbonitride phase by solvothermal method. *Diamond & Related Materials, 13*, 1757-1760.

IHS Incorporation (2011). *Report on Boron minerals and chemicals*. Retrieved February 2, 2014, from http://www.ihs.com/products/chemical/planning/ceh/boron-minerals.aspx

Jagannadham, K., Watkins, T.R., Lance, M.J., Riester, L. & Lamester, R.L. (2009). Laser physical vapor deposition of boron carbide films to enhance cutting tool performance. *Surface & Coatings Technology, 203*, 3151-3156.

Jain, A., Anthonysamy, S., Ananthasivana, K., Ranganathana, R., Mittal, V., Narasimhan, S.V. et al. (2008). Characterization of electrodeposited elemental boron. *Materials Characterization, 59*, 890-900.

Jain, A., Anthonysamya, S., Ghosh, C., Ravindran, T.R., Divakar, R. & Mohandas, E. (2013). Electroextraction of boron from boron carbide scrap. *Materials Characterization, 84*, 134-141.

Jankowski, A.F. & Hayes, J.P. (1998). Chemical bonding in hard boron-hexagonal boron nitride multilayer. *Diamond and Related Materials, 7*, 380-384.

Ji, X., Su, Z., Yang, D. & Zhang, T. (2008). Direct nucleation and growth of c-BN by the chemical reaction. *Materials Letters, 62*, 1721-1723.

Jung, C.H., Leeb, M.J. & Kima, C.J. (2004). Preparation of carbon free B_4C powder from B_2O_3 oxide by carbothermal reduction process. *Materials Letters, 58*, 609-614.

Kahraman, B. (2010). Economics of boron mining in Turkey. *II. International Symposium on Sustainable Development*, Sarajevo, 502-506.

Kanani, N. (Ed.). (2004). *Electroplating: Basic Principles, Processes and Practice*. Elsevier, 55-117.

Kavas, T. (2006). Use of boron waste as a fluxing agent in production of red mud brick. *Building and Environment, 41,* 1779-1783.

Khanra, A.K. (2007). Production of boron carbide powder by carbothermal synthesis of gel material. *Bulletin of Materials Sccience, 30* (2) , 93-96.

Kumar, R. (2006). *Development and validation of two-dimensional mathematical model of boron carbide manufacturing process*. M.S. Thesis, Indian Institute of Science, Department of Materials Engineering, India.

Liu, C.H., Peng, W. & Sheng, L.M. (2001). Carbon and boron nanoparticles by pulsed laser vaporization of boron carbide in liquids. *Carbon, 39*, 137-158.

Lou, H.H. & Huang, Y. (2006). Electroplating. *Encyclopedia of Chemical Processing*, Taylor & Francis, 1-10.

Lux, B., Kalss, W., Haubner, R. & Taniguchi, T. (1999). Nucleation of c-BN on various substrate materials under high-pressure-high-temperature conditions. *Diamond and Related Materials, 8*, 415-422.

Ma, R. & Bando, Y. (2002). High purity single crystalline boron carbide nano-wires. *Chemical Physics Letters, 364*, 314-317.

Mannan, M.A., Nagano, M., Hirao, N. & Baba, Y. (2008). Hexagonal BCN Films Prepared by RF Plasma-Enhanced CVD. *Chemistry Letter, 37* (1), 96-97.

Moriyoshi, Y., Shimizu, Y. & Watanabe, T. (2001). B-C-N nano-tubes prepared by a plasma evaporation method. *Thin Solid Films, 390*, 26-30.

Müller, F., Hüfner, S. & Sachdev, H. (2008). One-dimensional structure of boron nitride on chromium (110) – a study of the growth of boron nitride by chemical vapour deposition of borazine. *Surface Science, 602*, 3467-3476.

Naik, Y.A., Venkatesha, T.V. & Nayak, P.V. (2002). Electro-deposition of zinc from chloride solution. *Turkish Journal of Chemistry, 26*, 725-733.

Oganov, A.R. & Solozhenko, V.L. (2009). Boron: A hunt for superhard polymorphs. *Journal of Superhard Materials, 31*, 285-291.

Oganov, A.R., Solozhenko, V.L., Gatti, C., Kurakevych, O.O. & Godec, Y.L. (2011). The high-pressure phase of boron, γ-B28: disputes and conclusions of 5 years after discovery. *Journal of Superhard Materials, 33*, 363-379.

Onal, G. & Burat, F. (2008). Boron mining and processing in Turkey. *Gospodarka Surowcami Mineralnymi-Mineral Resources Management, 24* (4), 49-60.

Onoroa, J., Salvador, M.D. & Cambronero, L.E.G. (2009). High temperature mechanical properties of aluminum alloys reinforced with boron carbide particles. *Materials Science and Engineering A, 499*, 421-426.

Özdemir, M. & Kıpçak, I. (2010). Recovery of boron from borax sludge of boron industry. *Minerals Engineering, 23*, 685-690.

Paine, R.T. & Narula, C.K. (1990). Synthetic routes to boron nitride. *Chemical Reviews, 90* (1), 73-91.

Pei, L.Z. & Xiao, H.N. (2009). B_4C/TiB_2 composite powders prepared by carbothermal reduction method. *Journal of Materials Processing Technology, 209*, 2122-2127.

Rao, M.P.L.N., Gupta, G.S., Manjunatha, P., Kumara, S., Suri, A.K., Krishnamurthy, N. et al. (2009). *International Journal of Refractory Metals & Hard Materials, 27*, 621-628.

Rebillat, F., Guette, A., Naslain, R. & Brosse, R. (1997). Highly ordered pyrolytic BN obtained by LP-CVD. *Journal of the European Ceramic Society, 17*, 1403-1414.

Reynaud, S. (2010). *Fabrication and characterization of carbon and boron carbide nano structured materials*. Ph.D. Thesis, The State University of New Jersey, Materials Science and Engineering, New Jersey.

Rogl, P. & Bittermann, H. (1999). Ternary metal boron carbides. *International Journal of Refractory Metals & Hard Materials, 17*, 27-32.

Roy, T.K., Subramanian, C. & Suri, A.K. (2006). Pressureless sintering of boron carbide. *Ceramics International, 32*, 227-233.

Rubio, A., Corkill, J.L. & Cohen, M.L. (1994). Theory of graphitic boron nitride nanotubes. *Physical Review B, 49* (7), 5081-5084.

Rudolph, S. (1994). Boron nitride. *American Ceramic Society Bulletin, 73* (6), 89-90.

Ruh, R., Kearns, M., Zangvil, A. & Xu, Y. (1992). Phase and property studies of boron carbide-boron nitride composites. *Journal of the American Ceramic Society, 75*, 864-872.

Sachdev, H. & Strauß, M. (1999). Investigation of the chemical reactivity and stability of c-BNP. *Diamond and Related Materials, 8*, 319-324.

Sezer, A.O. & Brand, J.I. (2001). Chemical vapor deposition of boron carbide. *Materials Science and Engineering, 79*, 191-202.

Shi, L., Gu, Y., Chen, L., Qian, Y., Yang, Z. & Ma, J. (2003). A low temperature synthesis of crystalline B_4C ultrafine powders. *Solid State Communications,128*, 5-7.

Shi, X., Wang, S., Yang, H., Duan, X. & Dong, X. (2008). Fabrication and characterization of hexagonal boron nitride powder by spray drying and calcining-nitriding technology. *Journal of Solid State Chemistry, 181*, 2274-2278.

Singhala, S.K., Von der Gonnab, J., Noverb, G., Meurerb, H.J. & Singha, B.P. (2005). Synthesis of cubic boron nitride at reduced pressures in the presence of $Co[(NH_3)6]Cl_3$ and NH_4F. *Diamond & Related Materials, 14*, 1389-1394.

Sinha, A., Mahata, T. & Sharma, B.P. (2002). Carbothermal route for preparation of boron carbide powder from boric acid-citric acid gel precursor. *Journal of Nuclear Materials, 301*, 165-169.

Soh, H.T., Quate, C.F., Morpurgo, A.F., Marcus, C.M., Kong, J. & Dai, H.J. (1999). Integrated nano-tube circuits: Controlled growth and ohmic contacting of single-walled carbon nano-tubes. *Applied Physics Letters, 75*, 627.

Steinbrück, M. (2005). Oxidation of boron carbide at high temperatures. *Journal of Nuclear Materials, 336*, 185-193.

Streletskii, A.N., Permenova, D.G., Bokhonovb, B.B., Kolbaneva, I.V., Leonovc, A.V., Berestetskayaa, I.V. & Streletzkyd, K.A. (2009). Destruction, amorphization and reactivity of nano-BN under ball milling. *Journal of Alloys and Compounds, 483*, 313-316.

Sun, J., Liu, C. & Duan, C. (2009). Effect of Al and TiO_2 on sinterability and mechanical properties of boron carbide. *Materials Science and Engineering A, 509*, 89-93.

Tavşanoglu, T., Addemir, O. & Jeandin, M. (2010). Plazma-destekli manyetik alanda sıçratma teknigiyle B_4C ince film üretimi. *ITU Dergisi D, 9 (4) (In Turkish)*, 125-132.

Terrones, M., Grobert, N. & Terrones, H. (2003). Synthetic routes to nano-scale $B_xC_yN_z$ architectures. *Carbon, 40*, 1665-1684.

Thevenot, F. (1990). Boron carbide-A comprehensive review. *Journal of European Ceramic Society, 6*, 20-25.

TMMOB, Türkiye Metalurji Mühendisleri Odaları Birliği (2003). *Report on Boron*, Ankara, 1-50.

Tokmak, B. (2004). Boron end products and experiences of BM boron technologies. *IV. International Boron Symposium, Eskişehir (In Turkish)*, 105-108.

Torres, R., Caretti, I., Gago, R., Martin, Z. & Jimenez, I. (2007). Bonding structure of BCN nano-powders prepared by ball milling. *Diamond & Related Materials, 16*, 1450-1454.

Treacy, M.M.J, Ebbesen, T.W. & Gibson, J.M. (1996). Exceptionally high Young's modulus observed for individual carbon nano-tubes. *Nature, 381*, 678.

Ulrich, S., Holleck, H., Leiste, H., Niederberger, L., Nold, E., Sell, K. et al. (2005). Nano scale, multi-functional coatings in the material system B-C-N-H. *Surface & Coatings Technology, 200*, 7-13.

Wang, P., Fujii, H., Orimo, S. & Udagawa, M. (2004). Preliminary study on mechanically milled hydrogenated nano structured B_4C. *Journal of Alloys and Compounds, 363*, L3-L6.

Watanabe, M.O., Itoh, S., Mizushima, K. & Sasaki, T. (1996). Bonding characterization of BC_2N thin films. *Applied Physics Letter, 68,* 2962-2964.

White, C.T., Robertson, D.H. & Mintmire, J.W. (1993). Helical and rotational symmetries of nano-scale graphitic tubules. *Physical Review B, 47,* 5485.

Woodman, R.H., Klotz, B.R. & Dowding, R.J. (2005). Evaluation of a dry ball milling technique as a method for mixing boron carbide and carbon nano-tube powders. *Ceramics International, 31,* 765-768.

Wöhle, J., Ahn, H. & Rie, K.T. (1999). BCN coatings on polymer substrates by plasma CVD at low temperature. *Surface and Coatings Technology, 116-119,* 1166-1171.

Yanase, I., Ogawara, R. & Kobayashi, H. (2009). Synthesis of boron carbide powder from polyvinyl borate precursor. *Materials Letters, 63,* 91-93.

Yang, H.S., Iwamoto, C. & Yoshida, T. (2005). Peculiar deformation characteristics of turbostratic boron nitride thin film. *Thin Solid Films, 483,* 218-221.

Yersel, E., Tufan, B. & Batar, T. (2010). A study of various boron additives on the mechanical behavior and microstructure of ceramic tiles. *The Journal of Ore Dressing, 12* (24), 17-21.

Yılmaz, O. (2006). *Enrichment studies of boron process wastes from Balıkesir- Bigadiç plant by flotation method*. M.S. Thesis, Balıkesir University, Institute of Science, Department of Chemistry, Balıkesir.

Zhao, Y. & Wang, M. (2009). Effect of sintering temperature on the structure and properties of polycrystalline cubic boron nitride prepared by SPS. *Journal of Materials Processing Technology, 209,* 355-359.

Zhi, C.Y., Bai, X.D. & Wang, E.G. (2002). Raman characterization of boron carbonitride nano-tubes. *Applied Physics Letter, 80*, 3590-3592.

Zhuge, F. & Yamanaka, S. (2008). Ternary compound B_4CN_4 prepared by direct nitridation of B_4C. *Journal of Alloys and Compounds, 466*, 299-303.